NBS

Technical Note

No. 211
Volume 5

CONFERENCE ON NON-LINEAR PROCESSES IN THE IONOSPHERE DECEMBER 16-17, 1963

EDITORS

DONALD H. MENZEL AND ERNEST K. SMITH, JR.

Sponsored By

Voice of America

and

Central Radio Propagation Laboratory
National Bureau of Standards
Boulder, Colorado

U. S. DEPARTMENT OF COMMERCE
NATIONAL BUREAU OF STANDARDS

NATIONAL BUREAU OF STANDARDS

Technical Note 211, Volume 5

Issued April 24, 1964

CONFERENCE ON NON-LINEAR PROCESSES IN THE IONOSPHERE DECEMBER 16-17, 1963

Sponsored by
Voice of America
and
Central Radio Propagation Laboratory
National Bureau of Standards
Boulder, Colorado

NBS Technical Notes are designed to supplement the Bureau's regular publications program. They provide a means for making available scientific data that are of transient or limited interest. Technical Notes may be listed or referred to in the open literature.

For sale by the Superintendent of Documents, U. S. Government Printing Office
Washington, D.C. 20402
Price 60¢

Volume V

Table of Contents

---

*Session 3 paper continued from Volume IV, Technical Note No. 211.

**Session 4 papers continued in Volume VI, Technical Note No. 211.

ELECTROMAGNETIC WAVE REFLECTION FROM AN OSCILLATING, COLLISION-FREE MAGNETO-IONIC MEDIUM

O. E. H. Rydbeck

Research Laboratory of Electronics
Chalmers Institute of Technology
Gothenburg, Sweden

1. Introduction and Summary

A collision-free or low collision magneto-ionic medium is easily perturbed by a driving or pumping wave, even of moderate power. Unless the pump wave has longitudinal propagation, it will generate longitudinal electron velocities as well as differential space charge densities. These quantities, as well as the transverse, pump field electron velocities, will affect the propagation of any (low power) signal or probing wave propagating through the medium, which now has oscillating and travelling electron velocity and electron density ripples.

If the pump wave has an angular frequency ω_p, and that of the signal wave is ω_s, two first order sum and difference frequency ($\omega_{\pm 1} = \omega_p \pm \omega_s$), waves are generated in the medium. It is shown that the generation of these waves, for which specific refraction laws hold, is greatly enhanced if a parametric travelling wave resonance develops in the system or if the non-linear driving force experiences a local resonance. Under certain conditions, sum and/or difference frequency

waves, usually with two kinds of polarization, will radiate away from the resonance interaction region. This generation is dealt with in detail for homogeneous media, with a discontinuous boundary, and for slowly inhomogeneous ones.

Waves of this kind should be generated easily by a topside sounder of moderate power. It should also be possible, with present day techniques, to record sum and difference frequency "echoes" at the ground, if a very powerful pump wave transmitter were used. It is interesting to note that not only the true height of normal reflection ($N_0 e^2/m\epsilon_0 = \omega_s^2$) but also the electron density gradient, at the same level, should be obtainable by such measurements, provided $\omega_p \gg \omega_{s_{max}}$. Since ω_p could be left unchanged, while ω_s is swept through the sounding range of interest, the technical arrangements for such experiments, which might be very rewarding, should not be overly complicated.

2. Electromagnetic Wave Reflection from the Oscillating, Isotropic, Ionized Medium

a. Only electron density oscillations considered. Let us assume that two plane electromagnetic waves, one signal wave, of angular frequency ω_s and one high power (pump) wave, of angular frequency ω_p impinge upon a plane, homogeneous and isotropic as

shown in figure 1. We assume that the pumpwave is powerful enough to produce a differential charge density, ΔN, sufficiently large to affect the propagation of the much weaker signal wave. The influence of the electron velocities generated by the pump wave, which affects the propagation of the signal wave in a similar manner, will be considered in the following section b.

The differential electron density can be written

$$\Delta N = \eta\, N \cos(\omega_p t - \bar{k}_p \bar{r}), \tag{2.1}$$

where

$$k_p = \frac{2\pi}{\lambda_p} = \frac{\omega_p}{c_0} n_p \tag{2.1a}$$

and λ_p is the wavelength of the pump wave in medium II.

The wave equation for the signal field becomes

$$\frac{\partial}{\partial z^2} + \frac{\partial^2}{\partial x^2} - \frac{1}{c_0^2}\frac{\partial^2}{\partial t^2} - \frac{\omega_0^2}{c_0^2}\{1 + \eta\cos(\omega_p t - \bar{k}_p \bar{r})\}\psi = 0, \tag{2.2}$$

where ψ is related to E_y by the relation

$$E_y = \frac{1}{j\omega_s}\frac{\partial \psi}{\partial t}. \tag{2.2a}$$

If we neglect the field instabilities generated at or very near the parametric system resonances (for details see Rydbeck [1963]), E_y can be written

$$E_y = E_y^o \left[e^{+j(\omega_s t - k_{s_x} x)} \left\{ e^{-jk_{s_z} z} + \alpha_{\substack{+1 \\ -1}} e^{-j(k_{+1_z} - k_{p_z})z} + \right.\right.$$

$$\left. + \alpha_{\substack{-1_{+1}}} e^{-j(k_{-1_z} + k_{p_z})z} + \cdots \right\} + e^{+j(\omega_{+1} t - k_{+1_x} x)} \frac{\omega_{+1}}{\omega_s} \left\{ \alpha_{\substack{+1 \\ 0}} e^{-jk_{+1_z} z} + \right.$$

$$\left. + \alpha_{\substack{0_{+1}}} e^{-j(k_{s_z} + k_{p_z})z} + \cdots \right\} + e^{+j(\omega_{-1} t - k_{-1_x} x)} \frac{\omega_{-1}}{\omega_s} \left\{ \alpha_{\substack{-1 \\ 0}} e^{-jk_{-1_z} z} + \right.$$

$$\left. \left. + \alpha_{\substack{0_{-1}}} e^{-j(k_{s_z} - k_{p_z})z} + \cdots \right\} \right] + \text{higher order frequency terms,}$$

$$(z \geq 0), \qquad (2.3)$$

where k_{s_x}, k_{s_z} are the x and z components of $\bar{k}_s$, and

$$k_s = \frac{\omega_s}{c_0} \sqrt{1 - \frac{\omega_p^2}{\omega_s^2}} = \frac{\omega_s}{c_0} n(\omega_s) \qquad (2.4)$$

(c_0 = the electromagnetic velocity in vacuum).

Furthermore, ω_{+1} and ω_{-1} denote the sum and difference frequencies; i. e.,

$$\left.\begin{matrix} \omega_{+1} \\ \omega_{-1} \end{matrix}\right\} = \omega_s \pm \omega_p , \qquad (2.5)$$

and

$$k_{+1} = \frac{\omega_{+1}}{c_0} n(\omega_{+1}); \quad k_{-1} = \frac{\omega_{-1}}{c_0} n(\omega_{-1}). \qquad (2.6)$$

One finds that [Rydbeck, 1963] that $\alpha_{\substack{0_{+1}}}$ and $\alpha_{\substack{0_{-1}}}$ can be written

$$\left.\begin{matrix} \alpha_{\substack{0_{+1}}} \\ \alpha_{\substack{0_{-1}}} \end{matrix}\right\} = \frac{n}{2} \frac{\omega_p^2}{c_0^2} \frac{1}{k_{\pm 1}^2 - |\bar{k}_s \pm \bar{k}_p|^2} . \qquad (2.7)$$

These amplitude coefficients exhibit parametric travelling wave resonances and approach $\pm\infty$ (losses neglected, also possible instabilities at or near these resonances [Rydbeck, 1963]), when

$$\left.\begin{aligned} k_{+1} &\to \pm\,|\bar{k}_s + \bar{k}_p| \\ k_{-1} &\to \pm\,|\bar{k}_s - \bar{k}_p|. \end{aligned}\right\} \qquad (2.8)$$

Whether these resonances develop or not depends upon the boundary conditions which determine $\alpha_{0_{+1}}$, $\alpha_{0_{-1}}$, the amplitude coefficients of the natural, or unperturbed, sum and difference frequency waves of the medium. Since $\alpha_{\substack{+1\\-1}}$, $\alpha_{\substack{-1\\+1}}$ are proportional to these coefficients times η, they will be neglected in the following analysis ($\alpha_{0_{+1}}$ and $\alpha_{0_{-1}}$ will be proportional to η).

The boundary conditions at $z = 0$ require that

$$k_{s_x} + k_{p_x} = k_{+1_x} \quad \text{and} \quad k_{s_x} - k_{p_x} = k_{-1_x}, \qquad (2.9)$$

which yield the following reflection laws (in medium I) for the "reflected" sum and difference frequency waves, as shown in figure 2,

viz., $$\sin \varphi_{I_{\substack{+1\\-1}}} = \frac{1}{\omega_s \pm \omega_p} \left(\omega_s \sin \varphi_{I_s} \pm \omega_p \sin \varphi_{I_p}\right). \qquad (2.10)$$

In the case of degenerate parametric pumping, i.e., $\omega_p = 2\omega_s$, this relation yields the peculiar result

$$\sin \varphi_{I_{-1}} = -\sin \varphi_{I_0} \quad (\omega_p = 2\omega_s). \qquad (2.11)$$

If higher order sum and difference frequency terms were considered, one would obtain the more general relation

$$\sin \varphi_{I_{+n}} = \frac{1}{\omega_s \pm m\omega_p} \left(\omega_s \sin \varphi_{I_0} \pm m\omega_p \sin \varphi_{I_p} \right), \qquad (2.10a)$$

$$_{-n}$$

where $m = 1, 2, \ldots$.

If we next introduce the boundary reflection and transmission coefficients of the unperturbed signal wave, fiz.,

$$R_{s,0} = \frac{k^0_{s_z} - k_{s_z}}{k^0_{s_z} + k_{s_z}}; \quad T_{s,0} = \frac{2k^0_{s_z}}{k^0_{s_z} + k_{s_z}}, \qquad (2.12)$$

where $k^0_{s_z} = \omega_s / c_0$, the boundary conditions finally yield the following field relations in media I and II (E^0_y = amplitude of incident signal wave):

Medium I $(z \leq 0)$

$$E_y = E^0_y \left[e^{+j(\omega_s t - k^0_{s_x} x - k^0_{s_z} z)} + R_{s,0}\, e^{+j(\omega_s t - k^0_{s_x} x + k^0_{s_z} z)} + \right.$$

$$+ T_{s,0} R_{0,+1} \alpha_{0_{+1}} \frac{\omega_{+1}}{\omega_s} e^{+j(\omega_{+1} t - k^0_{+1_x} x + k^0_{+1_z} z)} +$$

$$\left. + T_{s,0} R_{0,-1} \alpha_{0_{-1}} \frac{\omega_{-1}}{\omega_s} e^{+j(\omega_{-1} t - k^0_{-1_x} x + k^0_{-1_z} z)} \right], \qquad (2.13)$$

where $k^0_{+1} = \omega_{+1}/c_0$, and $k^0_{-1} = \omega_{-1}/c_0$. The sum and difference "reflection" coefficients, $R_{0,+1}$ and $R_{0,-1}$, become

$$R_{0,+1} = \frac{k_{+1_z} - k_{s_z} - k_{p_z}}{k^0_{+1_z} + k_{+1_z}} , \tag{2.14}$$

$$R_{0,-1} = \frac{k_{-1_z} - k_{s_z} + k_{p_z}}{k^0_{-1_z} + k_{-1_z}} . \tag{2.15}$$

Medium II $(z \geq 0)$

$$E_y = E_y^0 T_{s,0} \left[e^{+j(\omega_s t - k_{s_x} x - k_{s_z} z)} + \alpha_{0_{+1}} \frac{\omega_{+1}}{\omega_s} e^{+j(\omega_{+1} t - k_{+1_x} x)} \left\{ e^{-j(k_{s_z} + k_{p_z})z} - T_{0,+1} e^{-jk_{+1_z} z} \right\} + \alpha_{0_{-1}} \frac{\omega_{-1}}{\omega_s} e^{+j(\omega_{-1} t - k_{-1_x} x)} \left\{ e^{-j(k_{s_z} - k_{p_z})z} - T_{0,-1} e^{-jk_{-1_z} z} \right\} \right] , \tag{2.16}$$

where

$$T_{0,+1} = \frac{k^0_{+1_z} + k_{s_z} + k_{p_z}}{k^0_{+1_z} + k_{+1_z}} , \tag{2.17}$$

$$T_{0,-1} = \frac{k^0_{-1_z} + k_{s_z} - k_{p_z}}{k^0_{-1_z} + k_{-1_z}} . \tag{2.18}$$

It is interesting to note that, for $k_p = 0$ (non-travelling pumpwave), these transmission and reflection coefficients ($T_{0,+1}$; $T_{0,-1}$; $R_{0,+1}$; $R_{0,-1}$) are the regular ones for a frequency shifting network.

By (2. 9), relation (2. 7) now can be written

$$\left.\begin{matrix} \alpha_{0_{+1}} \\ \alpha_{0_{-1}} \end{matrix}\right\} = \frac{\eta}{2} \frac{\omega_p^2}{c_0^2} \frac{1}{k_{\pm 1_z}^2 - (k_{s_z} \pm k_{p_z})^2} , \qquad (2.19)$$

which means that

$$R_{0,+1}\, \alpha_{0_{+1}} = \frac{\eta}{2} \frac{\omega_p^2}{c_0^2} \frac{1}{k^0_{+1_z} + k_{+1_z}} \cdot \frac{1}{k_{+1} + k_{s_z} + k_{p_z}} , \qquad (2.20)$$

$$R_{0,-1}\, \alpha_{0_{-1}} = \frac{\eta}{2} \frac{\omega_p^2}{c_0^2} \frac{1}{k^0_{-1_z} + k_{-1_z}} \cdot \frac{1}{k_{-1} + k_{s_z} - k_{p_z}} . \qquad (2.21)$$

Thus, to first order, only two parametric travelling wave resonances are left, viz. ,

and

$$\left.\begin{aligned} k_{+1} &= -(k_{s_z} + k_{p_z}) , \\ k_{-1} &= -(k_{s_z} - k_{p_z}) . \end{aligned}\right\} \qquad (2.22)$$

The other two resonances cancel out due to the boundary reflection effects. Since the energy balance at the boundary requires that the sign of $k_\pm$ be equal to the sign of $-(k_{s_z} \pm k_{p_z})$, this resonance is possible physically, if only the condition $|k_\pm| = |k_{s_z} \pm k_{p_z}|$ can be met (a condition that is more easily attainable in the magneto-ionic medium).

The natural sum frequency wave in medium II always travels in negative z-direction, i. e. , towards the boundary.

As far as the difference frequency wave is concerned, we have to distinguish between two cases, $\omega_p \gtrless \omega_s$. If $\omega_p > \omega_s$, the natural difference frequency wave travels in positive z direction if $k_{p_z} < k_{s_z}$, and in negative direction if $k_{p_z} > k_{s_z}$ When $\omega_p < \omega_s$ this situation is reversed.

A degenerate parametric resonance, $|k_{-1}| = |k_s|$. This resonance therefore is possible only if $2|k_s| > k_p$, i.e., if $n(\omega) > n_p$. If k_p is determined by the properties of the isotropic ionized layer only (for an unguided electromagnetic pump wave), this resonance is not possible for travelling waves.

If we assume that $k_p = 0$ (for example if $\omega_p^2 = \omega_0^2$), the degenerate parametric resonance requires

$$n_{s_z} = -j\sqrt{4 + \sin^2 \varphi_{I_0}} = n_{-1_z},$$

which yields one exponentially decreasing wave (with z) in medium II and one exponentially increasing; together they constitute a negative energy flow (at the frequency $\omega_s = \omega_p/2$), which generates the "amplified" signal returning at the peculiar angle $-\varphi_{I_0}$ from the boundary (see (2. 10)). The pumped ionized medium now acts as an amplifying wall or resonant reflection amplifier, the necessary power being supplied by the pump wave. Obviously one could consider parametric plasma amplifiers operating on this principle.

In an anisotropic medium, for example, the magneto-ionic one would have many more degrees of freedom to obtain parametric travelling wave resonances. Actually, resonance coefficients like $\alpha_{0_{\pm 1}}$, (2. 7), are quite general in nature, and similar expressions are obtained for the magneto-ionic medium, as will be shown in paragraph 4.

b. Electron velocity oscillations also considered. If we, for the sake of simplicity, assume that the electron velocity wave and the differential space charge density wave propagate with the same k_p-value (this is not always the case), it can be shown [Rydbeck, 1963] that η in (2. 7) has to be replaced by η_+ for $\alpha_{0_{+1}}$, and η_{-1} for $\alpha_{0_{-1}}$, where

$$\eta_{+1} = \eta \pm \frac{\omega_s \omega_p}{\omega_\pm^2} \frac{v_p n_s}{c_0} \cos (\varphi_{II_p}^{(v)} - \varphi_{II_0}). \qquad (2.23)$$

In this expression, v_p denotes the amplitude of the electron velocity caused by the pump wave, and $\varphi_{II_p}^{(v)}$ the angle that this velocity makes with the z-axis.

It is important that (1) the inclusion of the electron velocity does not change the parametric travelling wave resonances, and (2) that electrons oscillating transversely to the signal wave normal (in which case $\cos (\varphi_{II_p}^{(v)} - \varphi_{II_0}) = 0$) do not affect the propagation of the signal wave, as one might expect for the homogeneous medium. Since v_p is proportional to the pump wave amplitude (except when $\varphi_{II_p}^{(v)} = \varphi_{II_0}$)

and η is proportional to its square (for an electromagnetic pumpwaves in an isotropic medium), the electron velocity component normally would be the most active one in generating the sum- and difference frequency waves in an isotropic medium (see also paragraph 4).

3. Generation of Natural Sum and Difference Frequency Waves in a Slowly Inhomogeneous Medium

We have seen in the preceding paragraph how the boundary conditions at $z = z_0$ determine the possible parametric travelling wave resonances and the amplitudes of the sum and difference frequency waves. Naturally, one would like to know what happens in an inhomogeneous medium, if resonances occur at some specified level, $z = z_0$.

Let us therefore consider an inhomogeneous medium, but a slowly varying one, so that partial reflections of the signal and pump waves can be neglected. Furthermore, we limit ourselves, for the sake of simplicity, to an analysis of the difference frequency wave. Since the medium is slowly varying (in the z-direction) the signal wave assumes the form $\exp\{j(\omega_s t - k_{s_x} x - \int^z k_{s_z} dz)\}$, and similarly, the pumpwave can be written $\cos(\omega_p t - k_{p_x} x - \int^z k_{p_z} dz)$. The natural difference frequency waves are written

$$\Pi^{(2)}_{(1)} = e^{j(\omega_{-1}t - k_{-1_x}x \mp \int^{z} k_{-1_z}\,dz)}. \tag{3.1}$$

By (2.2) we now obtain for the difference frequency wave

$$\psi^{-} = \alpha\{\Pi^{(2)} \int_{z_1}^{z} \Pi^{(1)}\,\xi\,dz - \Pi^{(1)} \int_{z_3}^{z} \Pi^{(2)}\,\xi\,dz\}, \tag{3.2}$$

since

$$k_{-1_x} = k_{s_x} - k_{p_x},$$

$$\xi = \frac{\eta}{2}\,\frac{\omega_0^2}{c_0^2}\,e^{j(\omega_{-1}t - \int^{z} k_{s_z}\,dz + \int^{z} k_{p_z}\,dz)}, \tag{3.3}$$

and

$$\alpha = e^{j2\omega_{-1}t}\,\frac{\Pi^{(1)}}{\Pi^{(2)}} \int^{z} \frac{dz}{(\Pi^{(1)})^2}. \tag{3.4}$$

For a slowly varying medium, $\alpha \cong \frac{1}{2jk_{-1_z}}$, and therefore by (2.2a)

$$E_{y_-} \cong E_{y_0}\,e^{j\{\omega_{-1}t - k_{-1_x}(x - x_a)\}}\,\frac{\omega_-}{\omega_0}\,\frac{1}{2jk_{-1_z}}\,\frac{\eta}{2}\,\frac{\omega_0^2}{c_0^2} \cdot$$

$$\cdot \left\{ e^{+j\int_{z_a}^{z} k_{-1_z}\,dz} \int_{z_1}^{z} e^{-j\int_{z_a}^{z} (k_{s_z} - k_{p_z} + k_{-1_z})\,dz} - \right.$$

$$\left. - e^{-j\int_{z_a}^{z} k_{-1_z}\,dz} \int_{z_3}^{z} e^{-j\int_{z_a}^{z} (k_{s_z} - k_{p_z} - k_{-1_z})\,dz} \right\}. \tag{3.5}$$

One notices that the two coupling integrals may "generate" natural difference frequency waves at or near their respective travelling wave resonance levels, compare (2.7),

$$k_{-1_z} = -(k_{s_z} - k_{p_z}) \tag{3.6}$$

and

$$k_{-1_x} = k_{s_x} - k_{p_x} . \tag{3.7}$$

If, for example, $k_{p_z} < k_{s_z}$ and $\omega_p > \omega_s$, these resonances actually yield forward, natural difference frequency waves, and backward (i.e., "reflected" from the resonance region) waves if $k_{p_z} > k_{s_z}$.

If we assume that (3.6) holds at some specified level $z = z_0$, we can write as follows for the slowly varying medium:

$$\int_{z_0}^{z} (k_{s_z} - k_{p_z} + k_{-1_z})dz = \mathcal{H}(z - z_0)^2/2 = W^2, \tag{3.8}$$

where

$$\mathcal{H} = \left\{\frac{d}{dz}(k_{s_z} - k_{p_z} + k_{-1_z})\right\}_{z = z_0} . \tag{3.9}$$

Since we only need to know the electric field of the emerging natural, difference frequency wave (i.e., radiated from the interaction region), we can limit ourselves to such z-regions, or $|z - z_0|$ distances, for which $W^2 \gg 1$. If we make use of the asymptotic form of the Fresnel integral and assume that the condition for forward radiation is satisfied, relation (3.5) yields the following difference fields, viz.,

$$\underline{z < z_0, \quad W^2 \gg 1}$$

$$E_y^- = E_{y_0} e^{j\{\omega_{-1} t - k_{-1_x}(x - x_a) - \int_{z_a}^{z} (k_{s_z} - k_{p_z}) dz\}} \frac{\omega_{-1}}{\omega_s} \alpha_{0_{-1}}, \tag{3.10}$$

$$\underline{z < z_0, \quad W^2 \gg 1}$$

$$E_y^- = E_{y_0} e^{j\{\omega_{-1} t - k_{-1_x}(x - x_a) - \int_{z_a}^{z_0} (k_{s_z} - k_{p_z}) dz\}} \frac{\omega_{-1}}{\omega_s} \left\{ \alpha_{0_{-1}} - \right.$$

$$\left. - \frac{1}{2k_{-1_z}} \frac{\eta}{2} \frac{\omega_0^2}{c_0^2} \sqrt{\frac{\pi}{2\mathcal{H}}} e^{+j\left(\int_{z_0}^{z} k_{-1_z} dz + \pi/4\right)} \right\}. \tag{3.11}$$

Relation (3. 10) is as the difference frequency part of (2. 3). This wave, which alone does not satisfy the wave equation, is associated with the signal wave and can be considered as a "modulation" or side-band of the same. Its resonance is independent of the sign of $k_{s_z} - k_{p_z}$, as it shall be.

It appears from (3. 10) that $\sqrt{\frac{2\pi}{\mathcal{H}}}$ is a measure of the difference frequency radiation efficiency of the interaction region. If $\mathcal{H}$ is small, i. e., if the medium parameters vary very slowly, the radiation is large, provided the region is so extended that W^2 is large at its outer edges.

If we next consider the second resonance (3. 7), which takes place at the same frequencies as the former one, (3. 6), one finds that (3. 5) yields the same result as (3. 9) and (3. 10). The difference

between the two resonances thus is purely formal. This agrees with the results found in paragraph 2 for the discontinuous boundary case.

If $k_{p_z} \lesseqgtr k_{s_z}$, and $\omega_p \gtreqless \omega_s$, we obtain a "reflected" natural difference frequency wave, i. e., when the associated difference frequency wave (non-linear driving force) travels in a negative z-direction. When the opposite conditions hold, we get a forward difference frequency wave. Since the natural sum frequency waves radiate in the running direction of the associated sum frequency wave, a "reflected" sum frequency wave can be obtained only if the pumpwave runs in a negative direction with $-k_{p_z} > k_{s_z}$. This is in contrast to the case of the discontinuous boundary (paragraph 2) which always yields "reflected" sum and difference frequency waves.

The amplitude of the difference frequency reflection coefficient now can be written

$$|R_{0,-1}| = \frac{\omega_{-1}}{\omega_s} \frac{\eta}{2} \frac{\omega_0^2}{c_0^2} \frac{1}{2|k_{-1_z}|} \sqrt{\frac{2\pi}{|\mathcal{H}|}} , \qquad (3.12)$$

which corresponds to $|T_{s,0}\, R_{0,-1}|$ of (2.13).

The frequency dependent phase of the frequency shifted "echo" is

$$\phi_{0,-1} = \int_{z_a}^{z_0} (\underbrace{k_{s_z} - k_{p_z} - k_{-1_z}}_{\approx 2(k_{s_z} - k_{p_z})}) \, dz \qquad (\omega_p > \omega_s) . \qquad (3.13)$$

Since z_0 depends upon ω_s (as well as ω_p), the echo delay, τ, counted at the level z_a for a pulsed signal wave (φ_{I_s} and φ_{I_p} assumed to be zero) becomes

$$\tau = \frac{\partial \phi_{0,-1}}{\partial \omega_s} \cong \left\{ z_0 - z_a + \left(\frac{2k_{-1_z}}{\mathcal{H}} \right)_{z_0} \right\} \left(\frac{1}{v_{g_s}} + \frac{1}{v_{g_-}} \right), \qquad (3.14)$$

where v_{g_s} and v_{g_-} are the group velocities of the signal wave and the natural difference frequency wave. For a forward wave, emerging at $z = z_b$ ($>z_0$), one similarly obtains

$$\tau \cong (z_0 - z_a) \frac{1}{v_{g_s}} + (z_b - z_0) \frac{1}{v_{g_-}} + \left(\frac{2k_{-1_z}}{\mathcal{H}} \right)_{z_0} \left(\frac{1}{v_{g_s}} - \frac{1}{v_{g_-}} \right). \qquad (3.14a)$$

We thus get a change in effective reflection height of $(k_{p_z} / \mathcal{H})_{z_0}$ which may be a large quantity. It is a measure of the "frequency shift reflection thickness" of the interaction region. As the dispersion is very large, it is not sufficient to make use of the first phase-frequency derivative only to determine the time of arrival of the frequency shifted wave. Such a discussion lies outside the scope of the present communication.

Since

$$\left(k_{-1_z} \right)_{z_0} = - \left(k_{s_z} - k_{p_z} \right)_{z_0},$$

and

$$k_{-1_x} = k_{s_x} = k_{p_x},$$

one can sketch the frequency shifted wave normal paths about as shown in figure 3.

4. Electromagnetic Wave Reflection from the Oscillating Magneto-ionic Medium

Let us assume that the static magnetic field lies in the x-z plane, that its electronic angular gyrofrequency is ω_H with components $\omega_L = \omega_H \cos\theta$, $\omega_T = \omega_H \sin\theta$, along the z and x axes, respectively.

If we introduce the following operators, viz.

$$\wp_e^2 = -\frac{1}{\mu_0 \epsilon_0}\frac{\partial^2}{\partial z^2} + \frac{\partial^2}{\partial t^2}; \quad \wp_{em}^2 = \wp_e^2 + \omega_0^2; \quad \text{and} \quad \wp_p^2 = \frac{\partial^2}{\partial t^2} + \omega_0^2, \tag{4.1}$$

and limit ourselves to the case $\varphi_{I_s} = 0 = \varphi_{I_p}$ (i.e., vertical incidence) we obtain the following non-linear wave equations for the (second order) electron velocities, $v_y^{(2)}$, $v_x^{(2)}$, $v_z^{(2)}$, [Rydbeck, 1962],

$$D v_y^{(2)} = \wp_p^2 \left(\omega_L \wp_e^2 \psi_x + \wp_{em}^2 \frac{\partial \psi_y}{\partial t}\right) - \omega_T \wp_{em}^2 \wp_e^2 \psi_z = \Pi_y, \tag{4.2}$$

$$D v_x^{(2)} = \wp_p^2 \left(\omega_L \wp_e^2 S_1^{(2)} \psi_x + \wp_{em}^2 S_2^{(2)} \frac{\partial \psi_y}{\partial t}\right) - \omega_T \wp_{em}^2 \wp_e^2 S_2^{(2)} \psi_z = \Pi_x, \tag{4.3}$$

$$D \frac{\partial v_z^{(2)}}{\partial t} = \omega_T \left(\omega_L \wp_e^2 \frac{\partial^2 \psi_x}{\partial t^2} + \wp_{em}^2 \frac{\partial^3 \psi_y}{\partial t^3}\right) + \underbrace{\left(\wp_{em}^4 \frac{\partial^2}{\partial t^2} + \omega_L^2 \wp_e^4\right)}_{a} \psi_z = \Pi_z, \tag{4.4}$$

where Π_y, Π_x, Π_z are non-linear driving terms to be specified later. It is worth noting that $\underline{a}$ annihilates longitudinal magneto-ionic modes. Furthermore

$$D = \wp_{em}^2 \left(\wp_{em}^2 \wp_p^2 + \omega_T^2 \wp_e^2\right) \frac{\partial^2}{\partial t^2} + \omega_L^2 \wp_p^2 \wp_e^4. \tag{4.5}$$

By (4. 5) relation (4. 4) can be given in the alternate form

$$\rho_p^2 \frac{\partial v_z^{(2)}}{\partial t} = \omega_T \frac{\partial^2 v_y^{(2)}}{\partial t^2} + \psi_z . \tag{4.6}$$

The second order polarizations, $S_1^{(2)}$ and $S_2^{(2)}$, are related to each other as follows

$$S_1^{(2)} = \frac{(\rho_p^2 \rho_{em}^2 + \omega_T^2 \rho_e^2)\, \partial/\partial t}{\omega_L \rho_p^2 \rho_e^2} ; \quad S_2^{(2)} = -\frac{\omega_L \rho_e^2}{\rho_{em}^2 \partial/\partial t} ;$$

$$S_1^{(2)} = S_2^{(2)} \left(1 - \frac{D}{\omega_L^2 \rho_p^2 \rho_e^4}\right) . \tag{4.7}$$

Relation (4. 3) can now be transformed to

$$v_x^{(2)} = S_2^{(2)} v_y^{(2)} + \frac{\psi_x}{\rho_{em}^2 \partial/\partial t} = S_2^{(2)} \left(v_y^{(2)} - \frac{\psi_x}{\omega_L \rho_e^2}\right) . \tag{4.8}$$

Thus $S_1^{(2)} = S_2^{(2)}$, when $D = 0$, i. e., when one has a system (travelling wave) resonance. When this is the case $v_x^{(2)} = S_2^{(2)} v_y^{(2)}$.

Now D can be written

$$\rho_p^2 D = \rho_p^2 \underbrace{\left\{\left[\rho_e^2 \left(1 + \frac{\omega_T^2/2}{\rho_p^2}\right) + \omega_0^2\right] \frac{\partial}{\partial t} - \rho_e^2 \sqrt{\left(\frac{\omega_T^2/2}{\rho_p^2}\right)^2 \frac{\partial^2}{\partial t^2} - \omega_L^2}\right\}}_{D_o} \cdot$$

$$\cdot \underbrace{\rho_p^2 \left\{\left[\rho_e^2 \left(1 + \frac{\omega_T^2/2}{\rho_p^2}\right) + \omega_0^2\right] \frac{\partial}{\partial t} + \rho_e^2 \sqrt{\left(\frac{\omega_T^2/2}{\rho_p^2}\right)^2 \frac{\partial^2}{\partial t^2} - \omega_L^2}\right\}}_{D_x} . \tag{4.9}$$

The term D_o annihilates the natural ordinary magneto-ionic mode and the plasma oscillation (for which $\wp_p^2 = 0$), whereas D_x annihilates the natural extra-ordinary mode only. D can be used to study the transient behavior of the magneto-ionic medium.

By (4.9) one can also write

$$D = \left\{ \underbrace{(\omega^2 - \omega_0^2)(\omega^2 - \omega_H^2) - \omega_0^2 \omega_T^2}_{b} \right\} c_0^4 \left\{ \frac{\partial^2}{\partial z^2} + k_o^2(\omega) \right\} \left\{ \frac{\partial^2}{\partial z^2} + k_x^2(\omega) \right\}, \tag{4.10}$$

where

$$k_o(\omega) = \frac{\omega}{c_0} n_o(\omega); \quad \text{and} \quad k_x(\omega) = \frac{\omega}{c_0} n_x(\omega), \tag{4.11}$$

and n_o and n_x denote ordinary and extraordinary refractive indices, respectively. One notices that $b = 0$ at the fourth reflection level (referred to the angular frequency) at which $|n_x|^2 = \infty$. In the neighborhood of this level, D is conveniently written

$$D = -\wp_e^4 \wp_p^2 X_d \omega_0^2 \left(\frac{1}{1 - n_o^2} - \frac{1}{1 - n_d^2} \right) \left(\frac{1}{1 - n_x^2} - \frac{1}{1 - n_d^2} \right), \quad (X_d = \omega_0^2 / \omega_d^2), \tag{4.12}$$

where n_d is the effective refractive index of the wave, of angular frequency ω_d, upon which D operates.

Next, let us introduce the driving force polarization ratio'

$$S_d = j Q_d = j \frac{\omega_L}{\omega_d} \frac{1 - n_d^2}{1 - X_d - n_d^2}. \tag{4.13}$$

Relation (4. 2) now yields

$$\Pi_y = \omega_d^5 (1 - X_d)\ (1 - X_d - n_d^2) \{ Q_d \psi_x + j \psi_y + Y_{T_d} (1 - n_d^2) \psi_z \}$$

$$(Y_{T_d} = \omega_T / \omega_d). \quad (4.14)$$

If the pump (high power) wave has the v_y velocity

$$v_{p_y} = v_p \cos (\omega_p t - k_p z); \qquad (k_p = \omega_p\ n_p / c_0) \quad (4.15)$$

where, quite arbitrarily, k_p could refer to an ordinary or extra-ordinary pumpwave, the other pumpwave velocities become

$$v_{p_x} = - Q_p v_p \sin (\omega_p t - k_p z); \quad v_{p_z} = \frac{Y_{T_p}}{1 - X_p} \sin (\omega_p t - k_p z),$$

$$(X_p = \omega_0^2 / \omega_p^2) \quad (4.16)$$

with

$$Q_p = Y_{L_p} \frac{1 - n_p^2}{1 - X_p - n_p^2} \qquad (Y_{L_p} = \omega_L / \omega_p). \quad (4.17)$$

The differential space charge density becomes

$$\rho_p = \rho_0 \frac{n_p}{c_0} \frac{Y_{T_p}}{1 - X_p} v_p \sin (\omega_p t - k_p z) \qquad (\rho_0 = - e N_0). \quad (4.18)$$

The signal wave, of angular frequency ω_s, is written:

$$v_{s_y} = v_s e^{j(\omega_s t - k_s z)}; \quad v_{s_x} = - Q_s \frac{v_s}{j} e^{j(\omega_s t - k_s z)};$$

$$v_{s_z} = \frac{Y_{T_s}}{1 - X_s} \frac{v_s}{j} e^{j(\omega_s t - k_s z)}, \quad \rho_s = \rho_0 \frac{n_s}{c_0} \frac{Y_{T_s}}{1 - X_s} \frac{v_s}{j} e^{j(\omega_s t - k_s z)}$$

$$(k_s = \omega_s n_s / c_0; \quad X_s = \omega_0^2 / \omega_s^2; \quad Y_{T_s} = \omega_T / \omega_s). \quad (4.19)$$

where

$$Q_s = Y_{L_s} \frac{1 - n_s^2}{1 - X_s - n_s^2} \qquad (Y_{L_s} = \omega_L / \omega_s) \ . \tag{4.20}$$

The terms ψ_x, ψ_y, and ψ_z can be written [Rydbeck, 1962]:

$$\psi_x = \rho_e^2 P_x - \omega_0^2 \frac{\partial W_x}{\partial t}; \quad \psi_y = \rho_e^2 P_y - \omega_0^2 \frac{\partial W_y}{\partial t}; \quad \psi_z = \frac{\partial^2}{\partial t^2} P_z - \omega_0^2 \frac{\partial W_z}{\partial t}. \tag{4.21}$$

If we limit ourselves to a study of the sum and difference frequency terms only, we find that

$$P_x = P_{x_{sd}} = - v_{p_z} \frac{\partial v_{s_x}}{\partial z} \left(1 - \frac{X_s}{1 - n_s^2}\right) - v_{s_z} \frac{\partial v_{p_x}}{\partial z} \left(1 - \frac{X_p}{1 - n_p^2}\right), \tag{4.22}$$

$$P_y = P_{y_{sd}} = - v_{p_z} \frac{\partial v_{s_y}}{\partial z} \left(1 - \frac{X_s}{1 - n_s^2}\right) - v_{s_z} \frac{\partial v_{p_y}}{\partial z} \left(1 - \frac{X_p}{1 - n_p^2}\right), \tag{4.23}$$

$$P_z = P_{z_{sd}} = - \frac{\partial}{\partial z} (v_{z_s} v_{z_p}) - \frac{X_s}{1 - n_s^2} \left(\frac{\partial v_{s_y}}{\partial z} v_{p_y} + \frac{\partial v_{s_x}}{\partial z} v_{p_x}\right) -$$

$$- \frac{X_p}{1 - n_p^2} \left(\frac{\partial v_{p_y}}{\partial z} v_{s_y} + \frac{\partial v_{p_x}}{\partial z} v_{s_x}\right), \tag{4.24}$$

and

$$\overline{W} = \frac{1}{\rho_0} (\rho_s \overline{v}_p + \rho_p \overline{v}_s). \tag{4.25}$$

We evaluate next P_x, P_y, P_z, and $\overline{W}$ from these relations and obtain for the sum and difference terms (index + and − , respectively)

$$\psi_x^{\pm} = \mp j \frac{v_s v_p}{2} \omega_{\pm}^2 \left[(1 - n_{\pm}^2) \left\{ \alpha_s k_p Q_p \left(1 - \frac{X_p}{1 - n_p^2} \right) + \alpha_p k_s Q_s \left(1 - \frac{X_s}{1 - n_s^2} \right) \right\} + \right.$$

$$\left. + X_{\pm} \frac{\omega_{\pm}}{c_0} (\alpha_s n_s Q_p + \alpha_p n_p Q_s) \right] e^{j(\omega_{\pm} t - k_{\pm} z)}, \quad (4.26)$$

$$\psi_y^{\pm} = - \frac{v_s v_p}{2} \omega_{\pm}^2 \left[(1 - n_{\pm}^2) \left\{ \alpha_s k_p \left(1 - \frac{X_p}{1 - n_p^2} \right) \pm \alpha_p k_s \left(1 - \frac{X_s}{1 - n_s^2} \right) \right\} + \right.$$

$$\left. + X_{\pm} \frac{\omega_{\pm}}{c_0} (\alpha_s n_s \pm \alpha_p n_p) \right] e^{j(\omega_{\pm} t - k_{\pm} z)}, \quad (4.27)$$

$$\psi_z^{\pm} = j \frac{v_s v_p}{2} \omega_{\pm}^2 \left[\pm \alpha_s \alpha_p \{ k_{\pm} + X_{\pm} \frac{\omega_{\pm}}{c_0} (n_s + n_p) \} - \right.$$

$$\left. - \left(\frac{X_s}{1 - n_s^2} + \frac{X_p}{1 - n_p^2} \right) (1 \mp Q_s Q_p) \right] e^{j(\omega_{\pm} t - k_{\pm} z)}, \quad (4.28)$$

where

$$k_{\pm} = k_s \pm k_p; \quad X_{\pm} = \omega_0^2 / \omega_{\pm}^2; \quad \alpha_s = Y_{T_s} / (1 - X_s); \text{ and } \alpha_p = Y_{T_p} / (1 - X_p). \quad (4.29)$$

We now write (4.14) as follows:

$$\Pi_y^{\pm} = \omega_{\pm}^5 (1 - X_{\pm}) (1 - X_{\pm} - n_{\pm}^2) \left\{ \underbrace{Q_{\pm} \psi_x^{\pm} + j \psi_y^{\pm} + Y_{T_{\pm}} (1 - n_{\pm}^2) \psi_z^{\pm}}_{- j \frac{v_s v_p}{2} \xi^{\pm}} \right\}, \quad (4.30)$$

where

$$Q_{\pm} = Q_d \quad (\omega_d = \omega_{\pm}), \quad (4.31)$$

and by (4.26), (4.27), and (4.28) obtain

*Note: In what follows $\omega_{\pm}$ denotes $\omega_{\pm 1}$, etc.

$$\xi^{\pm} = \omega_{\pm}^2 \left[(1 - n_{\pm}^2) \left\{ \alpha_s k_p \left(1 - \frac{X_p}{1 - n_p^2} \right) (1 \pm Q_{\pm} Q_p) \pm \right. \right.$$

$$\pm \alpha_p k_s \left(1 - \frac{X_s}{1 - n_s^2} \right) (1 \pm Q_{\pm} Q_s) + Y_{T_{\pm}} \left[\pm \alpha_s \alpha_p \{ k_{\pm} + X_{\pm} \frac{\omega_{\pm}}{c_0} (n_s + n_p) \} - \right.$$

$$\left. \left. - \left(\frac{X_s k_s}{1 - n_s^2} + \frac{X_p k_p}{1 - n_p^2} \right) (1 \mp Q_s Q_p) \right] \right\} + X_{\pm} \frac{\omega_{\pm}}{c_0} \{ \alpha_s n_s (1 \pm Q_{\pm} Q_p) \pm$$

$$\left. \pm \alpha_p n_p (1 + Q_{\pm} Q_p) \} \right]_p e^{j(\omega_{\pm} t - k_{\pm} z)} . \qquad (4.32)$$

First we notice that $\xi^{\pm} = 0$, if $\omega_T = 0$. This is due to the fact that the differential space charges and the longitudinal velocities (which form longitudinal plasma wave pairs coupled to the transverse wave by ω_T) are zero in this case. Had we considered second order terms in the pumpwave field (which could easily have been done) this would not have been so. The transverse magnetic field thus is a very important factor in the non-linear interaction theory.

When $X_s \to 1$, or $X_p \to 1$, we have longitudinal driving force plasma resonance and $|\xi^{\pm}| \to \infty$ (in the collision-less case). In this connection it is worth noting that

$$\left. \begin{aligned} \frac{X}{1 - n_x^2} &\to - \frac{Y_T^2}{1 - X} + 1 - \frac{Y_L^2}{Y_T^2} (1 - X), \\ \frac{X}{1 - n_o^2} &\to 1 + \frac{Y_L^2}{Y_T^2} (1 - X), \end{aligned} \right\} \quad \text{if } X \to 1 \ (Y_T^2 \gg |2(1-X) Y_L|) .$$

If these driving force resonances occur in the travelling wave resonance region, the generation of sum and difference frequency wave may be

greatly enhanced. Even if there is no resonance of the latter kind, sudden driving force resonances may cause appreciable sum and difference frequency radiation.

Another level of considerable interest is the fourth reflection one, where $|n_s|$ or $|n_p| \to \infty$. At this level, determined by $b = 0$ (which indicates that it is gyro-plasma oscillation resonance coupling), all electron velocities (and the differential space charge density) become very large. This is in contrast to the plasma resonance level, where only the longitudinal velocity becomes large (and $\rho_{s,p}$ if $n_{s,p} = n_x$).

In ionospheric applications, this important resonance level is difficult to reach, except from a topside sounder. Moreover, travelling wave resonances, which are necessary, since D otherwise would grow to large values (see (4. 10)), might be critical to obtain at this level in practice. (b would have to be zero both for $\omega_\pm$ and for ω_s or ω_p.)

Before we continue the discussion, let us express the velocities in the corresponding E_y-fields. One has

$$v_s = \frac{1 - n_s^2}{X_s} \frac{e}{m\omega_s} E^0_{s_y}, \quad \text{and} \quad v_p = \frac{1 - n_p^2}{X_p} \frac{e}{m\omega_p} E^0_{p_y}, \qquad (4.33)$$

one finds that

$$E_y^{\pm} = -j \frac{m\omega_{\pm}}{e} \frac{X_{\pm}}{1 - n_{\pm}^2} \left\{ -j \frac{v_s v_p}{2} (n_s \alpha_s \pm \right.$$

$$\left. \pm n_p \alpha_p) \frac{1}{c_0} e^{j(\omega_{\pm} t - k_{\pm} z)} + v_y^{(2)} \right\}, \qquad (4.34)$$

$$E_x^{\pm} = -j \frac{m\omega_{\pm}}{e} \frac{X_{\pm}}{1 - n_{\pm}^2} \left\{ \pm \frac{v_s v_p}{2} (n_s \alpha_s Q_p + \right.$$

$$\left. + n_p \alpha_p Q_s) \frac{1}{c_0} e^{j(\omega_{\pm} t - k_{\pm} z)} + v_x^{(2)} \right\}. \qquad (4.35)$$

We now obtain the final formulas,

$$E_y^{\pm} = - \frac{E_{s_y}^0 E_{p_y}^0}{2} \frac{\tau_{\pm}}{\tau_s \tau_p} \left\{ \omega_{\pm}^5 (1 - X_{\pm}) (1 - X_{\pm} - n_{\pm}^2) \xi^{\pm} / D^{\pm} - \right.$$

$$\left. + \frac{n_s \alpha_s \pm n_p \alpha_p}{c_0} e^{j(\omega_{\pm} t - k_{\pm} z)} \right\}, \qquad (4.36)$$

$$E_x^{\pm} = - \frac{E_{s_y}^0 E_{p_y}^0}{2} \frac{\tau_{\pm}}{\tau_s \tau_p} \left\{ j Q_{\pm} \omega_{\pm}^5 (1 - X_{\pm}) (1 - X_{\pm} - n_{\pm}^2) \xi^{\pm} / D^{\pm} \pm \right.$$

$$\left. \pm j \frac{n_s \alpha_s Q_p + n_p \alpha_p Q_p}{c_0} e^{j(\omega_{\pm} t - k_{\pm} z)} \right\} + \tau_{\pm} \frac{\psi_x}{\omega_{\pm}^3 (1 - X_{\pm} - n_{\pm}^2)}, \qquad (4.37)$$

where

$$\tau_p = \frac{X_p}{1 - n_p^2} \frac{m\omega_p}{e}, \quad \text{etc.}$$

In order to study the stationary solutions, we present D (4.10) in an alternate form, viz.,

$$D^{\pm} = X_{\pm}^2 (1 - X_{\pm}) \frac{(n_{\pm}^2 - n_{o_{\pm}}^2)(n_{\pm}^2 - n_{x_{\pm}}^2)}{(1 - n_{o_{\pm}}^2)(1 - n_{x_{\pm}}^2)}, \qquad (4.38)$$

where

$$n_{\pm} = k_{\pm} / \omega_{\pm} \tag{4.39}$$

Since we want to study what happens at or near the travelling wave resonances ($D^{\pm} = 0$), especially to obtain the amplitudes of the natural sum and difference frequency waves, we neglect (in this particular case) the insignificant last terms in (4.36) and (4.37). By (4.38) we can write

$$E_y^{\pm} = -\frac{E_{s_y}^0 E_{p_y}^0}{2} \frac{e}{m\omega_0} \frac{\omega_p \omega_s}{\omega_0^5} \frac{(1 - n_p^2)(1 - n_s^2)}{1 - n_{\pm}^2} (1 - X_{\pm} - n_{\pm}^2) \cdot$$

$$\cdot \frac{(1 - n_{o_{\pm}}^2)(1 - n_{x_{\pm}}^2)}{(n_{\pm}^2 - n_{o_{\pm}}^2)(n_{\pm}^2 - n_{x_{\pm}}^2)} \cdot \xi^{\pm}, \tag{4.40}$$

$$E_x^{\pm} = j\, Q^{\pm} E_y^{\pm} . \tag{4.40a}$$

Next, let us, in analogy with paragraph 2, determine the natural waves that leave or approach the boundary $z = 0$ between the ionized medium (medium II) and vacuum (medium I).

We have the following sum and difference frequency waves to consider:

Medium II

$$\left.\begin{aligned} E_x &= E_x^{\pm} + T_{0,\pm 1}^{(o)} e^{j(\omega_{\pm} t - k_{o_{\pm}} z)} + T_{0,\pm 1}^{(x)} e^{j(\omega_{\pm} t - k_{x_{\pm}} z)}, \\ E_y &= E_y^{\pm} + \frac{1}{jQ_{o_{\pm}}} T_{0,\pm 1}^{(o)} e^{j(\omega_{\pm} t - k_{o_{\pm}} z)} + \frac{1}{jQ_{x_{\pm}}} T_{0,\pm 1}^{(x)} e^{j(\omega_{\pm} t - k_{x_{\pm}} z)}, \end{aligned}\right\} \tag{4.41}$$

where $j Q_{o_\pm}$ and $j Q_{x_\pm}$ are sum and difference frequency polarization ratios of the natural sum and difference frequency waves.

Medium I

$$\left.\begin{aligned} E_x &= R^{(1)}_{0,\pm 1}\, e^{j(\omega_\pm t + \omega_\pm z/c_0)}, \\ E_y &= R^{(2)}_{0,\pm 1}\, e^{j(\omega_\pm t + \omega_\pm z/c_0)}, \end{aligned}\right\} \tag{4.42}$$

If we break up the associated wave, $E^{\pm}_y$, in two components, $\alpha_\pm$ and $\beta_\pm$, with the (natural) polarization ratios $Q_{o_\pm}$ and $Q_{x_\pm}$, we obtain

$$\left.\begin{aligned} \alpha_\pm &= -\frac{Q_\pm / Q_{x_\pm} - 1}{Q^2_{o_\pm} + 1}, \\ \beta_\pm &= -Q^2_{o_\pm}\,\frac{Q_\pm / Q_{o_\pm} - 1}{Q^2_{o_\pm} + 1}. \end{aligned}\right\} \tag{4.43}$$

The boundary conditions now yield

$$T^{(o)}_{0,\pm 1} = \alpha_\pm j Q_{o_\pm}\,\frac{1 - n_\pm}{1 - n_{o_\pm}}; \qquad T^{(x)}_{0,\pm 1} = -\beta_\pm j Q_{x_\pm}\,\frac{1 - n_\pm}{1 - n_{x_\pm}}, \tag{4.44}$$

$$\left.\begin{aligned} R^{(1)}_{0,\pm 1} &= \alpha_\pm j Q_{o_\pm}\,\frac{n_\pm - n_{o_\pm}}{1 - n_{o_\pm}} + \beta_\pm j Q_{x_\pm}\,\frac{n_\pm - n_{x_\pm}}{1 - n_{x_\pm}}, \\ R^{(2)}_{0,\pm 1} &= \alpha_\pm\,\frac{n_\pm - n_{o_\pm}}{1 - n_{o_\pm}} + \beta_\pm\,\frac{n_\pm - n_{x_\pm}}{1 - n_{x_\pm}}. \end{aligned}\right\} \tag{4.45}$$

The "reflected" field, i.e., the wave leaving the boundary ($z = 0$) in medium I, thus is composed of two parts, with polarizations $Q_{o_\pm}$ and $Q_{x_\pm}$, respectively. Since the energy flow in the z-direction is

$$P_q^{(z)} = n_q (Q_q^2 + 1) |E_y^0|^2 / Z_0 ,$$

the energy balance at the boundary requires that

$$\left.\begin{array}{l} \text{Sign } (n_{o_\pm}) = \\ \\ \text{Sign } (n_{x_\pm}) = \end{array}\right\} - \text{Sign} \frac{\omega_s n_s \pm \omega_p n_p}{\omega_s \pm \omega_p} . \qquad (4.46)$$

For sum frequency waves $n_{o_\pm}$ and $n_{x_\pm}$ are thus always negative (if we assume n_p to be positive, i.e., a pumpwave incident upon the boundary in medium I). The natural sum frequency modes travel always toward the boundary in medium II. When $\omega_p < \omega_s$, the natural difference frequency modes travel towards the boundary, if $k_p < k_s$, and away from it, when $k_p > k_s$. When $\omega_p > \omega_s$ the situation is reversed.

If we make use of the fact that

$$\frac{Q_\pm}{Q_{o_\pm}} - 1 = \frac{X_\pm}{1 - X_\pm - n_\pm^2} \frac{n_\pm^2 - n_{x_\pm}^2}{1 - n_{x_\pm}^2} , \qquad (4.47)$$

and

$$\frac{Q_\pm}{Q_{x_\pm}} - 1 = \frac{X_\pm}{1 - X_\pm - n_\pm^2} \frac{n_\pm^2 - n_{o_\pm}^2}{1 - n_{o_\pm}^2} , \qquad (4.48)$$

the "reflected", frequency shifted field in medium I can finally be written:

$$E_y = \frac{E_{s_y}^0 E_{p_y}^0}{2} \frac{e}{m\omega_\pm} \frac{\omega_p \omega_s}{\omega_0^4 \omega_\pm} \frac{(1-n_p^2)(1-n_s^2)}{1-n_\pm^2} \left\{ \frac{1}{Q_{o_\pm}^2+1} \frac{1+n_{o_\pm}}{n_\pm + n_{o_\pm}} + \right.$$

$$\left. + \frac{1}{Q_{x_\pm}^2+1} \frac{1+n_{x_\pm}}{n_\pm + n_{o_\pm}} \right\} \xi^\pm e^{j\omega_\pm (1+n_\pm) z/c_0}, \qquad (4.49)$$

$$E_y = \frac{E_{s_y}^0 E_{p_y}^0}{2} \frac{e}{m\omega_\pm} \frac{\omega_p \omega_s}{\omega_0^4 \omega_\pm} \frac{(1-n_p^2)(1-n_s^2)}{1-n_\pm^2} \left\{ \frac{jQ_{o_\pm}}{Q_{o_\pm}^2+1} \frac{1+n_{o_\pm}}{n_\pm + n_{o_\pm}} + \right.$$

$$\left. + \frac{jQ_{x_\pm}}{Q_{x_\pm}^2+1} \frac{1+n_{x_\pm}}{n_\pm + n_{x_\pm}} \right\} \xi^\pm e^{j\omega_\pm (1+n_\pm) z/c_0}, \qquad (4.50)$$

where it is to be remembered that $Q_{o_\pm} Q_{x_\pm} = -1$.

We notice from (4.49) and (4.50) that only two resonances remain (compare the similar situation in paragraph 2), viz.,

$$\begin{aligned} n_{o_\pm} = -n_\pm \quad \text{and} \quad n_{x_\pm} = -n_\pm, \quad \text{or} \\ -(\omega_0 \pm \omega_p) n_{o_\pm} = \omega_s n_s \pm \omega_p n_p, \\ -(\omega_0 \pm \omega_p) n_{x_\pm} = \omega_s n_s \pm \omega_p n_p. \end{aligned} \qquad (4.51)$$

It is also important to note that these resonances by (4.46) correspond to the correct signs for $n_{o_\pm}$ and $n_{x_\pm}$, and are thus physically possible, if $|n_{o_\pm}| = |(\omega_s n_s \pm \omega_p n_p)/(\omega_s \pm \omega_p)|$, or

if $|n_{x_\pm}| = |(\omega_s n_s \pm \omega_p n_p)/(\omega_s \pm \omega_p)|$.

The possibilities to obtain these resonances are considerable, since $n_{o_\pm}$, $n_{x_\pm}$, n_s and n_p may vary within wide limits in the magneto-ionic medium. The degenerate case $\omega_+ = 2\omega_s$, which is of particular interest if one wishes to study the possibilities of obtaining second harmonic radiation or second harmonic echoes ($E^0_{p_y} = E^0_{s_y}$ = amplitude of high power primary wave, $\omega_p = \omega_s$, etc.; $\xi^\pm$ assumes a simpler form), has been studied extensively by the author [Rydbeck, 1962].

The second degenerate case, $\omega_- = -\omega_s$ (which leads to the same resonance conditions, although ξ^- is different from ξ^+ of the previous case), is of particular interest, if one wishes to study the possibilities of degenerate parametric amplification in the magneto-ionic medium.

Finally, let us return to the influence of the resonances of the driving forces, a situation that is somewhat different when we discuss the magnitude of E_y instead of $v_y^{(2)}$.

1. Fourth reflection resonance. Assume that $|n_p| \to \infty$. We then find from (4.32) that

$$\xi^\pm \propto (1 - n_\pm^2)\, n_p ,$$

i.e.,

$$|E_y| \underset{\text{(medium I)}}{\propto} \left| n_p^3 \left\{ \frac{1 + n_{o_\pm}}{n_\pm + n_{o_\pm}} + \frac{1 + n_{x_\pm}}{n_\pm + n_{x_\pm}} \right\} \right| ,$$

which demonstrates that the influence of the driving force resonance is extremely strong. This appears to be the most interesting non-linear resonance in the magneto-ionic medium.

2. Plasma resonance.

$$X_p \to 1; \quad n_p^{(o)} \to 0, \quad n_p^{(x)} \to 1.$$

a. $n_p = n_p^{(x)}$. One finds that

$$|E_y| \underset{\text{(medium I)}}{\propto} \frac{1 - n_s^2}{1 - n_\pm^2} \left\{ \frac{1 + n_{o_\pm}}{n_\pm + n_{o_\pm}} + \frac{1 + n_{x_\pm}}{n_\pm + n_{x_\pm}} \right\},$$

In contrast to what might be expected, this driving force resonance produces no enhanced effects.

b. $n_p = n_p^{(o)}$. One now finds that

$$|E_y| \propto \frac{1 - n_s^2}{1 - n_\pm^2} \frac{1}{1 - X_p} \left\{ \frac{1 + n_{o_\pm}}{n_\pm + n_{o_\pm}} + \frac{1 + n_{x_\pm}}{n_\pm + n_{x_\pm}} \right\},$$

i. e., the effect of the driving force resonance is very profound. A more detailed study of sum and difference frequency generation caused by this resonance will appear in the final paragraph 6 of this communication.

* * *

A further analysis of the travelling wave resonances (4. 51), interesting as it may be, is outside the scope and aim of the present communication. That this interesting phenomena, applicable to topside sounder ionogram interpretations, can be found seems certain.

5. Generation of Natural Sum and Difference Frequency Waves in a Slowly Varying Magneto-ionic Medium

In order to analyze the resonance radiation of sum and difference frequency magneto-ionic modes, we make use of (4. 36), which by (4. 10) for our present purposes can be written

$$\left(\frac{d^2}{dz^2} + k_{o_\pm}^2\right)\left(\frac{d^2}{dz^2} + k_{x_\pm}^2\right) E_y^\pm \cong -\frac{1}{c_0^4 b_\pm} \frac{E_{s_y}^0 E_{p_y}^0}{2} \frac{\tau_\pm}{\tau_s \tau_p} \omega_\pm^5 (1 - X_\pm) \cdot$$

$$\cdot (1 - X_\pm - n_\pm^2)\, \xi^\pm = \psi^\pm e^{j(\omega_\pm t - \int_{z_a}^{z} (k_s \pm k_p)\, dz)}, \qquad (5.1)$$

For the slowly varying medium the solution to (5. 1) now can be written

$$E_y^\pm \approx -\frac{j}{2} \frac{\psi^\pm e^{+j\omega_\pm t}}{k_{o_\pm}^2 - k_{x_\pm}^2} \left\{ \frac{1}{k_{x_\pm}} \left(e^{+j\int_{z_a}^{z} k_{x_\pm} dz} \int_{z_1}^{z} e^{-j\int_{z_a}^{z} (k_s \pm k_p + k_{x_\pm}) dz} dz - \right.\right.$$

$$\left. - e^{-j\int_{z_a}^{z} k_{x_\pm} dz} \int_{z_2}^{z} e^{-j\int_{z_a}^{z} (k_s \pm k_p - k_{x_\pm})\, dz} dz \right) -$$

$$- \frac{1}{k_{o_\pm}} \left(e^{+j\int_{z_a}^{z} k_{o_\pm} dz} \int_{z_3}^{z} e^{-j\int_{z_a}^{z} (k_s \pm k_p + k_{o_\pm}) dz} dz - \right.$$

$$\left.\left. - e^{-j\int_{z_a}^{z} k_{o_\pm} dz} \int_{z_4}^{z} e^{-j\int_{z_a}^{z} (k_s \pm k_p - k_{o_\pm}) dz} dz \right) \right\}. \qquad (5.1a)$$

If we assume that resonance takes place at some specified level z_0, where, for example

$$k_{x_\pm} = -(k_s \pm k_p) \quad ,$$

and conditions are such (see paragraph 3) that a forward extra-ordinary magneto-ionic mode is generated, we obtain (for definition of W and $\mathcal{H}$ see paragraph 3)

$\underline{z < z_0}$ $\quad (W^2 \gg 1)$

$$E_y^{\pm} \approx \frac{\psi^{\pm} e^{j(\omega_\pm t - \int_{z_a}^{z} (k_s \pm k_p)\, dz)}}{\{k_{o_\pm}^2 - (k_s \pm k_p)\}\{k_{x_\pm}^2 - (k_s \pm k_p)^2\}} \quad , \tag{5.2}$$

$\underline{z > z_0}$ $\quad (W^2 \gg 1)$

$$E_y^{\pm} \approx \psi^{\pm} e^{j(\omega_\pm t - \int_{z_a}^{z_0} (k_s \pm k_p) dz)} \left[\frac{e^{-j \int_{z_0}^{z} (k_s \pm k_p)\, dz}}{\{k_{o_\pm}^2 - (k_s \pm k_p)^2\}\{k_{x_\pm}^2 - (k_s \pm k_p)^2\}} - \right.$$

$$\left. - \frac{e^{+j(\int_{z_0}^{z} k_{x_\pm} dz + \pi/4)}}{(k_{o_\pm}^2 - k_{x_\pm}^2) 2 k_{x_\pm}} \cdot \sqrt{\frac{\pi}{2\mathcal{H}}} \right] . \tag{5.3}$$

Although the amplitude coefficients are much more complicated than in the isotropic case, dealt within paragraph 3, the radiation feature is essentially the same. Furthermore, it should be pointed out (see (4.32) that the pumpwave, for example, does not have to be of extra-ordinary kind in order to generate an extra-ordinary

natural mode. This is a typical feature of the non-linear propagation theory.

In conclusion a few words should be said about the ray paths. Since we are dealing with an anisotropic medium these will deviate from the phase paths. In order to make the discussion more general, we assume arbitrary incidence and noting the direct similarity between the coupling integrals of (3.5) and (5.2), write the phase of the downcoming difference frequency wave as follows:

$$\phi^- = \int_{z_a}^{z_0} (k_{s_z} - k_{p_z} - k_{-z})\, dz + \frac{1}{c_0} (\omega_s \sin \varphi_{s_0} - \omega_p \sin \varphi_{p_0})(x_2 - x_1), \quad (5.4)$$

where x_1 and x_2 are the ray positions corresponding to z_a, i.e., x_2 for the downcoming difference frequency wave (note: $\varphi_{s_0} = (\varphi_s)_{N_0 = 0}$, etc.).

If the signal wave carries the information, for example, in pulses, the position of the downcoming difference frequency wave is determined by the condition that

$$\frac{\partial \phi^-}{\partial \varphi_{s_0}} = 0 , \quad (5.5)$$

and by

$$\frac{\partial \phi^-}{\partial \varphi_{p_0}} = 0 , \quad (5.5a)$$

if the pumpwave carries the information. The ray direction of the associated wave, $\exp. [j \{\omega_{\pm} t - (k_{s_x} \pm k_{p_x}) x - \int^{z} (k_{s_z} \pm k_{p_z}) dz \}]$, thus

has the ray direction of the signal wave or the pumpwave, if the former or the latter carries the information. This is another typical feature of the non-linear propagation theory.

Since $n_{s_z} = \sqrt{n_s^2 - \sin^2 \varphi_{s_0}}$, etc., and

$\sin \varphi_{-1_0} = \frac{1}{\omega_-} (\omega_s \sin \varphi_{s_0} - \omega_p \sin \varphi_{p_0})$, we obtain

$$\frac{\partial \phi_{0,-1}}{\partial \varphi_{s_0}} = - \frac{\omega_s}{c_0} \cos \varphi_{s_0}$$

$$\left[\int_{z_a}^{z_0} \underbrace{\left\{ \tan \varphi_s + \frac{1}{\cos^2 \varphi_s} \left(\frac{1}{n_s} \frac{d n_s}{d \theta} \right)_{\varphi_s} + \tan \varphi_- + \frac{1}{\cos^2 \varphi_-} \left(\frac{1}{n_-} \frac{dn_-}{d \theta} \right)_{\varphi_-} \right\}}_{\mu_-} dz + \right.$$

$$\left. - (x_2 - x_1) + \left(\frac{2k_{-1_z}}{\mathcal{H}} \right)_{z_0} \mu_- \right] \qquad (5.6)$$

For a very slowly varying medium, $x_2 - x_1$ thus approximately becomes (compare (3.14))

$$x_2 - x_1 \cong \left\{ z_0 - z_a + \left(\frac{2k_{-1_z}}{\mathcal{H}} \right)_{z_0} \right\} \mu_- \qquad (5.7)$$

Due to the "height dispersion," the ray path of the downcoming difference frequency wave is deformed, as if the frequency shift reflection took place at the level $z_0 + \left(\frac{2k_{-1_z}}{\mathcal{H}} \right)_{z_0}$, instead of at z_0. For this change, the wave normal paths in figure 3 have not been corrected.

Returning to our present case of magneto-ionic vertical incidence ($\varphi_s = 0 = \varphi_{-1}$), we obtain

$$x_2 - x_1 \cong \left\{ z_0 - z_a + \left(\frac{2k_{-1z}}{\mathcal{H}} \right)_{z_0} \right\} \left\{ \left(\frac{1}{n_s} \frac{d n_s}{d \theta} \right)_0 + \left(\frac{1}{n_-} \frac{d n_-}{d \theta} \right)_0 \right\} . \quad (5.7a)$$

The difference frequency wave therefore does not come down where the signal wave enters, if $\frac{1}{n_s} \frac{d n_s}{d \theta} + \frac{1}{n_-} \frac{d n_-}{d \theta} \neq 0$.

Since

$$\left(\frac{1}{n_s} \frac{d n_s}{d \theta} \right)_{\substack{0 \\ x}} = \mp Y_{T_s} Y_{L_s} (1 - n_{s_0}^2) \frac{1}{\sqrt{Y_{T_s}^4 - 4(1 - X_s)^2 Y_{L_s}^2}} , \quad (5.8)$$

θ would have to be equal to 0° or 90° for μ_- safely to be equal to zero. Since the non-linear driving terms disappear if $\theta = 0°$ (unless we consider second order quantities in the high power pump field), we have to select $\theta = 90°$, i. e., transverse magneto-ionic propagation, in order to obtain reliable travelling wave resonance effects recorded at the same transmitting and receiving site (for example in a topside sounder).

6. Sum and Difference Frequency Generation when the Non-Linear Driving Forces Have a Resonance

For the sake of simplicity we limit ourselves to one resonance only and assume that the signal wave experiences longitudinal plasma resonance at some specified level $z = z_0$. If H is the scale

height of the electron density, we write accordingly

$$X_s = 1 + \frac{z - z_0}{H} \quad . \tag{6.1}$$

We now have to include (a modest) collision frequency ν_s, and replace $\alpha_s = Y_{T_s}/(1 - X_s)$ by $\alpha_{s_\nu} = Y_{T_s}/(1 - X_s j\delta_s)$, where $\delta_s = \nu_s/\omega_s$.

If the signal wave is of ordinary type, $n_s = n_s^{(o)}$ (see 2, b. of paragraph 4), $\xi^{\pm}$ near and at the resonance level can be written

$$\xi^{\pm} \cong \omega_{\pm}^2 (1 - n_{\pm}^2) \frac{Y_{T_s}}{1 - X_s - j\nu_s} \frac{\omega_p}{c_0} \left\{ \left(1 - \frac{X_p}{1 - n_p^2} \right) (1 \pm Q_{\pm} Q_p) \pm \frac{Y_{T_p}^2}{1 - X_p} \cdot \right.$$

$$\left. \cdot (n_{\pm} + n_p X_{\pm}) \, e^{j\{\omega_{\pm} t - \int_{z_a}^{z} (k_s \pm k_p)\, dz\}} \right\}, \quad (X_p \neq 1) \tag{6.2}$$

where $k_s \cong 0$. We have (naturally) neglected triple split coupling of the signal wave and likewise have assumed it to be of practically constant amplitude through the important part of the resonance region, a helpful but somewhat crude approximation.

Noticing that $b_{\pm}$ can be written

$$b_{\pm} = \omega_{\pm}^4 (1 - X_{\pm}) X_{\pm}^2 \frac{1}{(1 - n_{o_{\pm}}^2)(1 - n_{x_{\pm}}^2)}, \tag{6.3}$$

Relation (5.1) yields

$$\left(\frac{d^2}{dz^2} + k_{o_{\pm}}^2 \right) \left(\frac{d^2}{dz^2} + k_{x_{\pm}}^2 \right) E_y^{\pm} \cong \frac{\psi^{\pm}}{1 - X_s - j\delta_s} e^{j\{\omega_{\pm} t - \int_{z_a}^{z} (k_s \pm k_p)\, dz\}}, \tag{6.4}$$

where

$$\Psi^{\pm} = - E^0_{s_y} \frac{v_{p_{y\pm}}}{2} (1 - n_p^2)(1 - n_s^2)(1 - n_{o_\pm}^2)(1 - n_{x_\pm}^2) \frac{1}{X_\pm} \frac{\omega_p^2 \omega_s \omega_\pm}{c_0^4} (1 - X_\pm - n_\pm^2) \cdot$$

$$\cdot Y_{T_s} \left\{ \left(1 - \frac{X_p}{1 - n_p^2} \right) (1 \pm Q_\pm Q_p) \pm \frac{Y_{T_p}^2}{1 - X_p} (n_\pm + n_p X_\pm) \right\}, \qquad (6.5)$$

and

$$v^0_{p_{y_\pm}} = E^0_{p_y} e/m \omega_\pm , \qquad (6.6)$$

i.e., the ac electron velocity that the pumpwave would generate in an isotropic medium.

Since the evaluation of ordinary and extra-ordinary natural sum and difference frequency waves follows the same procedure, we take the ordinary sum and difference frequency waves as characteristic examples. By (5.1) we obtain approximately

$$E^+_{y(o)} = + \frac{j}{2} \frac{\Psi^+ e^{j\omega_+ t}}{k_{o_+}^2 - k_{x_+}^2} \frac{1}{k_{o_+}} e^{+j \int_{z_a}^{z} k_{o_+} dz} \cdot \underbrace{\int_{+\infty}^{z} e^{-j \int_{z_a}^{z} (k_s + k_p + k_{o_+}) dz} \frac{dz}{1 - X_s - j\delta_s}}_{H \mathfrak{J}_+ e^{-j \int_{z_a}^{z_0} (k_s + k_p + k_{o_+}) dz}} , \qquad (6.7)$$

where it has to be remembered that k_{o_+} must be positive for a down-coming wave. The coupling integral, $\mathfrak{J}_+$, now becomes (since $k_s \approx 0$)

$$\mathfrak{F}_+ = \mathfrak{F}^*(y,\sigma) = \int_{-\infty}^{y} \frac{e^{+jy}}{y - j\sigma}\, dy, \qquad (6.8)$$

where

$$\sigma = \delta_s H (k_p + k_{o_+}), \quad \text{and} \quad y = (z_0 - z)(k_p + k_{o_+}) \qquad (6.9)$$

One finds that

$$\mathfrak{F}^*(+\infty, \sigma_+) = \begin{cases} j\,2\pi e^{-\sigma}, & \sigma > 0 \\ j\pi, & \sigma = 0 \\ 0, & \sigma < 0 \end{cases} . \qquad (6.10)$$

Assuming k_p to be positive (pumpwave running in positive z-direction), we thus find that a sum frequency "echo" is obtained only if the electron density gradient is positive. This is in accordance with the physical situation, since the signal wave runs in the direction of increasing X_s.

In order to demonstrate how the "reflected" difference frequency wave is being built up in the driving force resonance region, we have in figure 4 presented the amplitude of the coupling integral as a function of y. One notes the (infinite) plasma resonance for $\sigma = 0$ and the moderate field perturbation in the resonance region when $H < 0$.

If we assume that the pump frequency is larger than $2\omega_s$, so that a difference frequency wave, in principle, could propagate away from the resonance region, the coupling integral becomes

$$\mathfrak{I}_{-} = \mathfrak{I}(y,\sigma) = \int_{-\infty}^{y} \frac{e^{-jy}}{y + j\sigma}\, dy, \tag{6.11}$$

where

$$\sigma = \delta_s H(k_p + k_{o_-}), \quad \text{and} \quad y = (z_0 - z)(k_p + k_{o_-}). \tag{6.12}$$

It appears from (6.10) that

$$\mathfrak{I}(+\infty, \sigma) = \begin{cases} -j2\pi e^{-\sigma}, & \sigma > 0 \\ -j\pi, & \sigma = 0 \\ 0, & \sigma < 0 \end{cases} \tag{6.13}$$

Also in the difference frequency case $(\omega_p > 2\omega_s)$ a positive electron density gradient is required for a downcoming wave to be generated.

For the ordinary forward sum frequency wave, the coupling integral becomes

$$\left.\begin{aligned} \mathfrak{I}_{+} = \mathfrak{I}(y,\sigma), \quad \text{where} \begin{cases} \sigma = \delta_s H(k_p - k_{o_+}) \\ y = (z - z_0)(k_p - k_{o_+}) \end{cases} \quad (k_p > k_{o_+}) \\ \mathfrak{I}_{+} = \mathfrak{I}^{*}(y,\sigma), \text{where} \begin{cases} \sigma = \delta_s H(k_{o_+} - k_p) \\ y = (z - z_0)(k_{o_+} - k_p) \end{cases} \quad (k_p < k_{o_+}) \end{aligned}\right\} \tag{6.14}$$

Thus, even the generation of a forward wave requires a positive electron density gradient.

The downcoming sum frequency wave, at the level $z = z_a$, finally can be written

$$E^{+}_{y_{(o)}} \cong R^{(o)}_{0,+1}\, E^{0}_{s_y}, \tag{6.15}$$

where

$$R^{(o)}_{0,+1} = -\frac{1}{2}\frac{v^{0}_{p_y}}{c_0}\left(\underbrace{\pi k_{o_+} H\, e^{-\delta_s H |k_p + k_{o_+}|}}_{P}\right)_{z=z_0} \cdot$$

$$\cdot\, e^{j(\omega_+ t - \int_{z_a}^{z_0} (k_s + k_p + k_{o_+})\, dz)} \cdot$$

$$\cdot \left[\frac{\omega_p^2 \omega_s}{\omega_0^2 \omega_+} \frac{(1 - n_p^2)(1 - n_{o_+}^2)(1 - n_{x_+}^2)}{(n_{o_+}^2 - n_{x_+}^2)\, n_{o_+}^2} (1 - X_+ - n_+^2) : \right.$$

$$\left. \cdot\, Y_{T_s}\left\{\left(1 - \frac{X_p}{1 - n_p^2}\right)(1 - Q_+ Q_p) - \frac{Y^2_{T_p}}{1 - X_p}(n_+ + X_+\, n_p)\right\}\right]_{z=z_0} . \tag{6.16}$$

Since

$$P = P_{max} = \frac{\omega_s}{\nu_s}\frac{\pi}{e}\frac{k_{o_+}}{|k_p + k_{o_+}|}, \quad \text{for} \quad H = \frac{\omega_s}{\nu_s}\frac{1}{|k_p + k_{o_+}|} \tag{6.17}$$

an optimum that should be attainable at some levels in the ionosphere, the order of magnitude of $|R^{(o)}_{0,+1}|$ is $v^{0}_{p_y}\, \omega_c / c_0\, \nu_s$, if ω_p is moderately larger than $2\omega_s$.

If we assume the pumpwave (the high power wave) to be pulsed, and the signal wave to be continuous, the sum frequency "echo" delay becomes

$$\tau_+^{(o)} = \frac{\partial}{\partial \omega_p} \int_{z_a}^{z_0} (k_s + k_p + k_{o_+})\, dz \cong \frac{2}{c_0} \left\{ z_0 - z_a + H \left(\frac{2\omega_p}{\omega_s} + 1 \right) \right\}. \quad (6.18)$$

if ω_p is so large that $(n_p)_{z_0} \cong 1$. For the difference frequency "echo" delay we similarly obtain

$$\tau_-^{(o)} \cong \frac{2}{c_0} \left\{ z_0 - z_a + H \left(\frac{2\omega_p}{\omega_s} - 1 \right) \right\}, \quad (6.19)$$

provided that $\omega_p - \omega_s$ is so great, that $(n_{o_-})_{z_0} \cong 1$. These relations yield

$$H = \frac{c_0}{4} \left(\tau_+^{(o)} - \tau_-^{(o)} \right), \quad (6.20)$$

and

$$z_0 = z_a + \frac{c_0}{4} \left\{ \tau_+^{(o)} + \tau_-^{(o)} - \left(\tau_+^{(o)} - \tau_-^{(o)} \right) \frac{2\omega_p}{\omega_s} \right\}. \quad (6.20a)$$

By sum and difference frequency pulse "echo" measurement of this kind it is thus in principle possible (if $\omega_p - \omega_s$ is large enough) to obtain not only the true ordinary reflection height, z_0 ($X_s = 1$), but also the electron density gradient, N_0/H, at the same. Since the pulse measurements have to be made at relatively high frequencies, for example $f_s = 30$ Mc/s, $\tau_+^{(o)}$ and $\tau_-^{(o)}$ can be determined with much greater accuracy than at the unshifted signal frequency ω_s. Another advantage is the fact that ω_p, if it is large enough, can remain unchanged, while ω_s is swept through the probing frequency range of interest.

The immediate question one asks oneself is the following: is it practically possible to perform sum and difference frequency pulse echo measurements of the type just discussed, using ground-based equipment? If $\omega_p^2 \gg \omega_0^2$, the amplitude of $R^{(o)}_{0,+1}$ by (6.16) approximately becomes

$$|R^o_{0,+1}| \approx \frac{1}{4} \frac{v^0_{p_y}}{c_0} \frac{\omega_s}{\nu_s} \underbrace{\frac{\pi}{e} u e^{1-u}}_{\mu} \frac{\omega_0^4}{(\omega_p + \omega_s)^3 \omega_p} Y_{T_s}, \qquad (6.21)$$

where

$$u = \frac{\nu_s}{\omega_s} H |k_p + k_{o_+}|. \qquad (6.22)$$

If we assume u to lie in the range 0.08 to 4, i.e., within a u-ratio of 50, $\mu \geq 0.20$ ($\mu_{max} = 1$), and $\omega_p/2\pi = 30$ Mc/s, $\omega_s/2\pi = 5$ Mc/s, we obtain

$$|R^o_{0,+1}| \approx \frac{2 v^0_{p_y}}{c_0} \frac{f_s}{\nu_s} 10^{-4} Y_{T_s},$$

which with $\nu_s = 10^3$ yields $|R^o_{0,+1}| \approx \frac{v^0_{p_y}}{c_0} Y_{T_s}$ If the ground-based pump transmitter has an effective radiation aperture A, and the ionospheric absorption is neglected at the pump frequency, $v^0_{p_y}$ becomes

$$v^0_{p_y} \approx \frac{e}{m} \frac{1}{\pi c_0 r} \sqrt{\frac{A Z_0 P_0}{2}}, \qquad (Z_0 = \sqrt{\frac{\mu_0}{\epsilon_0}})$$

where P_0 is the transmitter power and r the distance from the ground to the z_0-level. Considering the fact that the returning sum

(or difference) frequency travels practically without absorption and that the atmospheric noise level at the sum (or difference) frequency is very low, compared to at f_s = 5 Mc/s, we may assume that a $v^0_{p_y}/c_0$-ratio of 10^{-5} would yield a detectable echo at the ground (provided the regular ionosonde at 5 Mc/s is powerful enough). With an effective antenna area of 10^4 m^2, and r_0 = 300 km, P_0 becomes 5 Mw. It thus seems to lie within the possibilities of present day techniques to perform ionospheric sum and difference frequency measurements as outlined. Beyond doubt practical experiments of this type would be very interesting and probably also rewarding.

Acknowledgements

The research reported in this communication was partly done at the Ionosphere Research Laboratory (IRL), Pennsylvania State University, and partly at the Research Laboratory of Electronics, Gothenburg, Sweden. The author is much indebted to the IRL and to the U. S. Air Force, for support under Contract AF 61(052)-451.

7. References

Rydbeck, O. E. H. (1962), Dynamic non-linear wave propagation in ionized media, Part 2, The Magneto-Ionic Medium, Res. Rept. No. 28, Research Laboratory of Electronics, Chalmers University of Technology, Gothenburg, Sweden.

Rydbeck, O. E. H. (1963), Electromagnetic non-linear interaction and reflection from a plane ionized medium, Sci. Rept. No. 183, IRL, Pennsylvania State University.

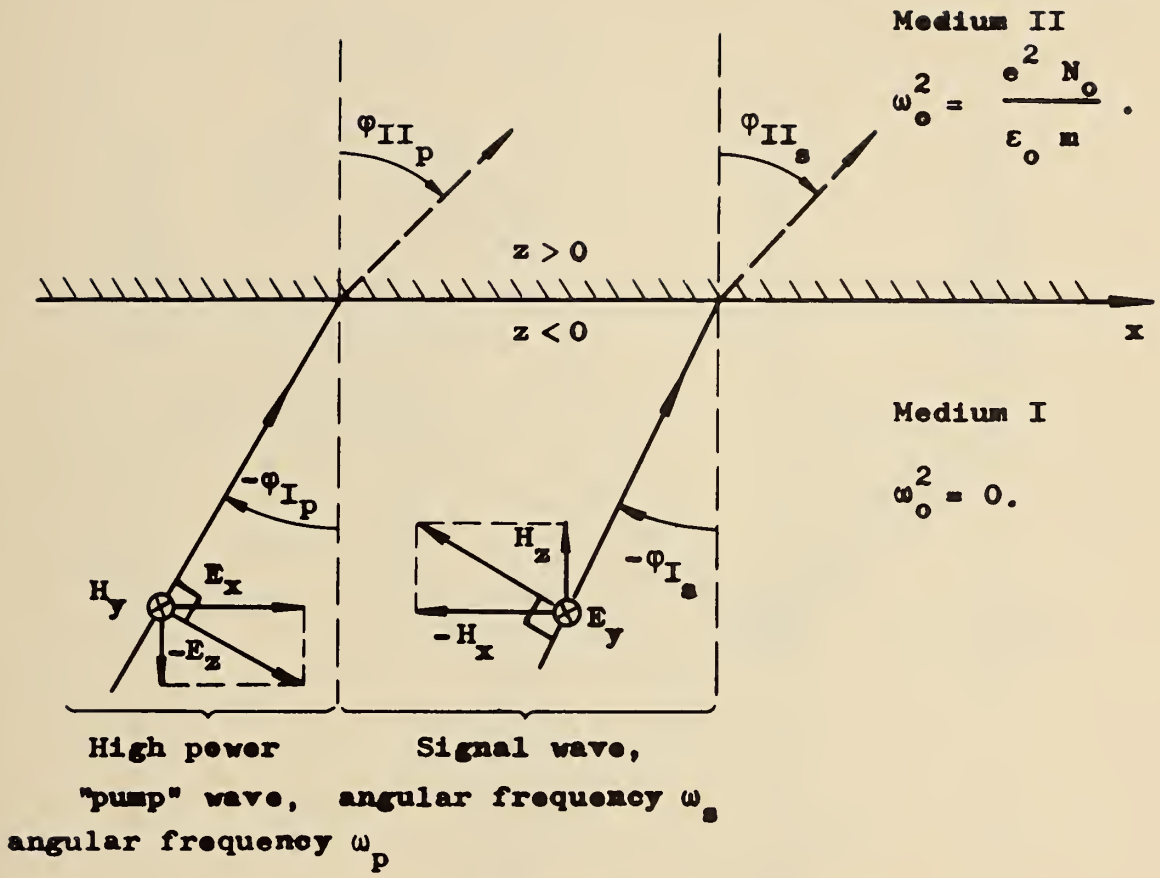

Figure 1. Depicting polarizations and angles of incidence of signal and pump waves.

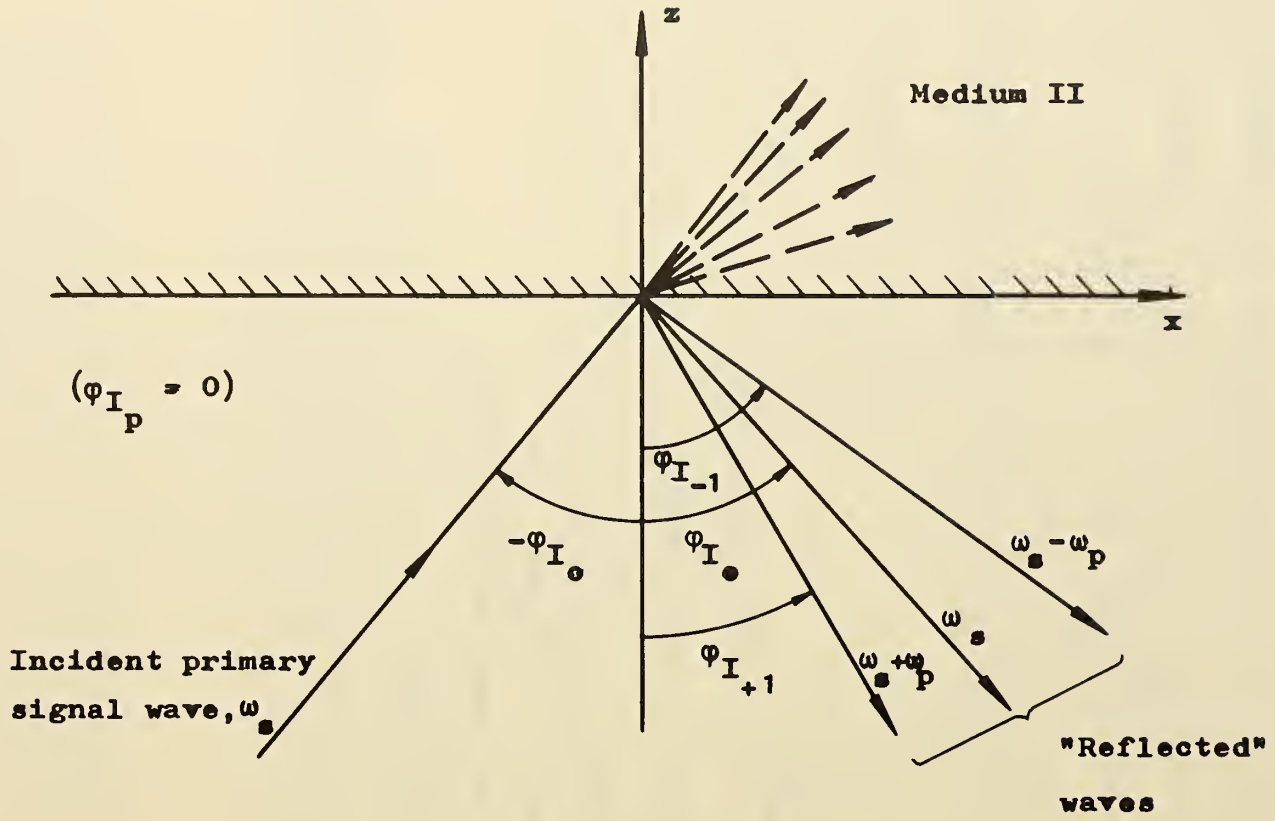

Figure 2. Demonstrating first order wave spectrum obtained from the pumped, ionized medium.

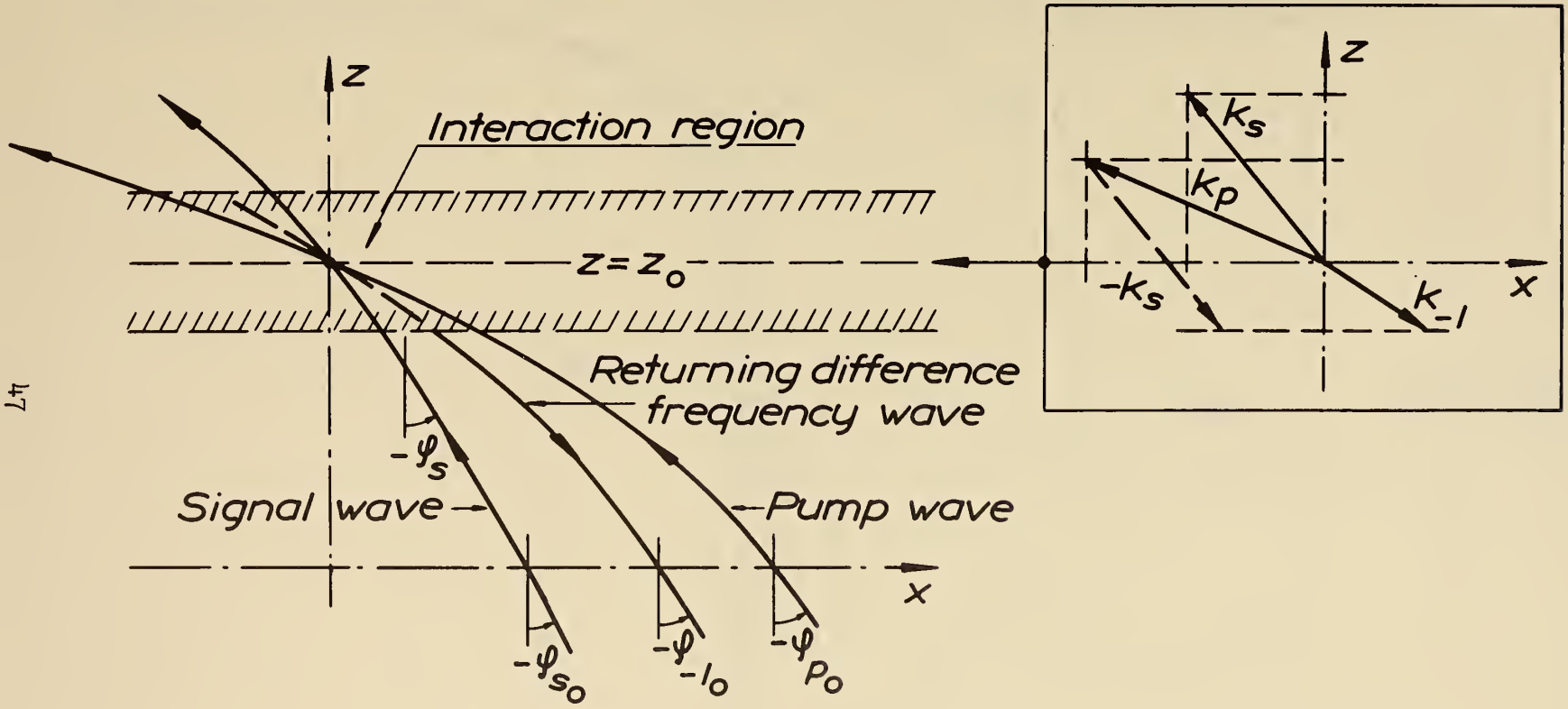

Figure 3. Demonstrating wave normal path of the frequency shifted downcoming wave.

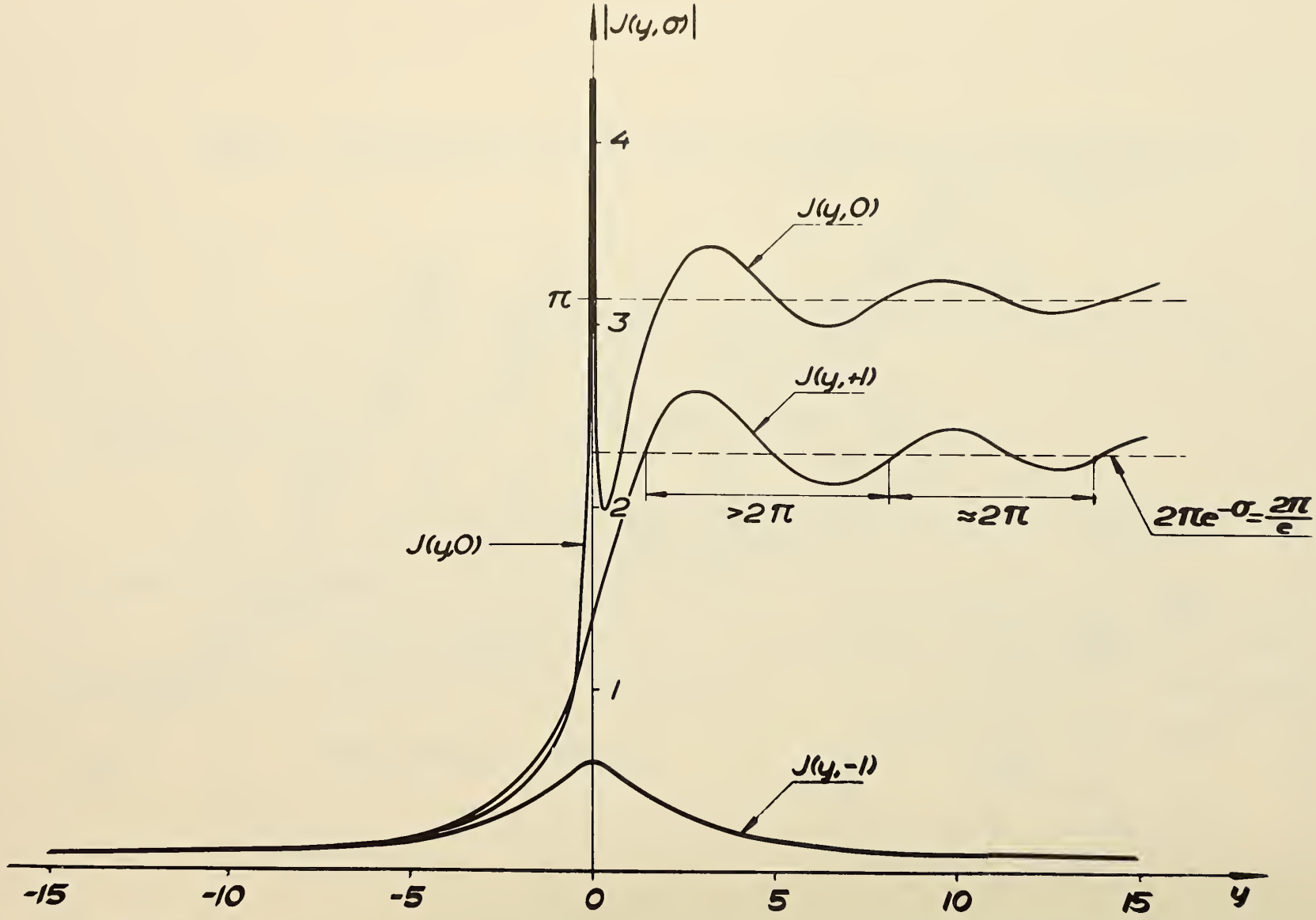

Figure 4. Depicting build-up of downcoming sum frequency wave.

Non-Linear Interaction Coefficients for Electrons in Nitrogen and Air*

A. V. Phelps
Westinghouse Research Laboratories
Pittsburgh, Pennsylvania

An analysis of measured electron transport coefficients for nitrogen and oxygen has yielded a consistent set of energy dependent cross sections for the momentum transfer and inelastic scattering of electrons in these gases. These results are used with the appropriate Boltzmann transport equation to predict the effects of the heating of electrons in nitrogen and air by radio frequency fields. The rapid increase in mean energy with electric field predicted by Altshuler at high frequencies is obtained, but the calculations do not show the predicted hysteresis effect. These procedures have made possible the direct calculation of cross modulation coefficients rather than the usual procedure of first evaluating the change of mean energy produced by an electric field and then calculating the change in propagation constant.

*This work was supported in part by the Air Force Weapons Laboratory.

I. Introduction

The purpose of this paper is to present the results of improved calculations of non-linear interaction coefficients for electrons in nitrogen and in air. In the past the lack of accurate electron collision cross section data and of accurate procedures for determining electron energy distribution functions has made it necessary to calculate the effect of electric fields on the electron transport coefficients and reaction rates under simplifying assumptions regarding the electron energy distribution and the electron energy loss processes. Recent studies have considerably improved our theoretical understanding of electron collision cross sections at low energies [1, 2][1] and have led to the determination of reasonably accurate and realistic electron collision cross sections in nitrogen [3, 4] and to the approximate collision cross sections for electrons in oxygen given in this paper. When these cross sections are used with an accurate form of the Boltzmann transport equation to determine the electron energy distribution function and various electron transport coefficients we expect to obtain accurate values for the various

[1] Italicized figures in brackets indicate the literature reference at the end of this paper.

coefficients describing the non-linear interaction of electromagnetic waves in weakly ionized nitrogen and air. The collision cross section data and the appropriate Boltzmann equation are summarized in Section II. In Section III, the variation of the mean electron energy with electric field strength obtained from our calculations is compared with the results of various approximate calculations. In Section IV, a comparison is made of experimental and theoretical determinations of the coefficient of cross modulation for waves of nearly equal frequency.

II. Cross Sections and Boltzmann Equation

The cross sections for momentum transfer and inelastic collisions for electrons in nitrogen and oxygen which are used in our analysis are shown in Figures 1 and 2. The cross sections shown in Figure 1 for nitrogen have been derived to be consistent with dc measurements of electron drift velocity, of the ratio of the electron diffusion coefficient to electron mobility, and of excitation and ionization coefficients [4]. As has been pointed out previously [3], although the cross sections derived by this technique are not unique they are much more accurate than previously available data and are consistent with most of the known experimental data. These effective cross sections are believed to be accurate to $\pm$ 10% or better. The cross sections shown for oxygen were determined by the same techniques as used for H_2 and

and N_2 [3,4]. These results are tentative largely because of the lack of consistent experimental data. Our primary concern is with the cross section, Q_{vib}, for vibrational excitation of O_2 which has been neglected in most previous calculations in spite of the fact that it is the dominant energy loss mechanism in air for energies between 0.2 and 1.7 eV. From the agreement between calculated and measured values of the drift velocity and the ratio of the diffusion coefficient to the mobility, we believe that the effective cross section for vibrational excitation is accurate to $\pm$ 30% in this energy range. The momentum transfer cross section is believed to be accurate to $\pm$ 20% in the energy range from 0.2 to 20 eV. Outside these energy ranges the momentum transfer and excitation cross sections shown are much less certain but are the best available at present. In particular, we have not shown rotational excitation cross sections for O_2 since theory [5] indicates cross sections which are an order of magnitude smaller than for N_2.

The Boltzmann equation and the integrals for the evaluation of the electron mobility applicable to the calculation of the behavior of electrons in weakly ionized N_2 and air are given by Equations (1) through (7) of an earlier paper [7]. The mean energy of the electrons is given by

$$\bar{\varepsilon} = \int_0^\infty \varepsilon^{3/2} f(\varepsilon)\, d\varepsilon \qquad (1)$$

where $\mathcal{E}$ is the electron energy and $f(\mathcal{E})$ is the normalized electron energy distribution function [7].

III. Mean Electron Energy

Most previous calculations of non-linear effects have made use of approximate analytical forms for the electron energy distribution function, e.g., a Maxwellian energy distribution. As a result, it has been convenient to calculate the changes in the mean electron energy resulting from the disturbing electromagnetic field and then calculate the corresponding changes in observable quantities such as the attenuation coefficient for an electromagnetic wave. In the present discussion we will be concerned with the rather large changes in mean electron energy such as those considered in calculations which lead to a prediction of a "hysteresis effect" in the curve of mean energy as a function of electric field, E, at high frequencies [8]. In Altshuler's investigation expressions were derived for the mean electron energy which are based on the assumptions that a) the electrons lose energy to nitrogen molecules only by rotational excitation, b) the effective electron collision frequency is a linear function of the mean electron energy and c) the electron energy distribution function is Maxwellian. Since these expressions were not expected to be valid at the higher mean energies where other inelastic collision processes are important, we have obtained progressively more accurate

values for the mean energy by relaxing assumptions (a), (b), and (c).

One simple way of including the effect of vibrational excitation is to equate Altshuler's expression [8] for the power input per electron in the radio frequency case to the power input per electron at the same average electron energy in the dc limit and solve for the ac field required to maintain the electrons of this mean energy. If assumptions (b) and (c) are correct then this procedure should yield the same result as a more accurate analytical or machine calculation. Thus,

$$\frac{\beta \bar{\varepsilon}\ e^2E^2}{m(\omega^2 + \beta^2\bar{\varepsilon}^2)} = \frac{e^2E_{dc}^2}{m\beta\ \bar{\varepsilon}} \tag{2}$$

where e is the electronic charge, m is the electron mass, E and E_{dc} are the rms ac and the dc electric fields required to maintain the mean electron energy at $\bar{\varepsilon}$, and $\beta\ \bar{\varepsilon}$ is the effective value of the frequency of momentum transfer collisions. In the high frequency limit Eq. (2) reduces to

$$\frac{E}{\omega} = \frac{E_{dc}}{\beta\ \bar{\varepsilon}} = \frac{(E_{dc}/N)}{(\beta/N)\ \bar{\varepsilon}}. \tag{3}$$

Since no measurements of mean electron energy as a function of E_{dc}/N are available,[1] we have used the results of calculations [4]. The value of the

[1] The author does not know of any technique for the measurement of mean electron energy in gases where the electron energy distribution may depart significantly from Maxwellian.

coefficient β in Eq. (3) is taken to be the mean of the effective collision frequencies in the low frequency and high frequency limits [9]. The results of the application of Eq. (3) to N_2 at $77^{\circ}K$ are shown by the short dashed curve of Figure 3. This curve shows that calculated values of $\bar{\varepsilon}$ are a multivalued function of the electric field parameter, E/ω, at both low energies where rotational excitation is the dominant energy loss and at high energies where vibrational and electronic excitation are dominant. We note that the decrease in E/ω with increasing $\bar{\varepsilon}$ is only about 10% and that if the calculations had been made at significantly higher gas temperatures no decrease in E/ω would have been obtained.

Our next step in improving the accuracy of the calculation is to take into account the fact that at the higher electron energies the electron collision frequency is considerably smaller than that assumed in Eqs. (2) and (3). A simple approximate way to take this into account is to replace the expression for the effective collision frequency in terms of the mean energy by the effective frequency of momentum transfer collisions, ν_m/N, determined directly from measurements of the electron drift velocity at a given Edc/N [3, 7]. Thus, we use the relation

$$\frac{E}{\omega} = \frac{(E_{dc}/N)}{(\nu_m/N)} , \qquad (4)$$

to calculate the curve of $\bar{\varepsilon}$ vs E/ω shown by the short-dash, long-dash curve of Figure 3. We see that the results are essentially unchanged at low energies where the electron collision frequency is approximately a linear function of the electron energy but that at large mean energies the values of E/ω required to maintain a given mean energy are considerably larger than obtained with Eq. (3).

Finally we can relax the assumption that the electron energy distribution is independent of frequency for a given mean energy by calculating the distribution function using the Boltzmann equation appropriate to the ac electric field [7] and the cross sections shown in Figure 1. The resultant values of $\bar{\varepsilon}$ as a function of E/ω, as indicated by the solid line of Figure 3, show that although the values of E/ω required to produce a given value of $\bar{\varepsilon}$ are not much different from those predicted by the approximate calculations, the values of $\bar{\varepsilon}$ are now a single valued function of E/ω. The explanation for the different character of the $\bar{\varepsilon}$ vs E/ω curves is that the shape of the electron energy distribution function varies considerably with frequency. This is shown in Fig. 4 where the calculated electron energy distribution, $\varepsilon^{1/2} f(\varepsilon)$, are shown for a dc case, $E/N = 1.2 \times 10^{-18}$ V-cm^2, and a very high frequency ac case, $E/\omega = 2 \times 10^{-10}$ V-cm and ω/N 6×10^{-7} cm^3/sec. In both cases the mean electron energy is 0.067 eV. Also shown is a Maxwellian electron energy distribution having the same mean energy. Of particular interest

is the fact that, although the energy distribution in the dc case is intermediate between the Maxwellian and Druyvesteyn forms [3], the distribution in the ac case peaks at very low energies and has a very long "tail" at high energies. Since the energy loss processes are the same in both cases, the differences are due to the energy dependence of the energy gain term [8]. At the highest $\bar{\varepsilon}$ of Figure 3 the electron energy distribution functions for a given mean energy are much more nearly independent of the frequency.

Figure 3 also shows a curve of mean energy as a function of E/ω for air at $232^{\circ}K$ as calculated using the cross section data of Figures 1 and 2. Here we see a much more uniform rise in $\bar{\varepsilon}$ with E/ω which is due in part to the higher gas temperature and in part to the large energy electron energy losses in vibrational excitation of the oxygen at low $\bar{\varepsilon}$.

IV. Cross Modulation Coefficients

In this section we are concerned with the accuracy of cross modulation coefficients calculated using various approximations to the true electron behavior in air. Throughout this discussion we will assume that a) the electric field strength present in the gas produces an arbitrarily small perturbation of the electrons from their thermal equilibrium conditions, b) the electric field occurs in the form of a pulse whose duration is long compared to energy relaxation times but short compared to the time required

for significant changes in the electron density, c) that magnetic field effects may be neglected, and d) the effects of electron collisions with oxygen molecules, with minor constituents such as water vapor, and with other electrons, ions or excited species can be neglected. As a result of assumption (d) the density, N, referred to is the nitrogen density. If further investigation of the properties of electrons in oxygen supports the tentative curves for Q_m below 0.2eV shown in Fig. 2, then the effects of oxygen will have to be included in any more accurate analysis.

It is convenient to use as a basis for our discussion of cross modulation effects the theory developed by Barrington and Thrane [10] and discussed more recently by Rumi [11]. This theory is based on the assumption that the collision frequency for momentum transfer collisions is a linear function of energy [9], that the electron energy distribution is accurately represented by a Maxwellian distribution, and that the attenuation per wavelength is small. The theoretical results for the fractional modulation $\delta E/E$ of a wave at an angular frequency ω_2 resulting from electron heating by a wave at ω_1 can be written in the following form

$$\frac{\delta E}{E} = \frac{\omega_p^2}{\omega^2} \frac{\Delta h}{\lambda} \frac{e^2E^2}{2m\omega^2kT} \frac{\omega}{N} R , \tag{5}$$

where $$R = \frac{4\pi}{3} \frac{e}{GkT} \frac{N}{\omega} \frac{kT}{e} a_2^2 f_1(a_2) a_1 f(a_1), \tag{6}$$

$$a_2 = \omega_2/\nu_2, \quad a_1 = \omega_1/\nu_2,$$

$$f_1(a) = \frac{25}{4}\left[C_{5/2}(a) - \frac{7}{5}C_{7/5}(a)\right], \tag{7}$$

and $f(a) = \frac{5}{2}\ C_{5/2}(a)$.

Here $\omega_p^2 = ne^2/m\varepsilon_o$ is the plasma resonance frequency where n is the electron density and ε_o is the permittivity of free space; ν_2 is the electron collision frequency for electrons with an energy of kTas defined in reference 9; Δh is the length of path over which the absorption occurs; λ is the free space wavelength; k is Boltzmann's constant; T is the gas temperature; G is the effective value of the energy loss per momentum transfer collision; N is the nitrogen density; and C_p (a) is a function defined and tabulated by Dingle, Arndt and Roy [12]. The particular form of the function R in Eq. (6) was chosen because it is approximately symmetrical with respect to frequencies above and below the electron collision frequency and because it yields a function which is roughly independent of temperature. This function is shown by the solid curves of Figure 5 and 6 for the case in which $\omega_1 = \omega_2$, i.e., for the case in which the wanted wave and the disturbing wave have essentially the same frequency, as in the case of many laboratory experiments or in self modulation experiments. The curves of Figures 5 and 6 were calculated for $\nu_2/N = 1.2 \times 10^{-7}(kT/e)cm^3/sec$ and for $G = 3 \times 10^{-3}(300/T)$. The value of

GT was chosen to fit the results of laboratory dc measurements at temperatures of interest in the ionosphere. For this assumption regarding the temperature dependence of G the solid curves in Figs. 5 and 6 are independent of temperature.

The only high frequency laboratory measurements known to the author in which the assumptions listed above are satisfied are those of Phelps, Fundingsland and Brown [13]. These results are shown by the points in Figure 6. Unfortunately these authors have not estimated the accuracy of their electric field measurements. The ionospheric measurements analyzed by Barrington and Thrane [10] using this theory indicated a G value of about half the value we have adopted in order to obtain a fit to the dc measurements. A reduced value of G such as this would give a better fit to the experimental points in Figure 6 but would require that the true R function deviate significantly from the curves shown. The obvious next step in this investigation is to solve the Boltzmann equation appropriate to near thermal conditions at high frequencies as has been done for the dc case in literature references 3 and 4. Calculations by the author for gases in which the only energy losses are due to elastic recoil show that it is not proper to assume that the perturbed electron energy distribution function is that of Maxwellian distribution at a slightly higher temperature.

V. Summary

The calculations of the dependence of the mean energy on the electric field show that one must take into account the changes in the form of the electron energy distribution which occur as the frequency of the applied signal is varied. Similarly, a comparison of the results of a simple theoretical evaluation of the cross modulation coefficients for N_2 and air suggests that it is not satisfactory to assume that the electron energy distribution function is Maxwellian.

The author wishes to acknowledge helpful discussions of this problem with his associates in the Atomic Physics Group, especially G. J. Schulz and A. G. Engelhardt.

References

1) E. Gerjuoy and S. Stein, Phys. Rev. 97, 1671 (1955) and 98, 1848 (1955).

2) A. Dalgarno and W. Moffett, Indian Academy of Sciences Symposium on Collision Processes, 1962 (unpublished).

3) L. S. Frost and A. V. Phelps, Phys. Rev. 127, 1621 (1962).

4) A. G. Engelhardt, A. V. Phelps and C. G. Risk, Paper E-2, 16th Gaseous Electronics Conference, Pittsburgh, Pa., October, 1963 and Bull. Am. Phys. Soc., Series II, 9, (1964).

5) A. Dalgarno, Ann. Geophys. 17, 16 (1961).

7) A. G. Engelhardt and A. V. Phelps, Phys. Rev. 131, 2115 (1963).

8) S. Altshuler, Jour. Geophys. Res. 68, 4707 (1963).

9) A. V. Phelps, Jour. Appl. Phys. 31, 1723 (1960).

10) R. E. Barrington and E. Thrane, J. Atmos. and Terrest. Phys. 24, 31 (1962).

11) G. C. Rumi, I.R.E. Trans. on Antennas and Propagation AP-10, 594 (1962). Our numerical values for $f_1(a)$ differ significantly from those given by Rumi for $a > 10$.

12) R. B. Dingle, D. Arndt and S. K. Roy, Appl. Sci. Res. 6B, 155 (1956).

13) A. V. Phelps, O. T. Fundingsland and S. C. Brown, Phys. Rev. 84, 559 (1951).

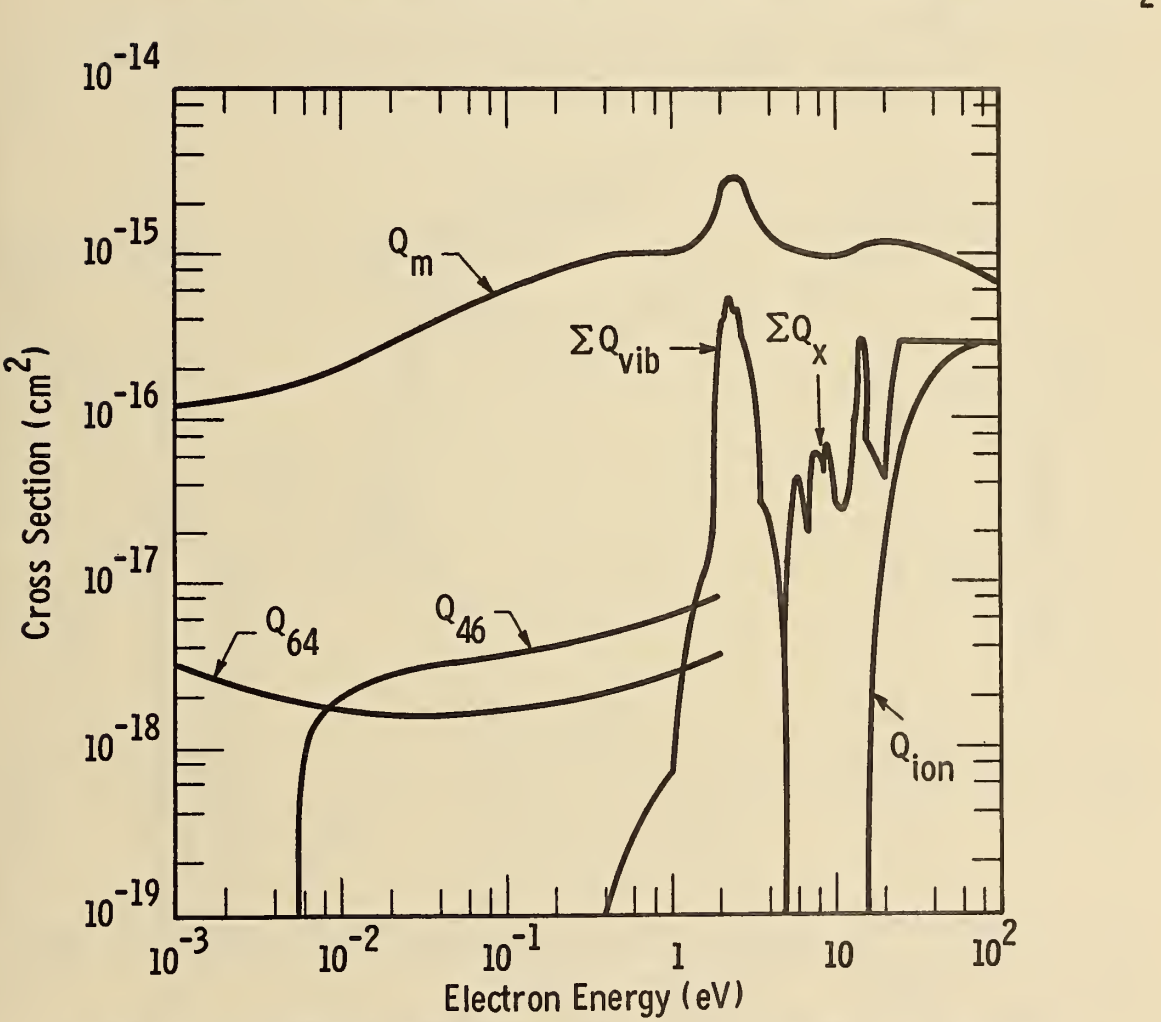

Fig. 1. Electron collision cross sections in N_2 for momentum transfer Q_m, rotational excitation and deexcitation Q_{ab}, vibrational excitation Q_{vib}, electronic excitation Q_x, and ionization Q_i. For clarity only one pair of rotational excitation and deexcitation curves is shown, i.e., Q_{46} for excitation from the J = 4 level and Q_{64} for deexcitation from the J = 6 level to the J = 4 level. Similarly, only the sums of the vibrational and electronic excitation cross sections are shown.

CURVE 568826-A

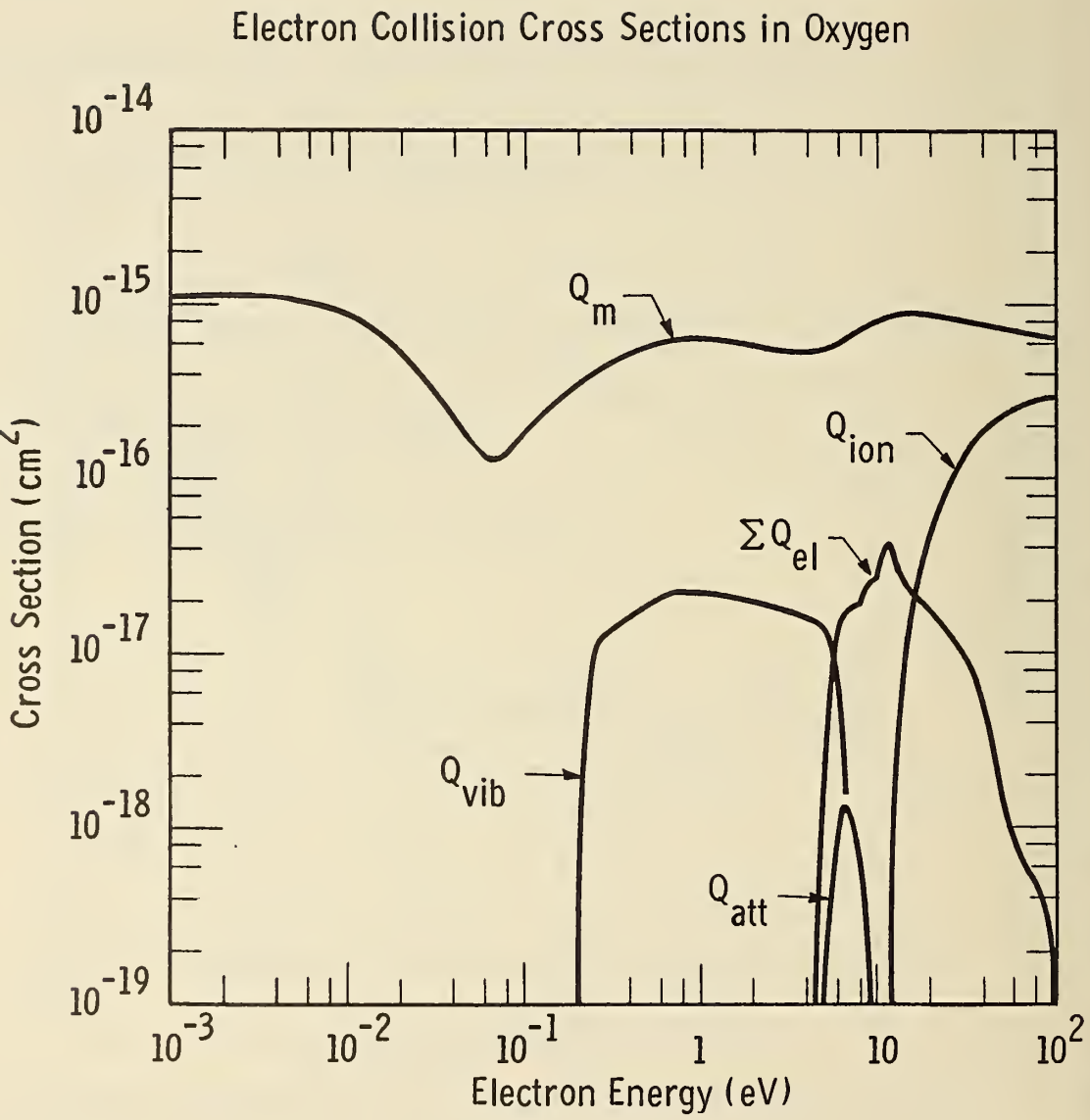

Fig. 2. Electron collision cross sections in O_2 for momentum transfer Q_m, vibrational excitation Q_{vib}, dissociative attachment Q_{att}, electronic excitation Q_{el}, and ionization Q_i. Only the sum of the various electronic cross sections is shown on this graph.

CURVE 568828-A

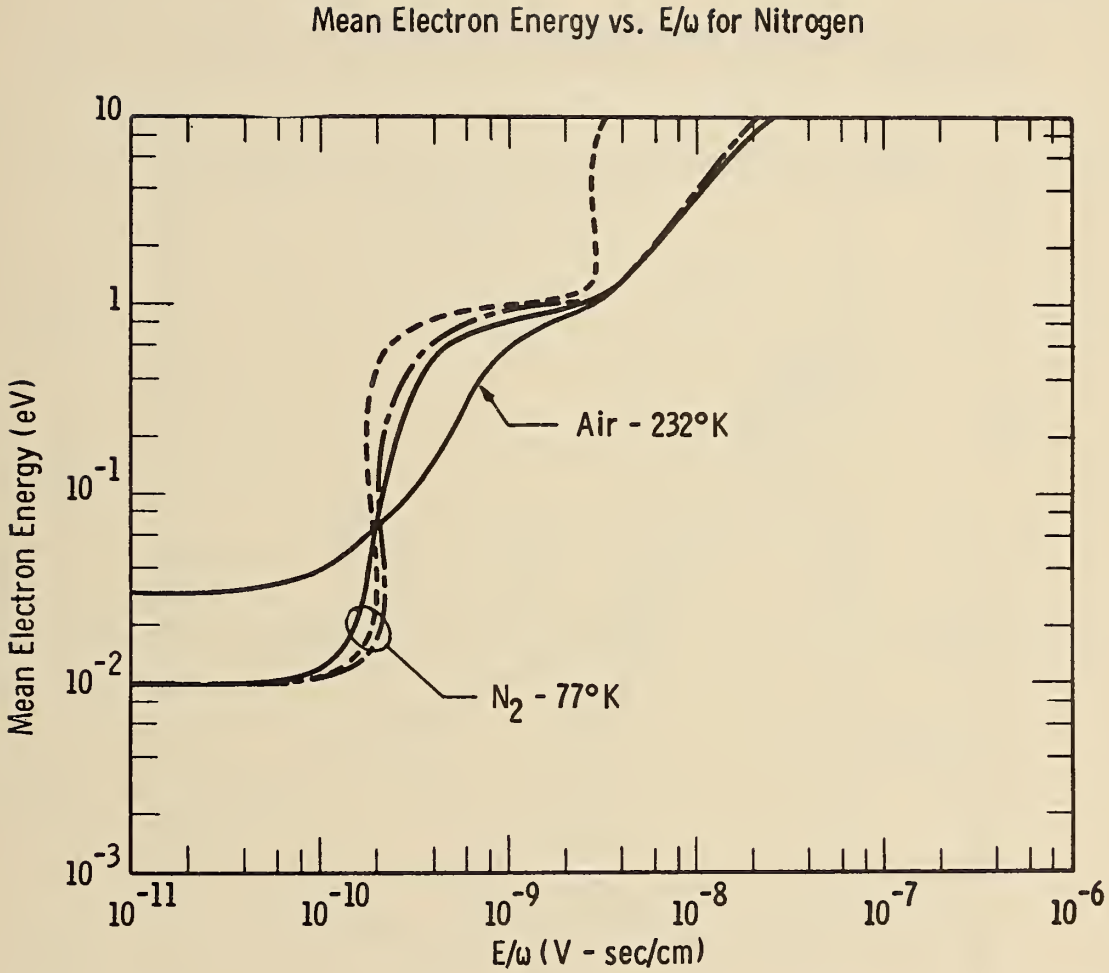

Fig. 3 Mean electron energy of electrons in N_2 at 77°K and air at 232°K as a function of E/ω at high frequencies. The calculations were made for $\omega/N = 6 \times 10^{-7}$ cm^3/sec for $E/\omega < 3.33 \times 10^{-9}$ $V\text{-}cm^{-1}\text{-}sec$ and for 6×10^{-6} cm^3/sec for $E/\omega < 3.33 \times 10^{-9}$ $V/cm^{-1}\text{-}sec$.

CURVE 568824-A

AC and DC Electron Energy Distribution Functions for N_2

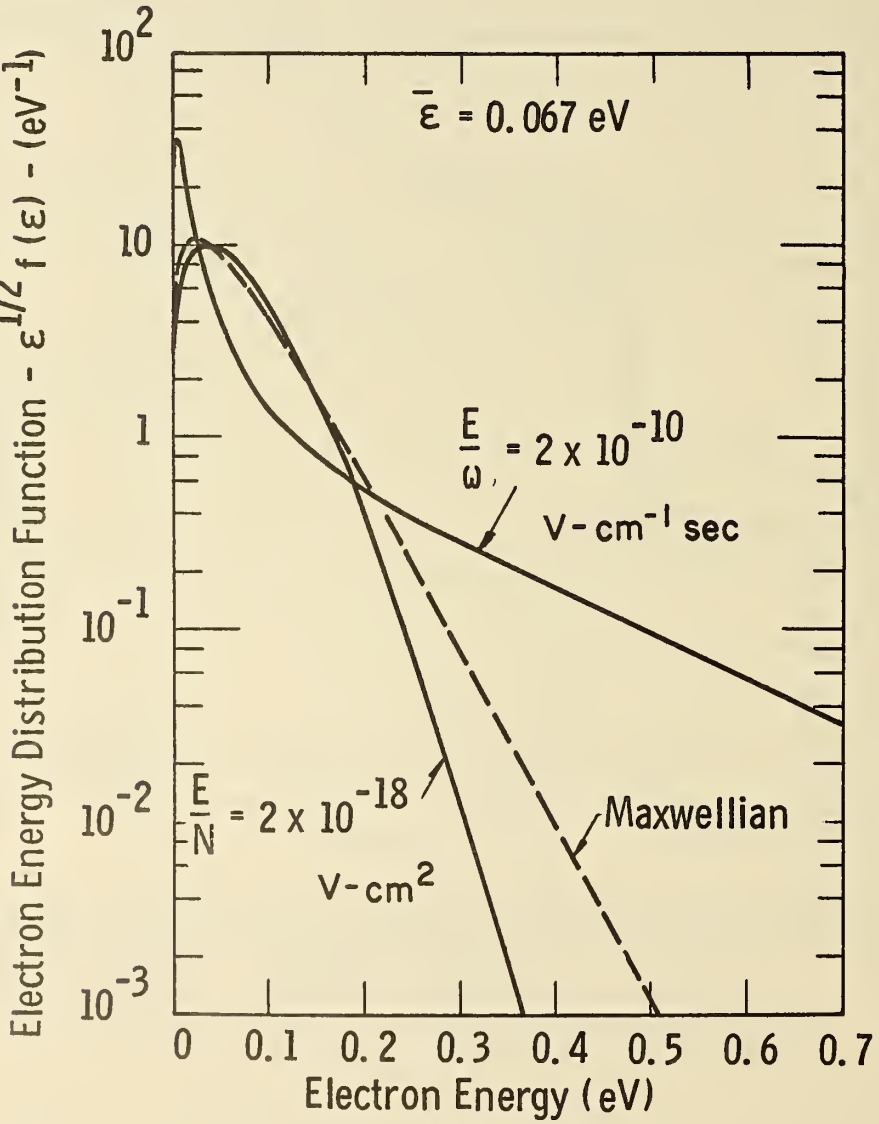

Fig. 4. Electron energy distribution functions for electrons in N_2 at 77°K.

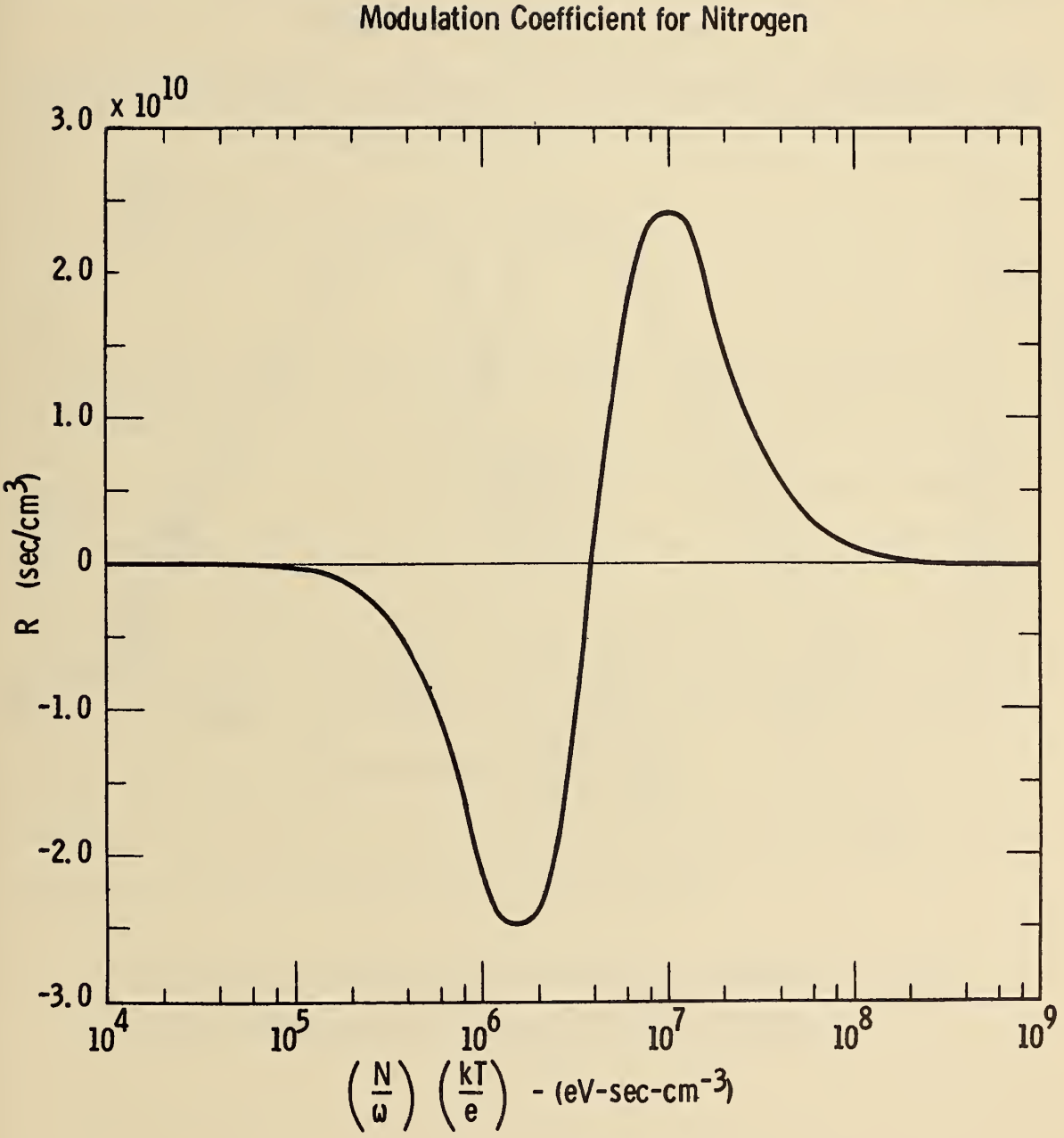

Fig. 5. Cross modulation function R.

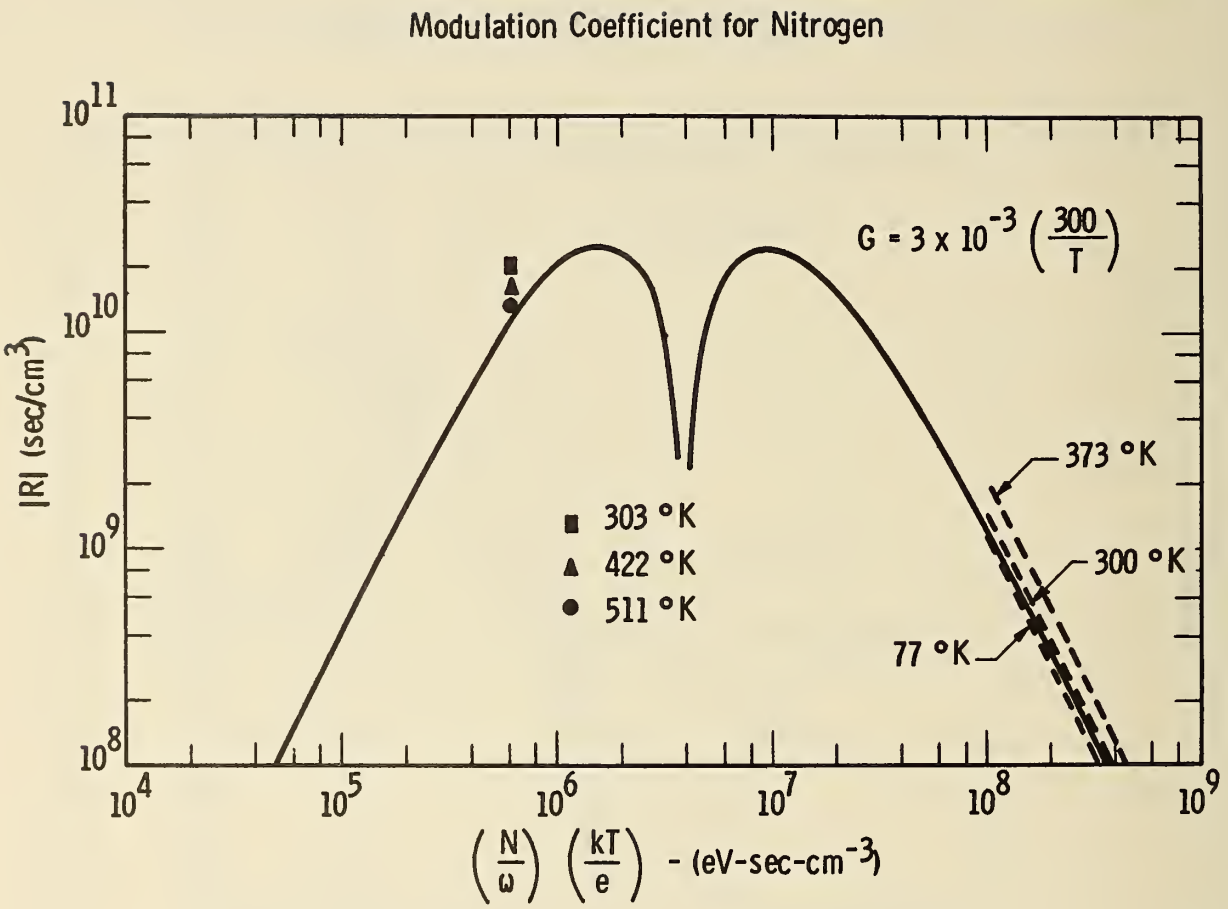

Fig. 6. Absolute magnitude of cross modulation function R showing theoretical curve and experimental data.

The Excitation of Optical Radiation by High Power Density Radio Beams

Lawrence R. Megill

Central Radio Propagation Laboratory, National Bureau of Standards,

Boulder, Colorado

We calculate the power density required to excite various states of O_2, and O which may be expected to radiate light observable from the ground. These calculations are made by first calculating the electrons energy distribution functions in the presence of the rf electric fields, and from this the rate of excitation of the radiating states. We discuss the feasibility of experiments to generate sufficient intensity to cause appreciable modification in the night airglow intensity. The possibility of performing experiments using the two body dissociative attachment of electrons is also considered, especially in regard to the performance of basic experiments in atomic physics.

1. Introduction

In the discussion of non-linear processes in the ionosphere, the excitation of optical radiation by a radio beam is an extreme case. Yet, if transmitters sufficiently powerful to excite optical radiation in the ionosphere existed, a great deal of quantitative information concerning the constitution of the ionosphere could be collected on a routine basis. It is, therefore, of some importance to investigate the conditions under which detectable optical radiation might be excited.

This problem has been considered by others, Bailey [1959], Clavier [1961]; but not in detail which we will apply. Authors in the past have estimated the intensity to be expected in the atmosphere based on laboratory data obtained in a discharge. Such a procedure is liable to considerable error, since conditions in a discharge differ greatly from those extant in the atmosphere. In particular, in discharges there exist many metastable states which change the power required to heat electrons and recombination processes which yield a great deal of the luminosity. In addition, the electron density in discharges is often such that the electron energy distribution is dominated by electron interactions, a condition which does not apply in the lower ionosphere. [Megill and Carleton, 1964]. We shall, in this paper, concern ourselves principally with the direct "heating" of the electrons already in existence in the ionosphere by means of electric fields and with the excitation of electronic states in the neutral gas by collisions with these electrons. The problem of "breaking down" the atmosphere will be discussed only briefly.

2. Excitation of Optical Radiation

If we know the distribution f(u) of electrons with energy, u, under the influence of electric and magnetic fields then we can calculate the total rate of excitation of a particular state ν_{ij} from

$$\nu_{ij} = N_i N_e \int_0^\infty \sigma_{ij} v f(u) u^{\frac{1}{2}} du; \tag{1}$$

where N_i is the number density of the gas, N_e is the number density of electrons, σ_{ij} is the cross section for excitation to state j, v is the electron velocity, and we have normalized the distribution function so that

$$\int_0^\infty f(u) u^{\frac{1}{2}} du = 1. \tag{2}$$

Carleton and Megill [1962] have described the calculation of the electron energy distribution function for altitudes of interest here. It is shown that the distribution function may be determined by solving the following differential equation.

$$[kT \delta \nu(u) + \gamma \alpha \nu(u)] \frac{\partial f}{\partial u} = - \delta \nu(u) f(u) - Q(u) \tag{3}$$

where

k is the Boltzmann constant

T is the temperature of the neutral particles

ν is the elastic collision frequency $\Sigma N_i \sigma_i v$ where N_i is the density of gas i and σ is the elastic scattering cross section for momentum transfer.

δ is the average fractional energy lost per elastic collision $\frac{2m}{M}$ where m is the electron mass and M is the mass of the gas particle.

γ is $\frac{2m}{3}\left(\frac{eE}{m}\right)^2$, e being the electronic charge and E the rms electric field,

$$Q(u) \text{ is } \sum_{ij} N_i\, u^{-3/2}\, (m/2)^{-1/2} \times$$

$$\int_0^\infty [u' + u_{ij})\, \sigma_{ij}\, (u' + u_{ij})\, f\, (u' + u_{ij}) - u'\, \sigma_{ij}\, (u')\, f\, (u')]\, du'$$

where σ_{ij} and N_i are as in equation (1) and u_{ij} is the energy required to excite the state u_{ij}. The summation is over all inelastic states j for each gas i.

α is a scaling parameter on the electric field expressed as

$$\frac{\nu^2 + \omega^2 + \omega_B{}^2}{[\nu^2 + (\omega - \omega_B)^2][\nu^2 + (\omega + \omega_B)^2}$$

where ω is the angular frequency of the exciting field E and ω_B is the gyro frequency of the electron in the earth's magnetic field B where $\omega_B = \frac{eB}{m}$.

The solution of (3) is carried out numerically in order to obtain the desired distribution function, using experimental cross sections where available, and theoretically estimated ones elsewhere. A list of the cross sections used for these and other calculations has been given by Megill and Carleton [1964].

3. Scaling Parameters

While one may calculate the expected excitation for any given power density, excitation frequency, and collision frequency, the number of such calculations required to cover all possible cases is very large. We search, therefore, for scaling parameters in the theory which will allow more general application of calculated values.

If we investigate (3) in detail, we find that (after dividing through by $\nu(u)$ for convenience) the left hand side of the equation constitutes a kind of "driving function" which describes the manner in which the electrons gain energy while the right hand side describes the mechanisms which will cause the electrons to lose energy. We further see that on the right hand side of (3) only the parameters of the gas enter. The only reference to the mechanism which increases the electron energy then, is inside the brackets on the left hand side of the equation ($kT\,\delta + \gamma\,\alpha$). Recall that we have divided the equation by $\nu(u)$.

The term $kT\delta$ presents a base energy (due to the neutral gas temperature) which is the electron energy for zero electric field. We have, then, as the driving function ϵ by which the electrons gain energy

$$\epsilon = \frac{2}{3} m\left(\frac{eE}{m}\right)^2 \frac{\nu^2 + \omega^2 + \omega_B^2}{[\nu^2 + (\omega - \omega_B)^2][\nu^2 + (\omega + \omega_B)^2]}. \tag{4}$$

Now let us examine expression (4) for limiting cases. In the ionosphere we have a rapidly decreasing number density with height so that the collision frequency $\nu = N\,\sigma\,v$ is also a rapidly varying function of height. Consider a beam of radiation extending upward through the ionosphere. It will, except for a small transition region, be in a situation in which $\nu \gg \omega \pm \omega_B$ or $\nu \ll \omega_B$. An exception is the condition $\omega = \omega_B$ about which more will be said later. We will, accordingly, consider these two cases in sequence.

When $\nu \ll \omega$ and if $\omega_B < \omega$,

$$\epsilon = \frac{2}{3}\frac{e^2}{m}\left(\frac{E}{\omega}\right)^2$$

which indicates that the mechanism by which the electrons gain energy is independent of the pressure of the gas and is only dependent upon its character as described by the right hand side of (3).

On the other hand, if $\nu \gg \omega \pm \omega_B$ then (4) reduces to

$$\epsilon = \frac{2}{3} \frac{e^2}{m} \left(\frac{E}{\nu}\right)^2$$

which, since $\nu \propto N$ and N is proportional to the pressure, yields the scaling factor E/P which is commonly used in gaseous electronics.

When $\omega = \omega_B$, gyro resonance exists. For purposes of calculating distribution functions, this may be considered to be the same as if there were a dc field. This is strictly true only if the radiation is circularly polarized in the extraordinary mode. For most purposes of interest in ionospheric problems, however, such an approximation is adequate.

In general, the electric field of importance in these calculations will be that present in the ionosphere at the height for which the calculations are being made. This field is, of course, dependent upon the power of the transmitter, the gain of the antenna and the absorption of the radiation below the point of interest. The calculation of the absorption of the radiation is in itself a difficult problem which is not discussed here.

We shall define two parameters then, in terms of which we shall present the data. These we will call the hf or high frequency and the lf or low frequency reduced power $(P_r)_{hf}$ and $(P_r)_{lf}$ where

$$(P_r)_{hf} = \frac{1}{\eta} \left(\frac{E}{\omega}\right)^2 \tag{5a}$$

and

$$(P_r)_{lf} = \frac{1}{\eta} \left(\frac{E}{N}\right)^2. \tag{5b}$$

If E is in volts per cm and η is in ohms then these quantities have units of watts $cm^{-2}sec^{2}$ and watts $cm^{-2}cm^{6}$ or watts cm^{4} if N is in units of number per cubic centimeter. These units, while they may appear unwieldly, are convenient for application to geophysical problems.

The power required from an antenna in order to generate a specific effect may in turn be calculated from

$$P_{antenna} = \frac{4\pi(P_r)_{hf}}{AG} h^2 \cdot \omega^2 \tag{6a}$$

or

$$P_{antenna} = \frac{4\pi(P_r)_{lf}}{AG} h^2 \cdot N^2 \tag{6b}$$

where h is the height at which the excitation rate is required, N is the number density at that height and G is the gain of the antenna. A is the amount of power absorbed below height h. For the purposes of our further calculations A is considered to be one.

4. Observable Radiations

Before calculating excitation rates of various states, let us first consider what radiations are likely to be visible from ground level. The first condition, of course, is that the experiment be done at night. Because we are dealing here with excitation by low energy electrons which already exist in the ionosphere as opposed to those created in a discharge we need consider radiation from states which can be excited from ground state atoms or molecules. The density of metastable states which can be excited to higher levels and will then radiate are negligible. Ground state rotational or vibrational states of the major molecular constituents will not radiate, and so, energy

put into these states will not result in visible radiation. We discuss here only the excitation of electronic levels in the atoms and molecules which may possibly re-radiate. In calculation of the distribution function, however, all inelastic states have been considered even though they are not discussed explicitly in this paper. In nitrogen, such states require so much energy to be excited (greater than 6.2 ev) that excitation is unlikely except in extremely powerful systems. In O_2 the three most easily excited electronic states are the $a^1\Delta_g$ (0.98 ev), the $b^1\Sigma_u^+$ (1.65 ev), and the $A^3\Sigma_u^+$ (4.47 ev). Of these, the first two have extremely small cross sections for direct excitation by electron collisions [Schulz and McDowell, 1962]*, so that we need to discuss only the excitation of the $A^3\Sigma_u^+$ state which radiates in the Herzberg bands. These bands are seen in the night airglow and are rendered difficult to observe because the energy is distributed into many lines in the band. However, fairly small amounts of excitation should be detectable with sophisticated techniques.

This leaves the ^1D (1.96 ev) and ^1S (4.17 ev) states of atomic oxygen. The former would be undetectable because it is strongly deactivated by collisions with O_2 at altitudes below about 140 km. These calculations do not apply in any practical situation for altitudes above 140 km because the dominant energy loss term there would be that due to diffusion out of the exciting beam, an effect which is not included in the calculation of the distribution function. $O(^1S)$ is the strongest line of the normal night airglow and

---

* These states are, of course, excited to some extent; but with the method of excitation considered here, we find it will never, at any power less than that which is required for breakdown, be possible to excite a detectable amount of radiation from them.

variations of intensity should be readily observed if excitation is accomplished. This leaves then, as the two most readily observed emissions $O_2(A^3\Sigma_u^+)$ and $O(^1S)$ both of which require more than 4 ev for excitation. The generation of electrons of this energy is particularly difficult in air because there is a very large cross section for energy loss to the vibrational states of N_2 for all electrons between about 1.7 and 4 ev [Schulz, 1959]. It is of interest to know, however, just what power would be required in order to obtain detectable intensities. In figures 1a and 1b, we plot specific rates of excitation for the above two states, as well as two body attachment rates and ionization rates, as a function of the two previously defined reduced powers. In order to obtain the excitation rate at a particular power and height, one needs to multiply the value given in the figure by electron density and constituent density. The cross section for the excitation of the $O_2(A^3\Sigma_u^+)$ is estimated from the data of Schulz [1962], that for the excitation of $O(^1S)$ from the theoretical calculations of Seaton [1953]. As an example let us suppose that we wish to know the power required to excite 100 rayleighs* of 5577 Å radiation (from $O(^1S)$ in a slab of the ionosphere between 90 and 100 km). Then this means that we must excite 100 atoms per cubic centimeter per second, which will later radiate. If we assume that there are on the average 500 electrons/cm^3 and 2×10^{12} oxygen atoms/cm^3 in the slab, then we would expect to see approximately 100 rayleighs for a specific excitation rate of $O(^1S)$ equal to 10^{-13} which requires from figure 1a a reduced hf power of 3.3×10^{-21} watts seconds. This results (using 5a) in a required power flux of 8×10^{-5} watts/cm^2, if

---

* The rayleigh is defined as 10^6 emissions per cm^2 column through the radiating medium.

we are considering a transmitter at 50 megacycles. Using (6a) it is found that 9×10^{10} watts are required for an isotropic radiator. If we have an antenna gain of 10^4, we then need 9 megawatts transmitted from the antenna. The very large power required for minimum detection conditions indicates that experiments resulting in the excitation of optical radiation may not be economically feasible unless the installation can be justified for other applications.

An additional consideration should be made at this point. The calculations made here yield average excitation rates while the power is turned on, and after a steady state has been established. The time required to establish equilibrium is approximately equal to the product of the average fractional energy loss per collision (averaged over all types of collisions) and the collision frequency. For air the average energy loss is not constant with energy, but for rough calculations may be assumed to be of the order of 10^{-3}. For the convenience of the reader and those who might wish to extend the calculations to include absorption we plot in figures 2a and 2b the average collision frequency, normalized to one particle/cm^{-3} and the average energy against the two previously defined reduced powers. The relaxation time will vary from the order of a microsecond at 60 km height to the order of a millisecond at 100 km height. Transmitters must, therefore, be operated with pulse lengths long compared to these times for steady state to be achieved. For the higher heights this puts severe requirements on the transmitter because of the long pulses required.

One other parameter which must be considered for the case of $O(^1S)$ is that the state has a mean life of the order of one second. For this reason the effect of pulsed operation will be to reduce the observed change in intensity by the duty cycle. It is to be noted that this does not mean that the

average power flux is the important quantity. The extremely non-linear nature of the intensity vs power curve indicates that the transmitter should be operated at as high a peak power as possible and then for as high a duty cycle as is compatible with this condition.

5. Modification of the Ionosphere by Attachment.

Another possible experiment of interest is the modification of the atmosphere by attaching the electrons to O_2 molecules. The problem has been discussed in some detail by Molmud [1964] for attachment by three body attachment,

$$O_2 + e + M \rightarrow O_2^- + M. \qquad (7)$$

The rate of this process is probably the easiest one to change with transmitted rf power because there is a maximum in the rate at about 0.1 ev average electron energy. [Chanin, Phelps, and Biondi, 1959].

There is a second process which occurs at higher energies. This is dissociative attachment of O_2, by the following reaction,

$$O_2 + e \rightarrow O^- + O. \qquad (8)$$

This process has a threshold at 4 ev with a maximum at 6.3 ev [Schulz, 1962]. We may calculate this rate in the same manner that one calculates attachment rates. These rates are given in figures 1a and 1b. In the example previously discussed, if we were exciting 100 rayleighs of the 5577 Å line we would expect electrons to attach at a rate of 3% per second. The electrons would effectively disappear at this rate until they are re-released either by collisional detachment or by the reverse of process (8). These rates are not well known and it might be that an ionospheric experiment would be one of the best with which to determine their rates.

6. Breakdown in the Ionosphere

The general technique of calculation used here can, in principle, be used to compute the power required to "breakdown" the ionosphere. In the lower ionosphere one may, to a large extent, ignore diffusion losses and may therefore compute the rate of attachment as a function of power and the rate of ionization as a function of power. As the ionization rate becomes the larger the ionization density will grow exponentially until some limiting process sets in. The details of an approximate treatment of some of these processes is given by Lombardini [1963]. In addition he gives comparisons to experimental data which indicate the order of the accuracy of the calculations. Specific rates of ionization as a function of $(P_r)_{hf}$ and $(P_r)_{lf}$ are shown in figures 1a and 1b.

7. F Region Emissions

In the investigation of possible modification of airglow intensities another possibility of interest presents itself in terms of the F region emission from $O(^1D)$ at 6300 Å. This radiation is presumably due to the two step recombination of O^+ by means of

$$O^+ + N_2 \rightarrow NO^+ + N \tag{9}$$

and

$$NO^+ + e \rightarrow N + O(^1D). \tag{10}$$

The rate of (9) is the slower and controls the emission rate so that the intensity of 6300 Å radiation is proportional to the product of the O^+ and N_2 densities.

Farley [1962, 1963] has shown that by using power at the plasma frequency it is possible with reasonable power to heat ($\sim$ 250 kw) the electrons

enough that the enhanced diffusion decreases the electron and ion density by about ten percent or more. This should, in turn, decrease the intensity of 6300 Å radiation by ten percent and serve as an experimental check on the recombination process in the F region. It should be noted that the mean life of the $O(^1D)$ state is 100 sec, so that a transmitter which will perform the described experiment must be operated cw.

8. Conclusions

The requirements on large power transmitters which can be expected to yield observable amounts of optical radiation have been expressed quantitatively for the two most likely radiations. We find that the size of the required installations is so large that such experiments may not be economically feasible at the present time.

9. Acknowledgements

The author wishes to recognize the very considerable contributions of Mrs. J. D. Droppleman in the performance of the calculations and the preparation of the figures.

References

Bailey, V.A. (1959), Some possible effects caused by strong gyrowaves in the ionosphere. J. Atmos. Terret. Phys. 14, 229-324.

Carleton, N.P., and Lawrence R. Megill (1962), Electron energy distribution in slightly ionized air under the influence of electric and magnetic fields, Phys. Rev. 126, 2089-2099.

Chanin, L.M., A.V. Phelps, and M. Biondi (1959), Measurements of the attachment of slow electrons in oxygen, Phys. Rev. Let. 2, 344.

Clavier, P.A. (1961), Man-made heating and ionization in the upper atmosphere, J. Appl. Phys. 32, 570-577 and erratum 2651.

Farley, D.T. (1963), Artificial heating of electrons in the F region of the ionosphere, J. Geophys. Res. 68, 401-413.

Lombardini, P.P. (1963), Non-linear Conference, NBS, Boulder, Colorado

Megill, Lawrence R., and J.H. Cahn, (1964), Calculation of electron energy distribution functions in the ionosphere, to be published.

Megill, Lawrence R., and N.P. Carleton (1964), Excitation by local electric fields in the aurora and airglow, J. Geophys. Res. 69, 101-122.

Molmud, P. (1963), Non-linear Conference, NBS, Boulder, Colorado

Schulz, G.J. (1959), Measurement of excitation of N_2, CO, and H_e, by electron impact, Phys. Rev. 116, 1141-1147.

Schulz, G.J. (1962), O_2, CO, and CO_2 by electron impact, Phys. Rev. 128, 178-

Schulz, G.J., and J.T. McDowell (1962), Excitation of vibrational and electronic levels in O_2 by electronic impact, Phys. Rev. 128, 178-

Seaton, M.J. (1953), The Hartree-Fock equations for continuous states with application to electron excitation of ground configuration terms of OI, Phil. Trans. Roy. Soc. 245, 469.

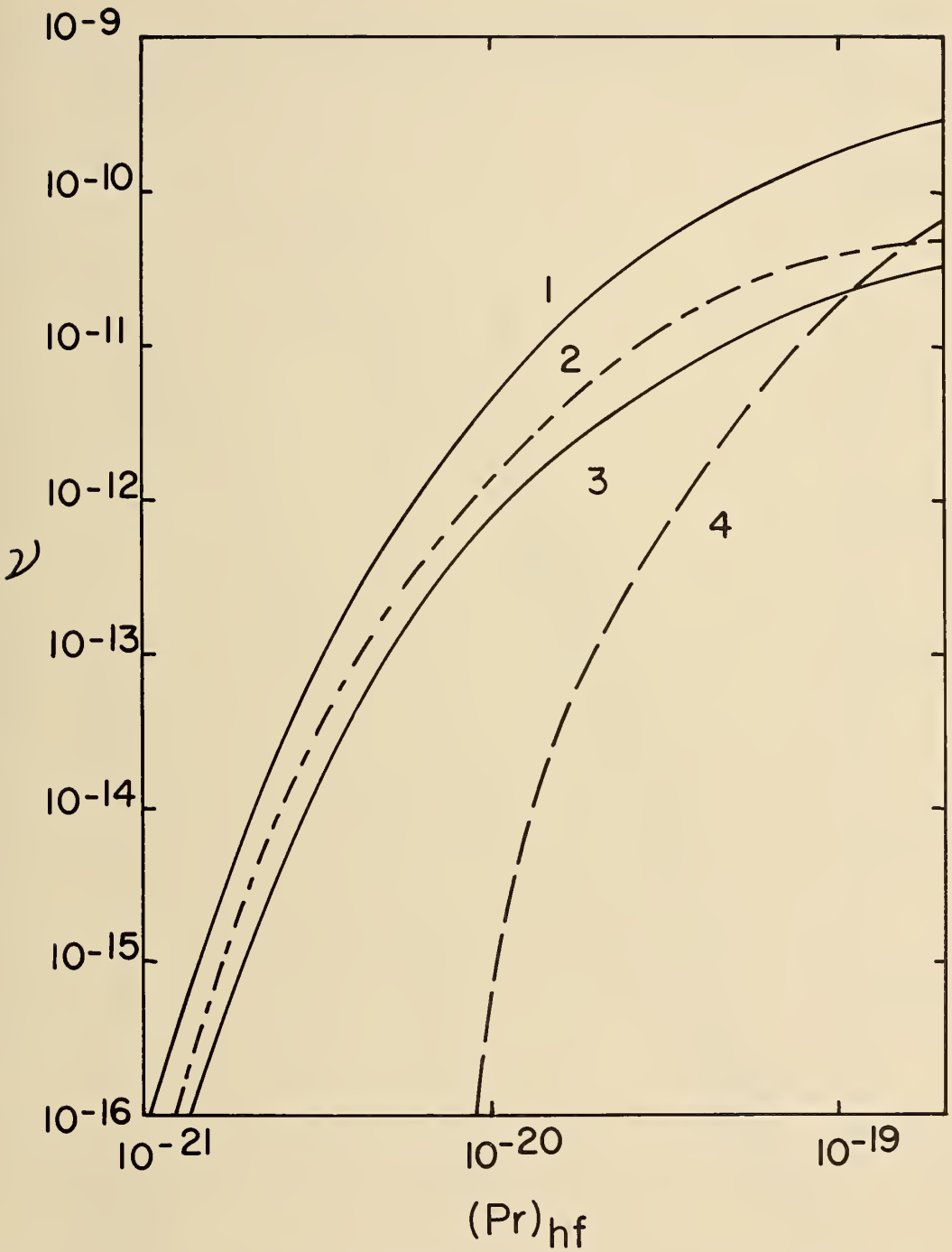

Figure 1a. This figure shows the rate of excitation of $O(^1D)$ (2), the rate of attachment to O_2, (3), the rate of excitation of $O_2(A^3\Sigma_u^+)$, and (4) the rate of ionization as a function of reduced power with high frequency excitation. To obtain an absolute rate the ordinate should be multiplied by the constituent density and the electron density. The power flux in watts cm^{-2} may be had by multiplying the abscissa by $(2\pi f)^2$ where f is the frequency of excitation. These curves should be used if $\upsilon < \omega \pm \omega_b$.

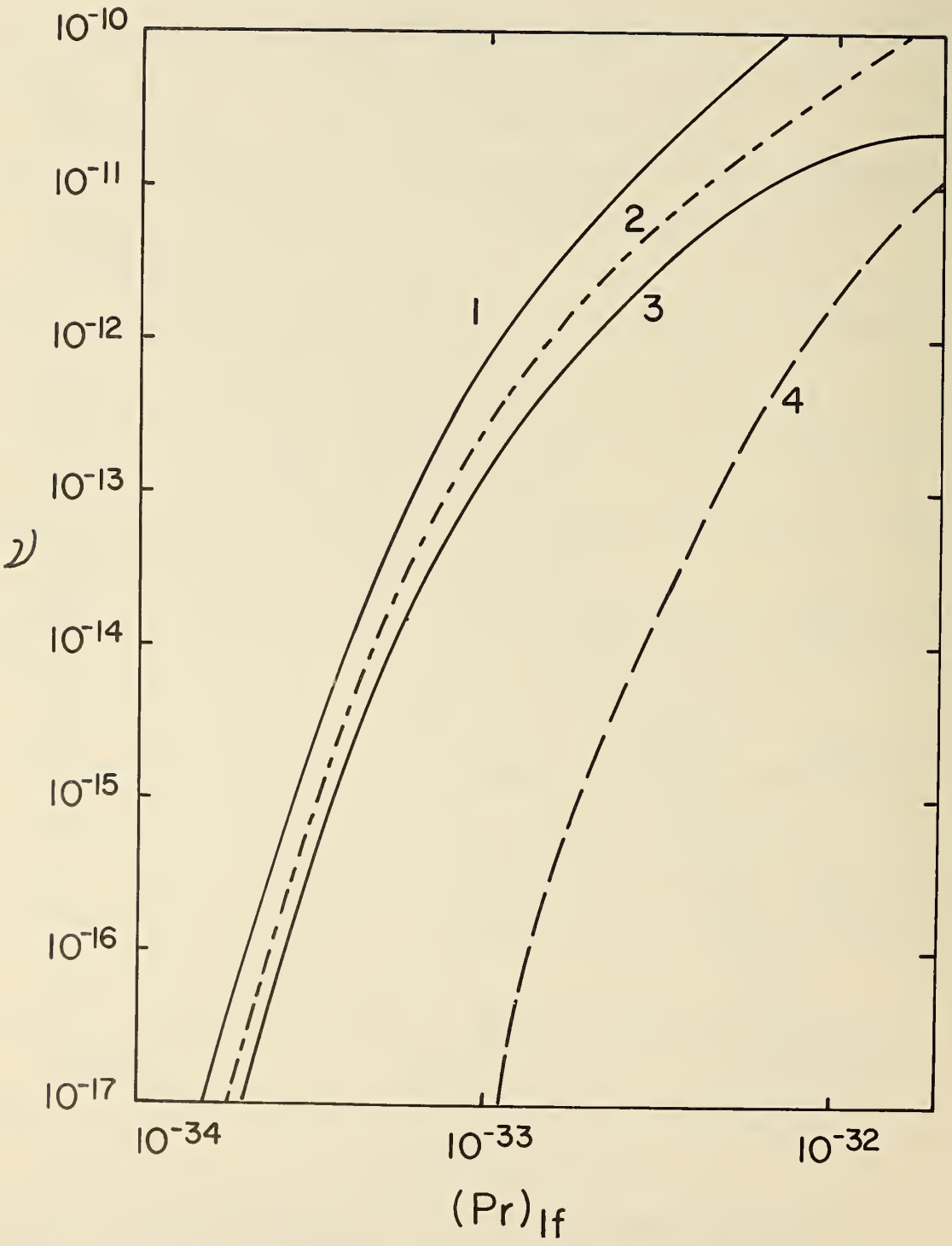

Figure 1b. This figure shows the same quantities as figure 1a except that they are plotted vs the reduced power for low frequency excitation. In this case the abscissa should be multiplied by the square of the total number density in particles per cm^3 to yield watts cm^2. These curves should be used when $\upsilon > \omega \pm \omega_b$ and for the gyro-resonance condition.

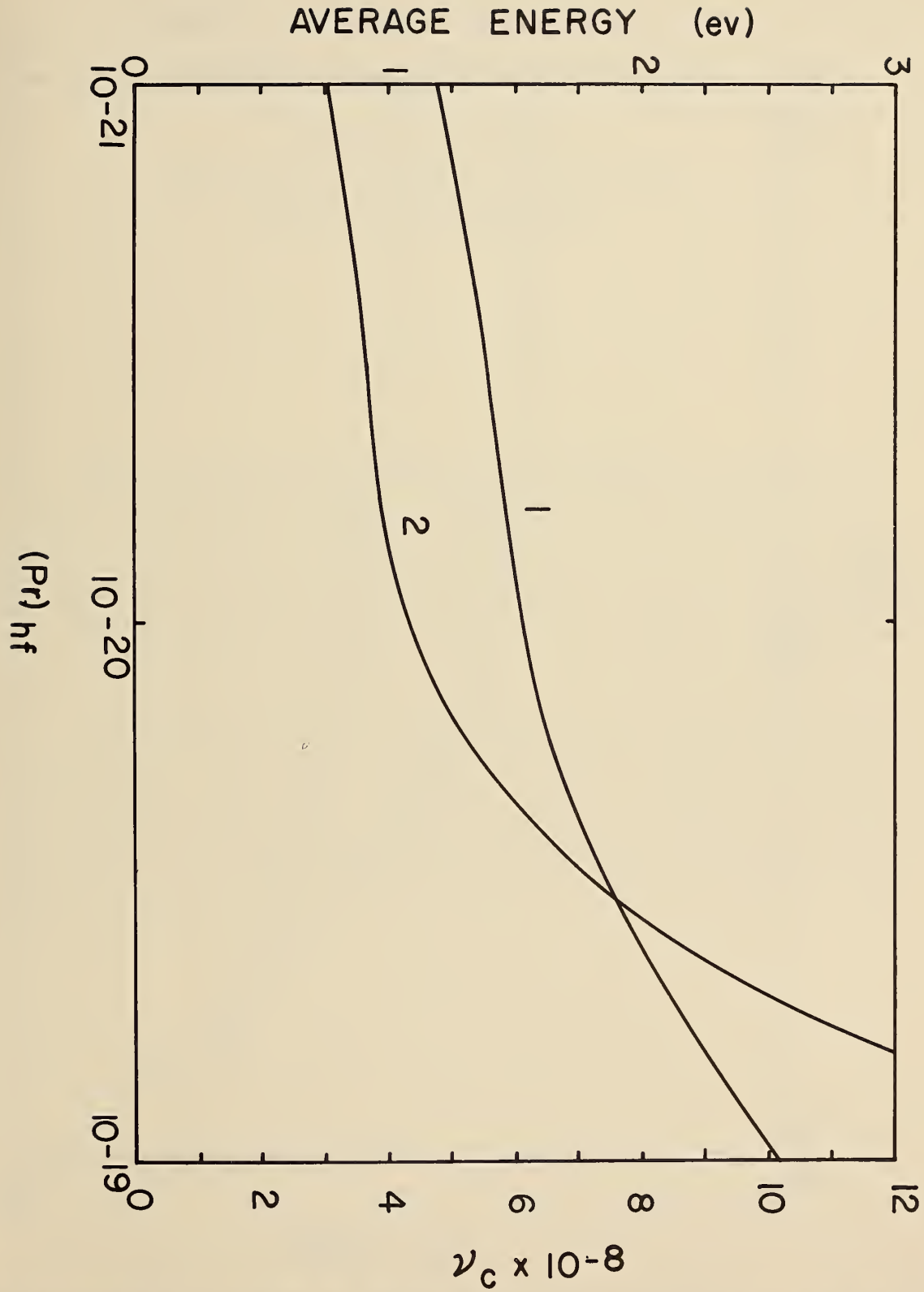

Figure 2a. The abscissa is as defined in fig. 1a while the ordinates are the average collision frequency (curve 2) per neutral particle in sec^{-1} and the average energy in ev (curve 1). The averages are over the calculated distribution functions.

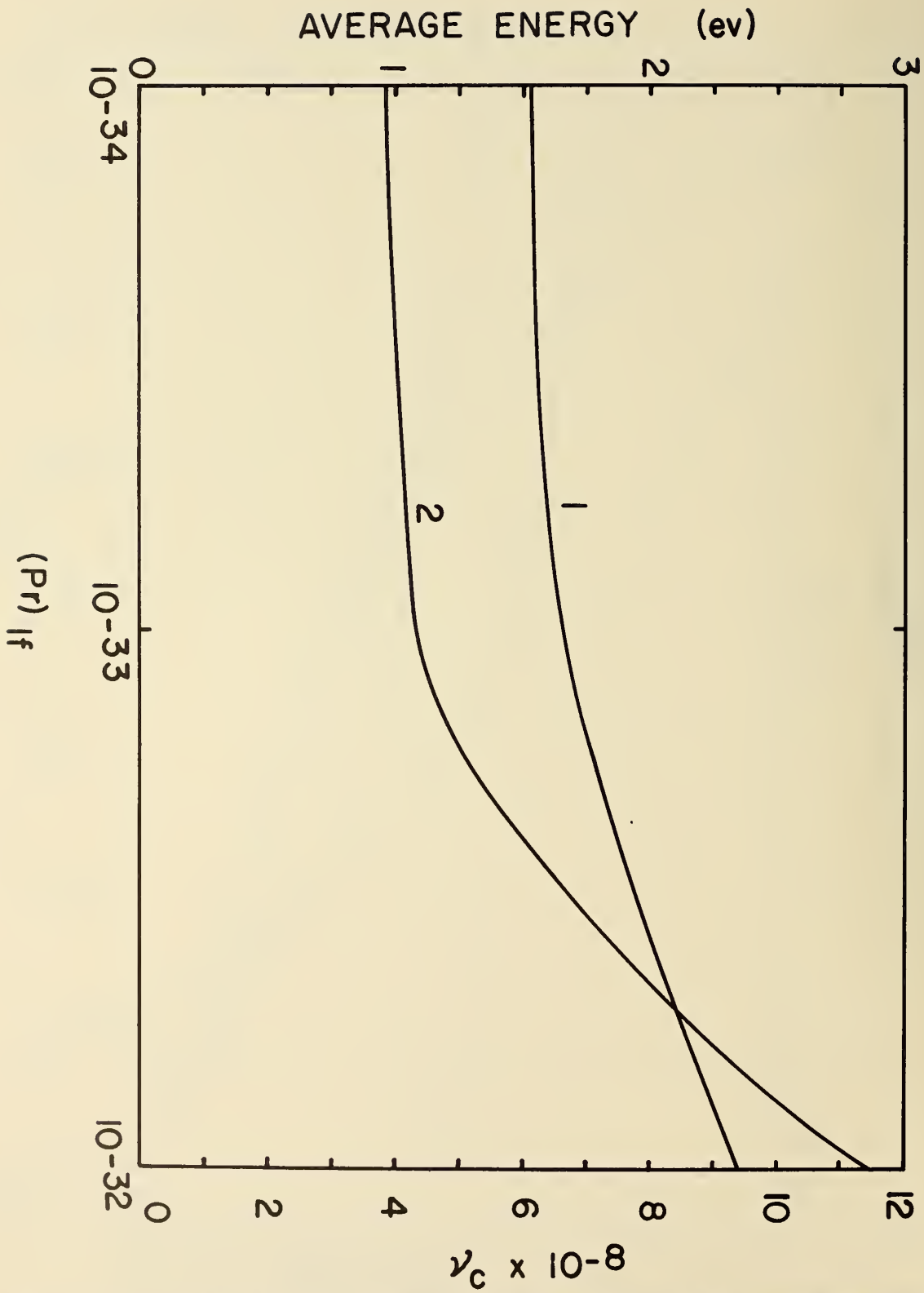

Figure 2b. The abscissa is as defined in fig. 1b while the ordinates are as defined in fig. 2a.

Alteration of the Electron Density of the Lower Ionosphere with Ground Based Transmitters

Pietro P. Lombardini

Moore School of Electrical Engineering
University of Pennsylvania

Using computational techniques as described by Carleton and Megill, and Megill to calculate the difference between rate of attachment of electrons to O_2 and the ionization rate in air as a function of electric field, the power required to create breakdown in the ionosphere has been calculated. These calculations are compared with extrapolated microwave breakdown data and found to agree satisfactorily.

The propagation of the primary beam is altered by the electrons created by it. This gives origin to a non-linear problem, which is very difficult to deal with in the general case. However, a steady state approximate solution has been found, considering diffusion in one dimension. The solution is applied to the design of a possible atmospheric experiment.

1. INTRODUCTION

The possibility of altering the characteristics of the lower ionosphere utilizing ground-based transmitters has been considered by several investigators. In particular, studies have been made concerning the achievement of a decrease in electron density [1], an increase in the electron collision frequency [2], and the excitation of air glow [3., 4]. Little attention, however, has been given to utilizing ground-based transmitters to achieve an increase of electron density. The aim of this paper is to investigate the paramters involved in obtaining such an increase.

The first step of the present work involves the definition of breakdown as created by a high frequency electromagnetic wave in a boundless, slightly ionized homogeneous medium. Experimental data for these conditions of breakdown are not available; however, the electric field necessary to initiate breakdown (breakdown threshold) may be obtained in either of the following two ways. One way consists in performing direct laboratory measurements of breakdown in finite enclosures, and then scaling the results to the open air case. The other way consists of computing the electron distribution function in the mixture of gases considered (N_2, O_2 and O) and in the presence of the electric field. This distribution function computed by utilizing the experimental data for the various cross sections involved is in turn used to evalute the "electron attachment and ionization frequencies" (i.e., ν_a and ν_i respectively). The breakdown threshold, E_b (defined as that field for which $\nu_i = \nu_a$), may therefore be calculated.

The breakdown threshold is shown to decrease for certain altitudes at a faster rate than that specified by the inverse of the distance law which applies to VHF waves in the far field of the transmitter. From this, it is concluded that breakdown can be achieved if the proper power is available. Furthermore, it is shown that once breakdown is obtained,

the steady state electron density is critically dependent upon the difference of the altitude rate of changes of the breakdown field and the inverse of the distance field.

Because of this dependence on the altitude rate of change of the exciting field, greater electron densities may be achieved using a sufficiently large antenna such that breakdown occurs in the near field.

A characterization of the attachment-ionization process is shown to indicate an altitude for which the optimum breakdown efficiency exists.

2. CHARACTERIZATION OF THE BREAKDOWN THRESHOLD ELECTRIC FIELD

A VHF radiowave traveling upward in the D or in the lower E region is assumed to be idealized as a plane wave propagating in a weakly ionized, quasi-homogeneous plasma. The breakdown conditions applicable may therefore be identified with those pertaining to an electric field of constant orientation and amplitude in a weakly ionized air. In general, the breakdown condition of an electric discharge is defined by the electric field (breakdown threshold, E_b) for which equilibrium is achieved between the gain of electrons due to ionizing collisions, and the loss due to the various mechanisms which remove electrons from the discharge region (e.g., attachment, recombination, and diffusion). Because of the absence of walls, and the weak ionization for the case considered, the breakdown is predominantly controlled by attachment, while diffusion has a negligible role. Conditions of this kind are rarely encountered in the laboratory where the walls confining the discharge play a considerable role in removing electrons. Brown and Rose [5] have shown that the experimental data of microwave breakdown threshold in air can be characterized by a curve of $\frac{E_{eff}}{p}$ versus the product pL, where E_{eff} is the "effective" breakdown electric field defined by the formula

$$E_{eff} = E_b \frac{\nu}{\sqrt{\nu^2 + \omega^2}} \qquad (1)$$

where,

ν = average electron collision frequency

ω = radian frequency of wave

p = air pressure

L = breakdown gap spacing .

This curve flattens out for increasing values of pL approaching the asymptotic value of 3×10^3 V/m x (mm of Hg). Introducing this value into Equation (1), considering a collision frequency as a function of pressure given by 5.3×10^9 p (cps) [6], one obtains the following simple equation relating the r m s value of the breakdown threshold field in air with the pressure,

$$E_b = 3 \times 10^3 \sqrt{1 + \left(\frac{\omega}{5.3 \times 10^9 \, p} \right)^2} \qquad (2)$$

Specification of breakdown conditions in open space may also be obtained utilizing a different approach. That is, the energy distribution function of the electrons under the influence of an oscillating electric field in a mixture of N_2, O_2 and O may be calculated. In this approach, the experimental data introduced are the collision cross sections of the electrons with the above mentioned components of air. Megill and Carleton [7] have given a detailed analysis of the problem of determining the electron energy distribution function under these conditions. Megill has constructed a computer program for the IBM 704 of Raytheon, which gives the electron energy distribution function, f (u), for the interval of electron energy, u, from 0.01 to 20.0 e.v., and having neutral particle, density, temperatures, geomagnetic field, frequency, and the electric

field intensity as parameters. The solution applies to a situation in which the total number of electrons does not change. Providing that the rate of change of the total number of electrons is small, and incorporating perturbation techniques, the solution f (u) may be used for evaluating the rate of increase of electrons due to ionizing collisions,

$$\nu_i = \frac{\sum_i N_i \int_o^\infty u\, f(u)\, \sigma_{iI}(u)\, du}{\left(\frac{m}{2}\right)^{1/2} \int_o^\infty u^{1/2} f(u)\, du} \tag{3}$$

or the rate of decrease of electrons due to attachment,

$$\nu_a = \frac{\sum_i N_i \int_o^\infty u f(u)\, \sigma_{iA}(u)\, du}{\left(\frac{m}{2}\right)^{1/2} \int_o^\infty u^{1/2} f(u)\, du} \tag{4}$$

where N_i, σ_{iI} and σ_{iA} are the concentration, ionization cross section and attachment cross section for the i^{th} component of air considered (i.e., N_2, O_2, and O) and m is the electron mass. In the actual computations, the only attachment phenomenon considered is the dissociative attachment, $O_2 + e \longrightarrow O + O^-$. Ionization and attachment collision frequency obtained in this way may be characterized as a function of the electric field intensity E, holding all other parameters constant. ν_a grows rapidly for moderate fields and quickly tends to saturate, while

ν_i starts a quick rise at higher field intensities. The crossing of the two curves ($\nu_i = \nu_a$) corresponds to the breakdown threshold E_b. Using the atmospheric model presented in the Handbook for Astronautical Engineering [8], extensive computations have been made for the following choice of parameters: f= 50 mc/s, geomagnetic field = 5×10^{-5} weber/m^2, and concentrations and temperatures corresponding to the height interval, 55 - 105 KM. The corresponding values of E_b as a function of altitude are shown in Figure 1 by the solid curve. In the same figure, the dotted curve shows the E_b altitude variation as obtained using Equation (2). The good agreement between the two methods of approach is apparent from this figure. The collision frequencies given by (3) and (4) are required for evaluating the rate of change of the total number of electrons given by

$$\frac{\partial N}{\partial t} = (\nu_i - \nu_a) N \cdot \qquad (5)$$

Computed values of $\nu_i - \nu_a$ are plotted in Figure 2 as a function of the excess of electric field, ΔE, and the same range of paramters previously specified for Figure 1. The relationship between $\nu_i - \nu_a$ and $\frac{\Delta E}{E_b}$ is approximately linear.

In Figure 3, $\nu_i - \nu_a$ is plotted vs. height for constant electric field above threshold breakdown. This figure shows that there exists an altitude at which the creation of new electrons occurs with a maximum efficiency. This optimum height corresponds to the condition for which the average collision frequency approximately equals the frequency of the electric field; i.e.,

$$\nu\ (h,\ E_b) \simeq f \quad . \qquad (6)$$

FIG. I BREAKDOWN THRESHOLD ELECTRIC FIELD VS. ALTITUDE FOR A FREQUENCY OF 50 mc/s

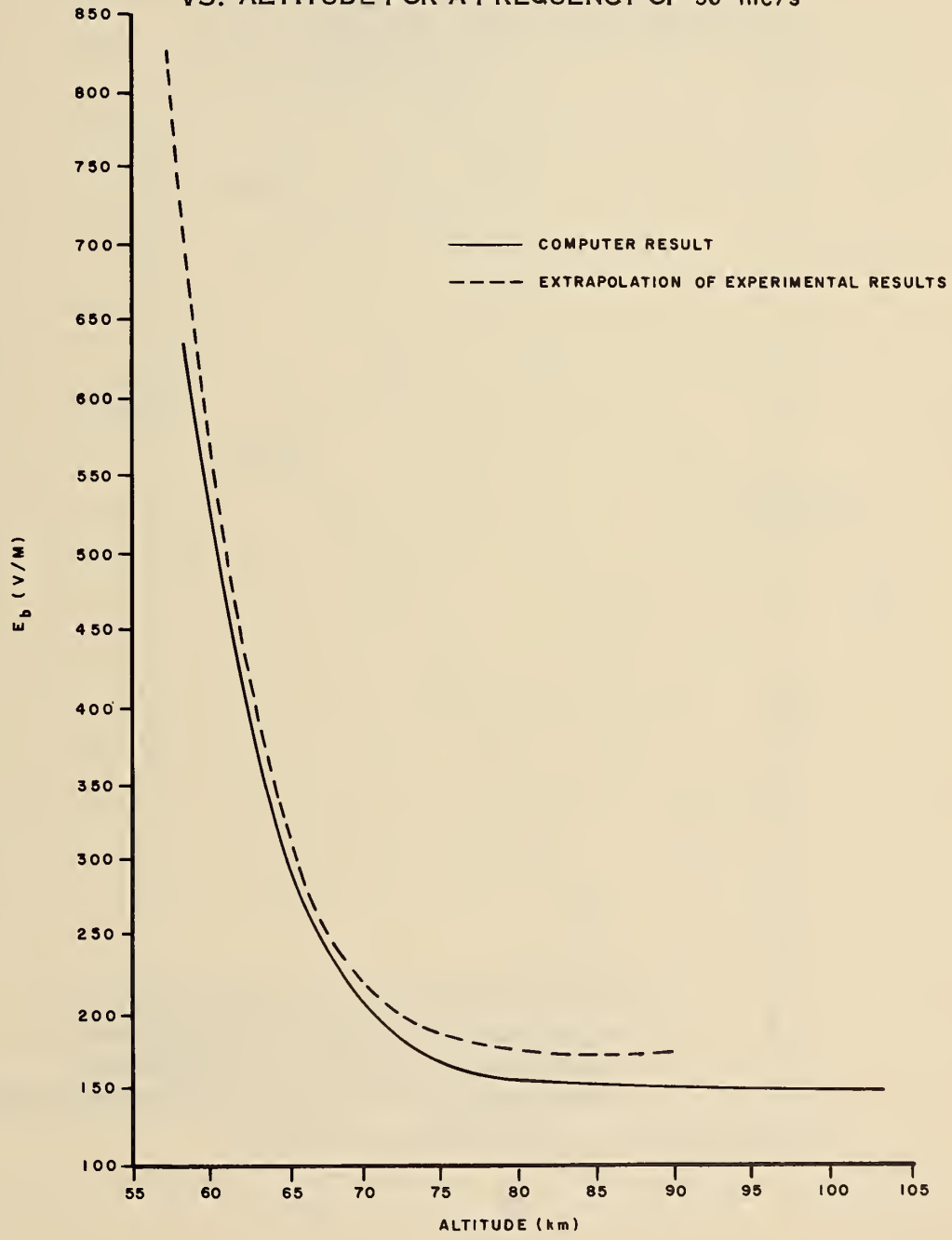

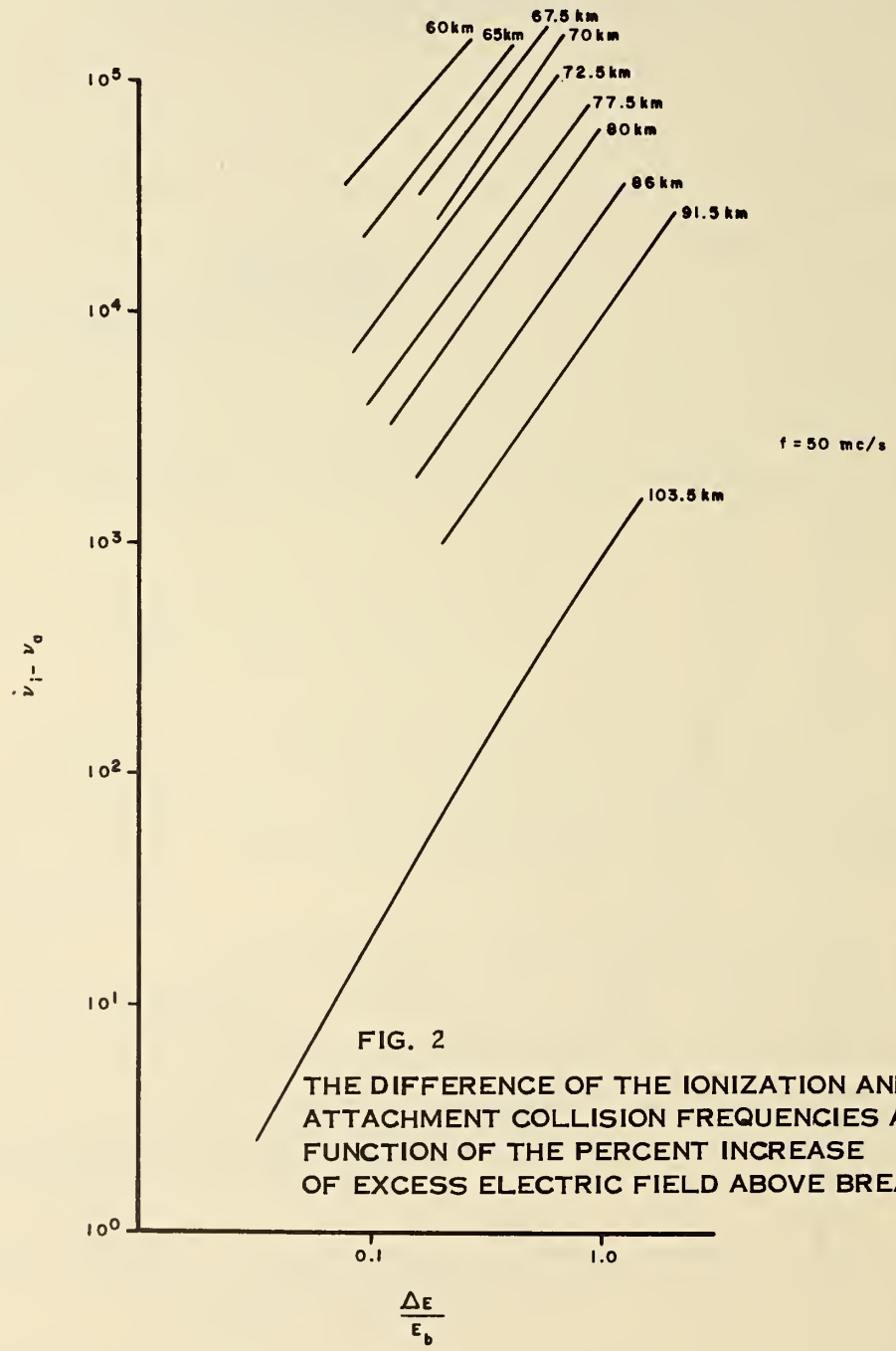

FIG. 2

THE DIFFERENCE OF THE IONIZATION AND ATTACHMENT COLLISION FREQUENCIES AS A FUNCTION OF THE PERCENT INCREASE OF EXCESS ELECTRIC FIELD ABOVE BREAKDOWN

FIG. 3 THE DIFFERENCE OF THE IONIZATION AND ATTACHMENT COLLISION FREQUENCIES AS A FUNCTION OF ALTITUDE FOR THE FIELD STRENGTHS INDICATED

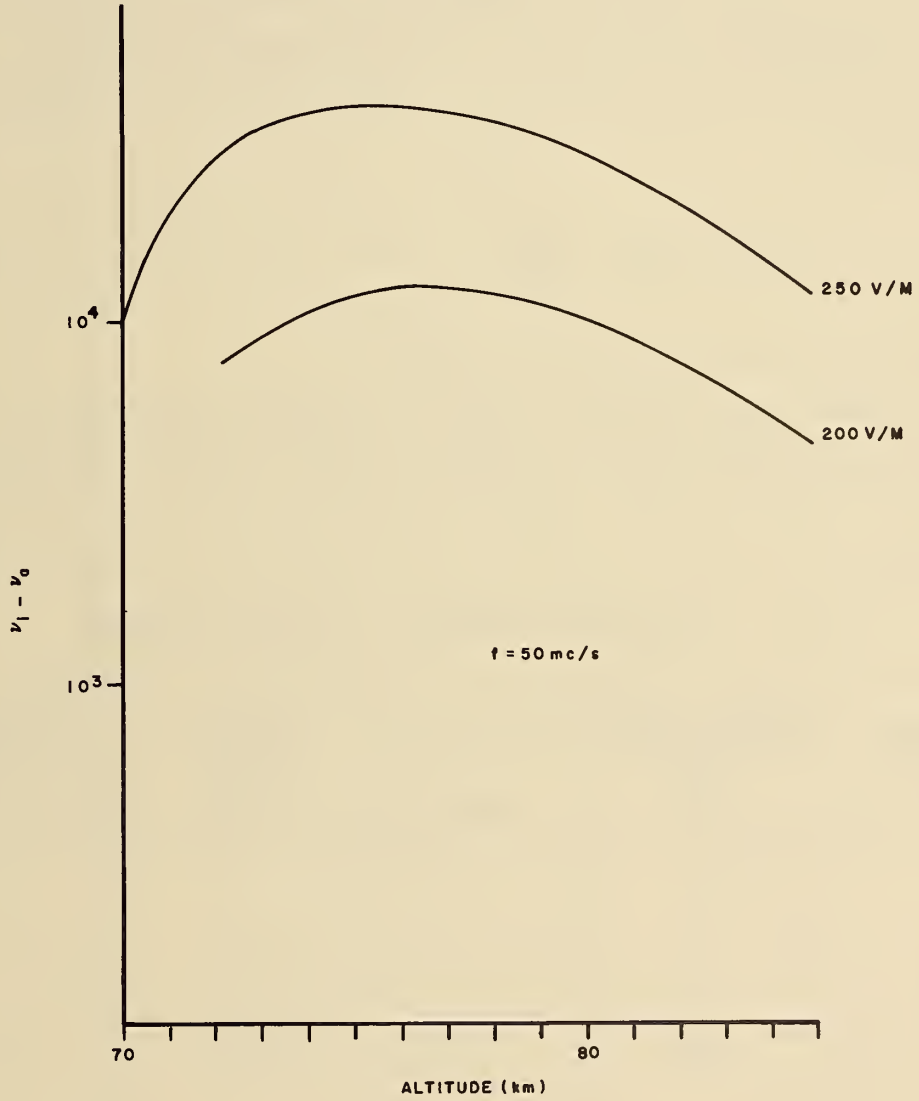

Figure 4 shows the relationship between frequency and altitude as obtained by Equation (6), using for ν, McDonald's [6] approximation. To each of these frequencies corresponds a breakdown threshold electric field, which may be determined using Equation (2). The ground-based upward radiating transmitter needed for obtaining the above defined electric field, E_b, at the altitude given by Figure 4, must have a power-gain product, PG, which for free wave propagation is given by

$$PG = 4 \pi h^2 \frac{E_b^2}{\eta_o} \qquad (7)$$

where η_o is the wave impedance in space.

In Table 1 are tabulated breakdown-transmitter parameters. In the last two columns of the table gain and power are given, assuming that the 1,000 foot Arecibo paraboloid antenna is used as the transmitter.

TABLE I - TRANSMITTER PARAMETERS TO ACHIEVE BREAKDOWN

BREAKDOWN ALTITUDE (km)	FREQUENCY FOR OPTIMUM IONIZATION EFFICIENCY (mc/s)	POWER X GAIN (WATT)	THEORETICAL GAIN USING ARECIBO ANTENNA	POWER NEEDED USING ARECIBO ANTENNA (MEGA WATT)
60	1,000	$1.2\ 10^{15}$	10^7	120
65	500	$3.8\ 10^{14}$	$2.5\ 10^6$	150
70	250	10^{14}	$6.0\ 10^5$	165
75	100	$2.0\ 10^{13}$	10^5	200
80	40	$3.5\ 10^{12}$	$1.6\ 10^4$	220
85	15	$5.0\ 10^{11}$	$2.2\ 10^3$	230

FIG. 4 FREQUENCY OF MAXIMUM IONIZATION EFFICIENCY VS. ALTITUDE

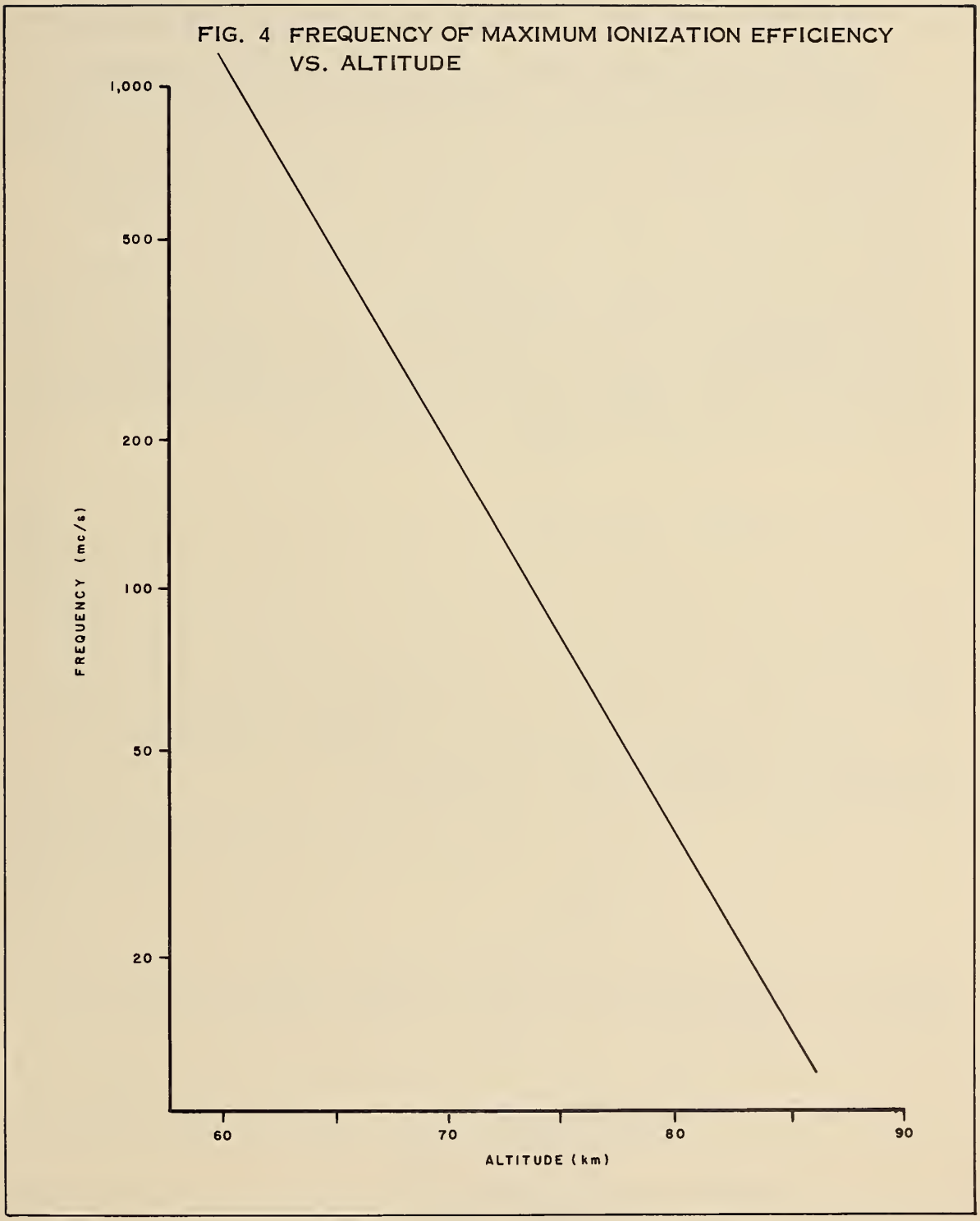

3. MAXIMUM ATTAINABLE INCREASE OF ELECTRON DENSITY

In the previous section, the conditions required for obtaining breakdown have been examined. The problem is now that of determining the maximum electron density which may be achieved using radio waves. For this purpose, consider a VHF wave propagating vertically upward. Under normal ionospheric conditions, a wave in this band of frequencies is negligibly absorbed by the ionosphere. However, when the electric field strength of the wave becomes larger than the breakdown threshold, the electron density will increase and hence the wave may suffer an exponential attenuation. In free space, the electric field of the wave may be expressed as:

$$E(x) = E_0 \, \Phi(x) \tag{8}$$

where E_0 is the amplitude of field intensity at an altitude, h_o, from the ground, where the source is assumed to be located. Here, x is the local vertical coordinate in a system whose origin is at a height, h_o, and $\Phi(x)$ represents the functional variation in the absence of absorption. In the "far field" of an antenna,

$$\Phi(x) = \frac{1}{1 + \frac{x}{h_o}} \tag{9}$$

Along the axis of a spherical antenna excited in phase and focused at h_o, $\Phi(x)$ is given by

$$\Phi(x) = \frac{\operatorname{Sin}\left(\frac{\pi D^2}{8 \lambda h_o^2} x\right)}{\left(\frac{\pi D^2}{8 \lambda h_o^2} x\right)} \tag{10}$$

where D is the antenna diameter and λ the wavelength.

If the propagation takes place in ionized air, the wave is subjected to exponential absorption. When the electron density is sufficiently low, the differential power absorbed along the wave path is

$$\frac{d}{dx}\left[\frac{E^2(x)}{\eta_o}\right] = -N(x)\,\frac{\frac{2}{3}\frac{(eE(x))^2}{m}\int_o^\infty u^{3/2}\,a(u)\,\frac{\partial f(u)}{\partial u}\,du}{\int_o^\infty u^{1/2} f(u)\,du} \qquad (11)$$

where N (x) is the electron density at the altitude $h_o + x$ and a (u) is given by,

$$a(u) = \frac{\nu}{\nu^2 + \omega^2} \qquad (12)$$

disregarding the earth's magnetic field. Proceeding to integrate Equation (11) in the interval x = 0 to the arbitrary distance x,

$$E(x) = E_0\,\Phi(x)\exp\left[-\int_o^x A(E, x)\,N(x)\,dx\right] \qquad (13)$$

where the quantity A (E, x) is a slowly varying function of E and x.

In order to simplify the problem, let us for the moment disregard diffusion. Assume that for the radio waves propagating upward with some spatial variation, $\phi(x)$ [e.g., inverse of the distance law] breakdown conditions are reached at the altitude h_1. The physical situation may be explained from Figure 5 where the spatial variation of the electric field of the wave and the breakdown threshold variation are plotted as a function of altitude. These two curves cross at two altitudes, h_1 and h_2. Consider a point located at the altitude $h_1 + x$, where the spatial variation field curve lies above the breakdown curve. Here the intensity of the wave will change with time because of the attenuation due to the time increasing electron density. Hence, assume the spatial variation curve of Figure 5 represents the established situation at time, $t = 0$. It follows at this point $(h_1 + x)$ that the electron density will start increasing exponentially with time according to the solution of Equation (5),

$$N(x, t) = N_0 \exp\left[(\nu_i - \nu_a)\, t\right] \tag{14}$$

where N_0 is the previously existing electron density. It has already been pointed out that the quantity $(\nu_i - \nu_a)$ is critically dependent upon the quantity $\Delta E = E - E_b$ (see Figure 2). Substituting Equation (14) into Equation (13),

$$\Delta E = E_0\, \Phi(x) \exp\left[-\int_0^x A(x)\, N_0 \exp\left[(\nu_i - \nu_a)\, t\right] dx\right] - E_b(x) \tag{15}$$

Equation (15) does not take into account any mechanism limiting the growth of electron density as a function of time, such as losses due to diffusion or recombination. Therefore, for increasingly large

FIG. 5

SKETCH OF THE VARIATION OF THE FREE SPACE FIELD STRENGTH (DASHED LINE), AND OF THE BREAKDOWN THRESHOLD (SOLID LINE) VS. ALTITUDE

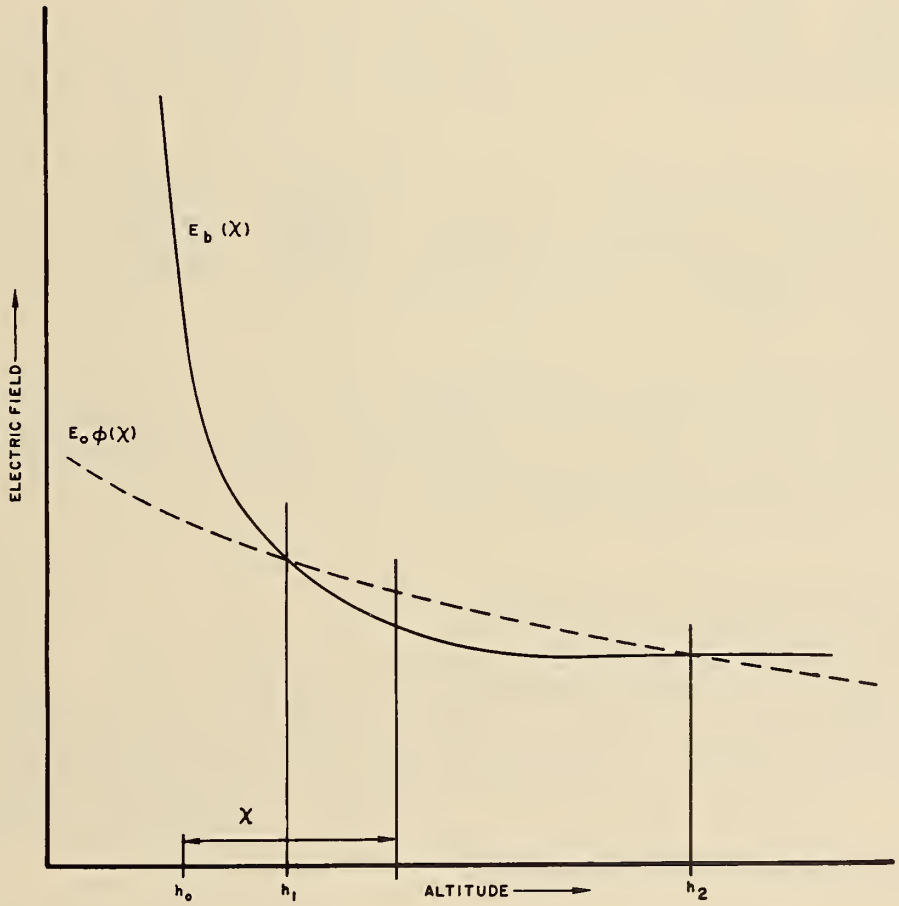

times, satisfaction of Equation (15) requires that ΔE approaches zero. In the limit condition,

$$\lim_{t \longrightarrow \infty} \int_{o}^{x} A(E, x)\, N(x, t)\, dx = - \ell n \frac{E_b(x)}{E_0\, \phi(x)} \tag{16}$$

$$N_{max} = \lim_{t \longrightarrow \infty} N(x, t) = \frac{1}{A(E, x)} \left[\frac{\frac{d\phi(x)}{dx}}{\phi(x)} \quad \frac{\frac{d E_b(x)}{dx}}{E_b(x)} \right] . \tag{17}$$

An important observation of Equation (17) is that the steady state distribution of N is critically dependent upon the slopes of the field and the breakdown threshold curves.

4. THE DIFFUSION PROBLEM

Equation (17) was obtained ignoring diffusion. The rigorous solution taking diffusion into account is unknown. However, for steady state, if the electric field and the density of the neutral components of air are slowly varying functions of the coordinates, the electron balance may be approximated by the equation:

$$D(E, x) \frac{d^2 N(x)}{dx^2} = - N(x) (\nu_i - \nu_a) \tag{18}$$

where,

$$D(E, x) = \frac{\int_0^\infty u^{3/2} \nu^{-1}(u) f(u)\, du}{\frac{3}{2} m \int_0^\infty u^{1/2} f(u)\, du} \qquad (19)$$

is the diffusion coefficient which is assumed to be a slowly varying function of the altitude and the electric field.

Equations (13) and (18) describe completely the steady state situation for N (x) and E (x). The system can be solved using the boundary conditions suggested by physical considerations (see Figure 6). The boundary conditions will thus be chosen at two altitudes h_1 and h_2, one below and the other above the crossing of the breakdown threshold. For this altitude, the value of N and $\frac{d N}{d x}$ are assumed to be known. Examining Equations(13) and (18) we note that while A (E, x) and D (E, x) are slowly varying functions of E and x, the function $\nu_i - \nu_a$ may undergo large changes for small changes of either variable (as shown in Figure 6). Thus, Equation (18) is very sensitive to small changes of E. This renders the system of Equations (13) and (18) highly nonlinear and difficult to deal with. This system has been solved numerically by Albertoni, Bocchieri, and Daneri [9] with the help of an IBM 7090 computer.

5. NUMERICAL EXAMPLES

Two cases are considered here which employ the results of the previous section. The first case deals with the "far field" of the transmitter. The parameters selected are,

$f = 50$ mc/s
$h_1 = 71$ KM
$E_b = 196$ V/m .

FIG. 6

VARIATION OF THE DIFFERENCE OF THE IONIZATION AND ATTACHMENT COLLISION FREQUENCIES AS A FUNCTION OF THE FIELD STRENGTH

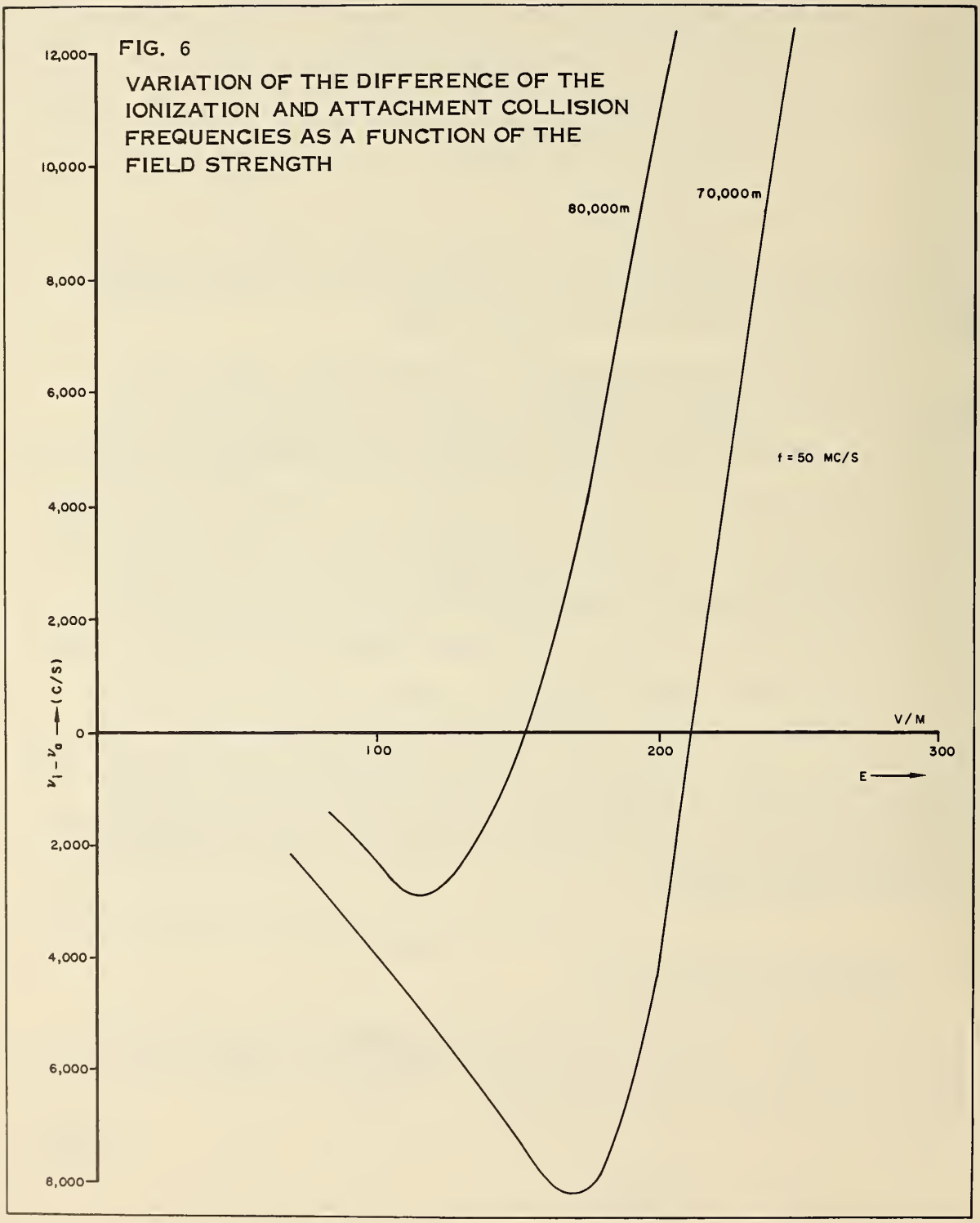

In Figure 7 is plotted the electron density distribution as obtained using Equation (14) (curve on the right). Also plotted (curves on the left; note the change in scale) are the solutions of the system of Equations (13) and (18). The two curves, which correspond to the different "trial" parameters chosen in the numerical integration, represent the physical solution as long as they coincide. Beyond the point of bifurcation they fail to indicate a physical solution. The region of coincidence could be prolonged with a better choice of parameters. However, the data in Figure 8 show that beyond the region considered, the approximation obtained neglecting diffusion Equation (14) is adequate.

The second case refers to a hypothetical transmitting antenna large enough such that the breakdown field is located at its focus. Here it is assumed that the antenna is a spherical basin whose surface is radiating in phase. The law of variation of the field intensity near the focus is thus assumed to be given by Equation (10), where

$$\frac{\pi D^2}{8\lambda h_1^2} = 1.7 \times 10^{-1}/\text{m}.$$

The other parameters are chosen such that in absence of electronic absorption, the electric field radiated reaches a maximum of 200 v/m at the altitude of 78 KM, where the focus of the antenna is assumed to be located. In Figure (8) is plotted the electron density variation with altitude obtained using Equation (17). Also plotted are the solution of the system of Equations (13) and (18) which is valid as a physical solution up to the point of bifurcation.

FIG. 7 ELECTRON DENSITY DISTRIBUTION FOR CASE I [f = 50 mc/s E_b = 196 V/M, FAR FIELD OF TRANSMITTER]

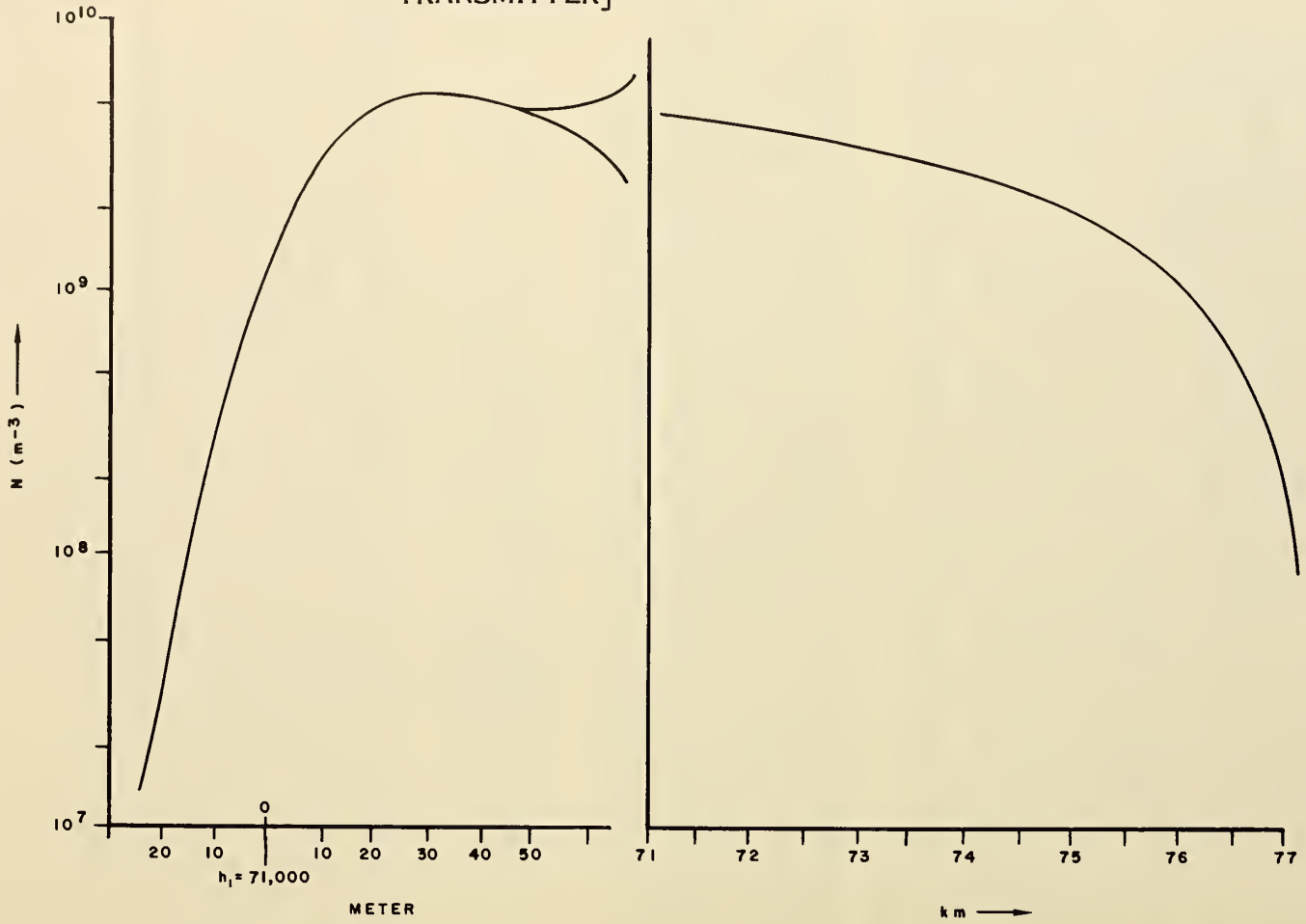

FIG. 8 ELECTRON DENSITY DISTRIBUTION FOR CASE 2
[f = 50 mc/s, $E(h_1) = 200$ V/M, $E_b = 156$ V/M, NEAR FIELD OF TRANSMITTER]

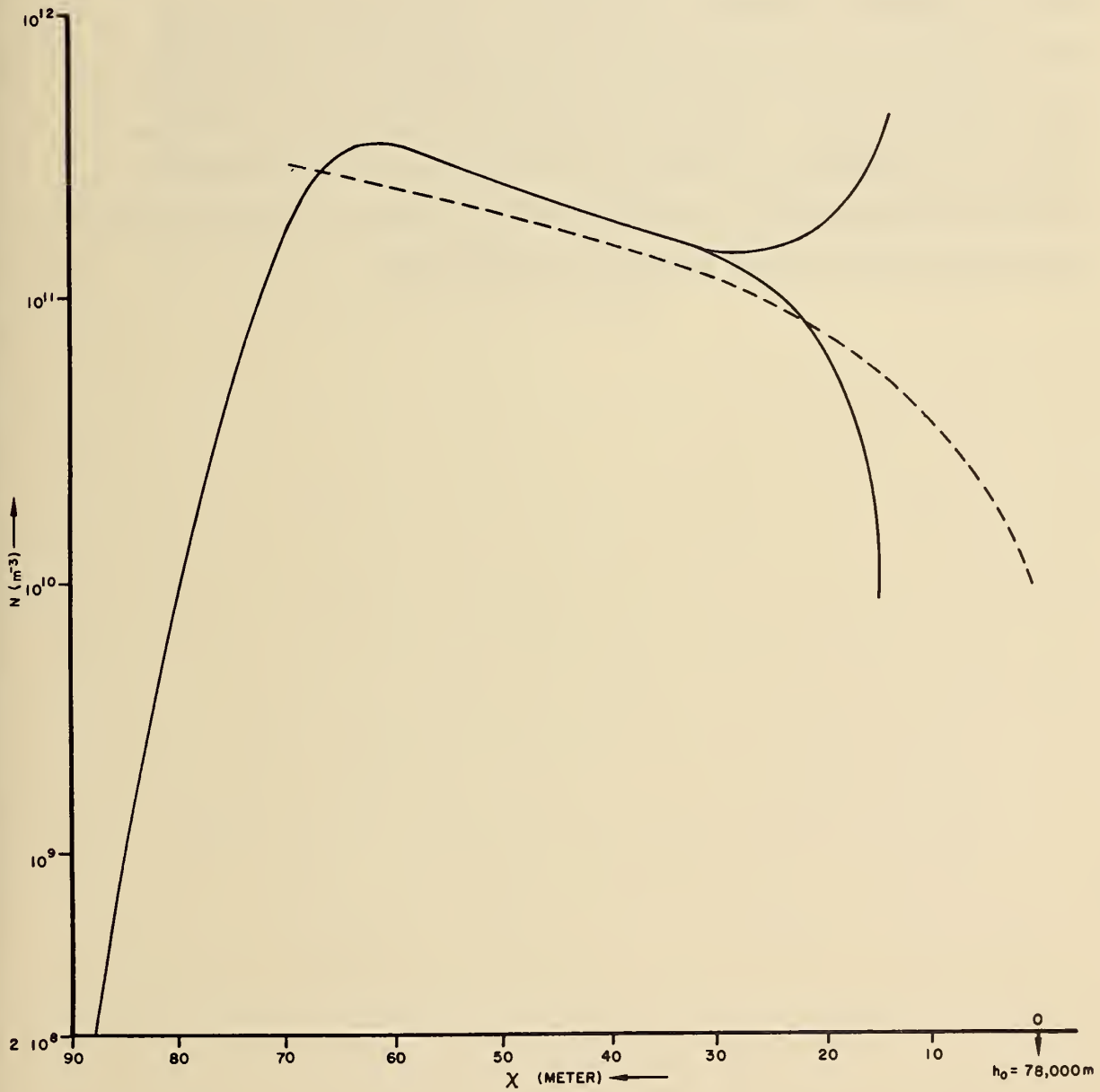

6. CONCLUSIONS

It has been shown that a radiowave radiated by a ground based transmitter may achieve breakdown in the D or lower E ionospheric regions. For each altitude, a frequency exists at which there corresponds an optimum ionization efficiency. The maximum electron density which can be obtained critically depends upon the altitude rate of change of both the breakdown field and the free space transmitted field strength. This characteristic automatically limits the maximum obtainable electron density which may be achieved in the far field of an antenna. This limitation may, however, be overcome by having breakdown take place in the near field.

ACKNOWLEDGEMENT

The study described in this paper has been totally supported by the Raytheon Company, for which the author is a Consultant. Acknowledgement should also be given to all the people who have worked on this project: L. R. Megill (National Bureau of Standards, Boulder, Colorado), S. Albertoni, P. Bocchieri, A. Daneri (Applications of Scientific Research, Milan, Italy), C. F. Eaton, and R. C. Gunther (Raytheon Company).

REFERENCES

[1] Molmud, P., "Use of Radio Transmitters to Decrease D-Region Electron Density," 1963. (in this issue)

[2] Farley, D. T. Jr., "Artificial Heating of the Electrons in the F-Region of the Ionosphere," J. Geoph. Research, 68, 1963, pp. 401.

[3] Bayley, V. A., "Some Possible Effects Cuased by Strong Gyrowaves in the Ionosphere," J. Atmos. Terrest. Phys. 14, 1959, pp. 229.

[4] Megill, L. R., "The Excitation of Optical Radiation by High Power Density Radio Beams," (in this issue)

[5] Brown, S. C., Rose, D., "Microwave Gas Discharge Breakdown in Air, Nitrogen and Oxygen," J. Appl. Phys. 28, 1957, pp. 561.

[6] Mac Donald, Gaskell, and , Gitterman, "Microwave Breakdown in Air, Oxygen, and Nitrogen," Phys. Rev. 130, 1963, pp. 1841.

[7] Carleton, N. P., Megill, L. R., "Electron Energy Distribution in Slightly Ionized Air Under the Influence of Electric and Magnetic Fields," Phys. Rev. 126, 1962, pp. 2089.

[8] Handbook of Astronautical Engineering, McGraw-Hill, 1961, pp. 2-9.

[9] Albertoni, S., Bocchieri, P., Daneri, A., Conference on Applications of Electronic Computers to Space Problems, Florence, 12-13 September 1963.

Nonlinear Effects in Radiation Generation Through the Coupling of Electron Beams with Diffraction Gratings

Winfield W. Salisbury, Sc.D.
Chief Scientist
Varo, Inc., 2201 Walnut St., Garland, Texas

The experimental studies of the Smith-Purcell effect which we have been pursuing in the Research Laboratory of Varo, Inc. have led to some unexpected results. The Smith-Purcell effect is the radiation of visual light by free electrons passing rapidly across the surface of a metallic diffraction grating. The early experiments reported by Smith and Purcell used electrons up to a little over 300 kv accelerating potential or having beta values in the region between 0.75 and 0.8. Our experiments have involved somewhat lower energies with beta values from about 0.4 to 0.75 or, roughly, in the range from 50 to 250 kv of accelerating potential. The wavelength formula given by Smith and Purcell is

$$\lambda = D \left(\frac{1}{\beta} - \text{Cos } \theta\right).$$

Where λ is the observed wavelength of radiation, D is the grating spacing; β is the ratio of the electron velocity to the velocity of light; and θ is the angle getween the direction of the electrons and the line of observation.

This formula has been found to be correct to a high degree of accuracy with one exception. The gratings which are normally available from optical work produce a spectrum rather than a single wavelength in a given direction. This spectrum can be accurately predicted if the profile shape of the grating lines is known. The alteration in the wavelength formula is simple. Dividing a grating spacing D by a number N, which may take on integral values, will give the correct spectrum, providing the integers represented by N are chosen to represent the index numbers of the Fourier series terms which represent the grating profile. Thus, a grating profile which is symmetrical around a perpendicular to the average surface of the grating will require only odd terms in its Fourier series, and only the odd integers will occur as appropriate values of N. In the case of a blazed grating, however, both even and odd terms occur in the representative Fourier series. Harmonics out to the seventh have been observed in this way.

These facts of wavelength and the occurance of a null in the radiation intensity in the direction where

$$\beta = \text{Cos } \theta$$

are compatible with a simple electrostatic image theory in which the electron and its supposed positive image below the grating surface form a moving oscillating dipole, which accounts for the radiation. (Figure 1). Several attempts to make an intensity theory based on this radiation have not so far proved very successful.

An experiment regarding the effect on electron distance from the grating sheds some light on this lack of agreement, and indicates the possibility of known linearities and a more complex requirement for theoretical explanation. Electron beams .025 mm thick have been used for most of our experiments.

This thickness is approximately 500 wavelengths for green light, which is frequently observed. For this reason, it has been expected that only a small fraction of the electrons very close to the grating would be effective in producing radiation. A series of experiments to test this, however, have given strong indications to the contrary. For example: An adjustable electron-slit gate was devised and the light intensity at a fixed angle measured as a function of the gate position. Surprisingly, the intensity proved to be an almost linear function of gate position in such a way as to indicate that electrons at the surface of the beam furthest from the grating were almost as effective in producing light as those next to the grating. (Figure 2.)

Movements of the grating away from the beam, however, extinguish the light with movements of an entirely different order of magnitude. This seems to indicate that the beam of electrons acts as a total entity, rather than a mere summation of the action of individual electrons. This should be explainable by some form of non-linearity. The usual ionosphere-type equations, however, do not seem adequate, as the plasma frequencies for the electron beam lie in the ordinary radio frequency region for the highest electron densities so far used (up to about 10^8 electrons per cubic centimeter).

The possibility has been considered that a plasma is formed by the electron beam in the residual gas in the vacuum. However, operation in vacuums from 10^{-6} torr to 10^{-8} torr have produced no appreciable change in intensity. Operation with pure argon gas between 10^{-5} and 10^{-6} torr pressure produce an increase in intensity of about 20% at the high pressure region. It seems reasonable to attribute this effect to increased current density in the beam, because of the effect of space charge neutralization, which is commonly known as gas focussing.

A word or two about experimental equipment seems desirable for the benefit of those who may wish to follow this research more in detail. In order to permit the study of electron beams up to 300 kv of accelerated potential, an experimental apparatus has been built in which the potential for acceleration is split in half by a concentrically enclosed division which is only open through the electron slit and some small alignment jig holes. (Figure 3.) This is in the form of concentric stems supported vertically by a tower of Pyrex glass insulators in oil. The electron emitter which is in the innermost surface mounted on a supporting stem consists of a ridge on an indirectly heated nickel cylinder. This ridge is placed between beam forming electrodes which are at the same potential as the emitter. The beam forming electrodes are sloped at a 67° angle to the electron beam in the manner of a Pierce gun designed for the formation of a sheet electron beam. A control slot is mounted ahead of this and is connected to an insulated power supply through the stem so that its potential with respect to the emitter can be independantly varied from 0 up to 5,000 volts with respect to the emitter. This is surrounded by a separate support stem and an outer sphere which is separately insulated. The whole arrangement is inserted into a ground potential chamber which contains the grating mounting and adjustment micrometers. The electron deflector and catcher system and an adjustable ground potential slot, which is the final focussing electrode for the electron beam formation, are shown clearly in the photograph. The innermost stem containing the emitter is operated at the full negative potential through which the electrons are accelerated. The support stem and spherical shield is operated at half this potential by means of a resistance voltage divider.

The electron beam focus is sufficiently good so that the electrons collected by the slot in this outer shield cause a negligible shift in the dividing potential. The usual arrangement is with the emitter blocked off by emitter potential shields so that a beam, 1 cm wide, is formed. This sheet beam is 1/4 mm thick. Good focussing is observed for total accelerating potentials of 50 kv and upwards. Various harmonics of the grating profile are observed in the form of visual light with accelerating voltages from 20 kv upwards. Visual light is expected to be observed with even lower potentials when a new grating, 76,000 lines per inch, is placed in the test position. Gratings of various profiles having 15,000, 20,000, 35,000, 45,000, and 55,000 lines per inch have been used with results which conform very closely to those expected insofar as the harmonic content and directional pattern of light intensity is concerned. Observed intensities have been considerably greater than should be expected on the basis of interaction with a layer of electrons having a depth of one wavelength or less for the emitted radiation, or having a depth of the order of one grating spacing.

A grating profile as determined from electron microscope photographs, showing the dimensions in microns, is shown in Figure 4. The Fourier series which represents this profile is as follows:

$$f(X) = 0.2263 - 0.0656 \cos \frac{\pi X}{D} - 0.0674 \sin \frac{\pi X}{D}$$
$$+ 0.0184 \cos \frac{2\pi X}{D} - 0.0645 \sin \frac{2\pi X}{D} + 0.0264 \cos \frac{3\pi X}{D}$$
$$+ 0.0204 \sin \frac{3\pi X}{D} + 0.00137 \cos \frac{4\pi X}{D} + 0.02025 \sin \frac{4\pi X}{D}$$
$$+ 0.01284 \cos \frac{5\pi X}{D} + 0.004028 \sin \frac{5\pi X}{D} \ldots .$$

A picture from the light from this grating is shown in Figure 5. This picture was obtained by photographing the electron beam through an 8,000 lines per inch transmission grating. The extra images on each side each represent a harmonic present in the emitted light. Beginning at the outside, away from the center image and counting inward toward it, we have the 4th, 5th, 6th, and faintly, the 7th harmonic of the Fourier analysis of this grating as separate images. This photograph is quite striking shown in the original color. The color of the light also depends on the angle of observation as indicated by the original wavelength equation. This is due to the Doppler effect introduced by the fact that the apparent source of radiation moves with the velocity of the electrons. This is not very troublesome, however, as the intensity at low angles in the forward direction may be hundreds of times that seen at an angle of 90° to the grating for example, and thousands of times the light seen at the minimum angle where some radiation may appear due to the observing lens taking in Azimuth angles other than 0.

Experiments are continuing and any suggestions regarding possible theoretical explanations will be gratefully received.

This work is sponsored by Varo, Inc., Garland, Texas, and by the United States Air Force, Aeronautical Systems Division, Wright Patterson Air Force Base, Dayton, Ohio.

References

Smith, Stephen J., and Edward M. Purcell (Nov. 15, 1953), Visible Light from Localized Surface Charges Moving Across a Grating, Letter, The Physical Review 92, No. 4, 1069.

Salisbury, Winfield W., United States Patent, Number 2, 634, 372, issued in April 1953.

Panofsky, Wolfgang K. H., and Melba Phillips, Classical Electricity and Magnetism, Para. 19-4, 306-307. (Addison-Wesley Publishing Company, Cambridge, Mass., 1955).

Palocz, Istvan, A Leaky Wave Approach to Cerenkov and Smith-Purcell Radiation, Dissertation submitted for the degree of Doctor of Philosophy at the Polytechnic Institute of Brooklyn. (Ann Arbor, Univ. Microfilms, 1962).

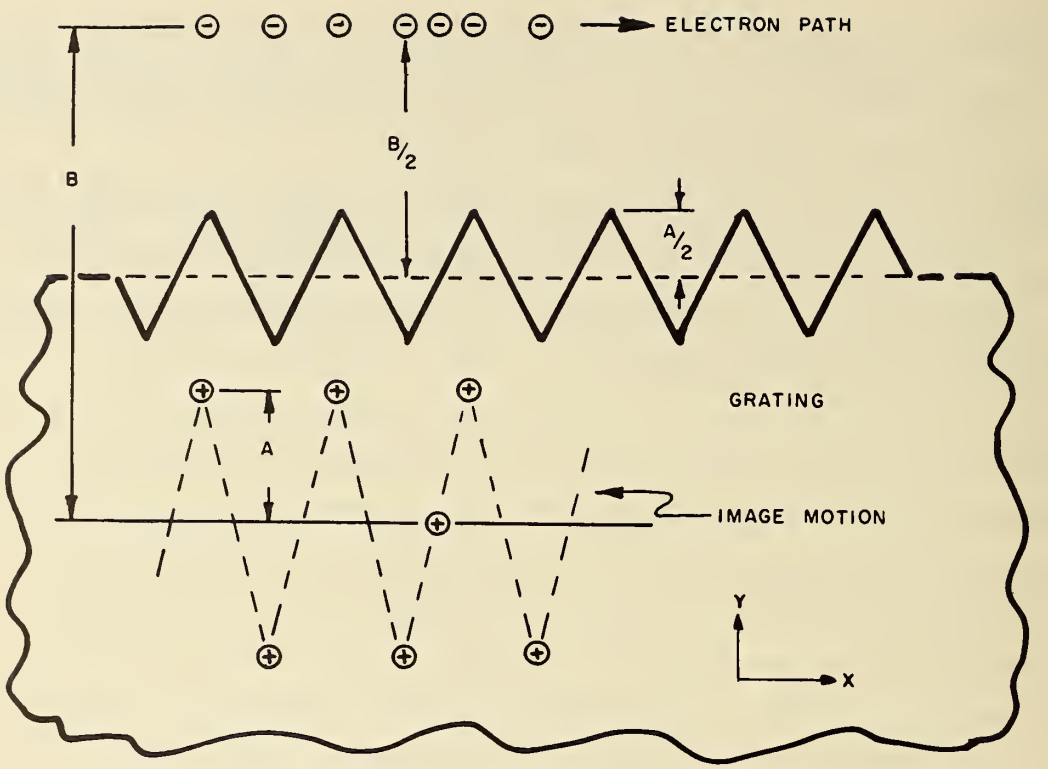
ELECTRON PATH
B
B/2
A/2
A
GRATING
IMAGE MOTION
Y
X

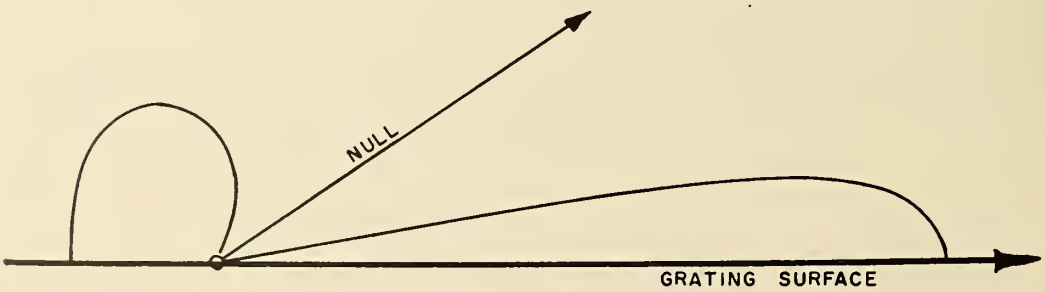
NULL
GRATING SURFACE

Figure 1.

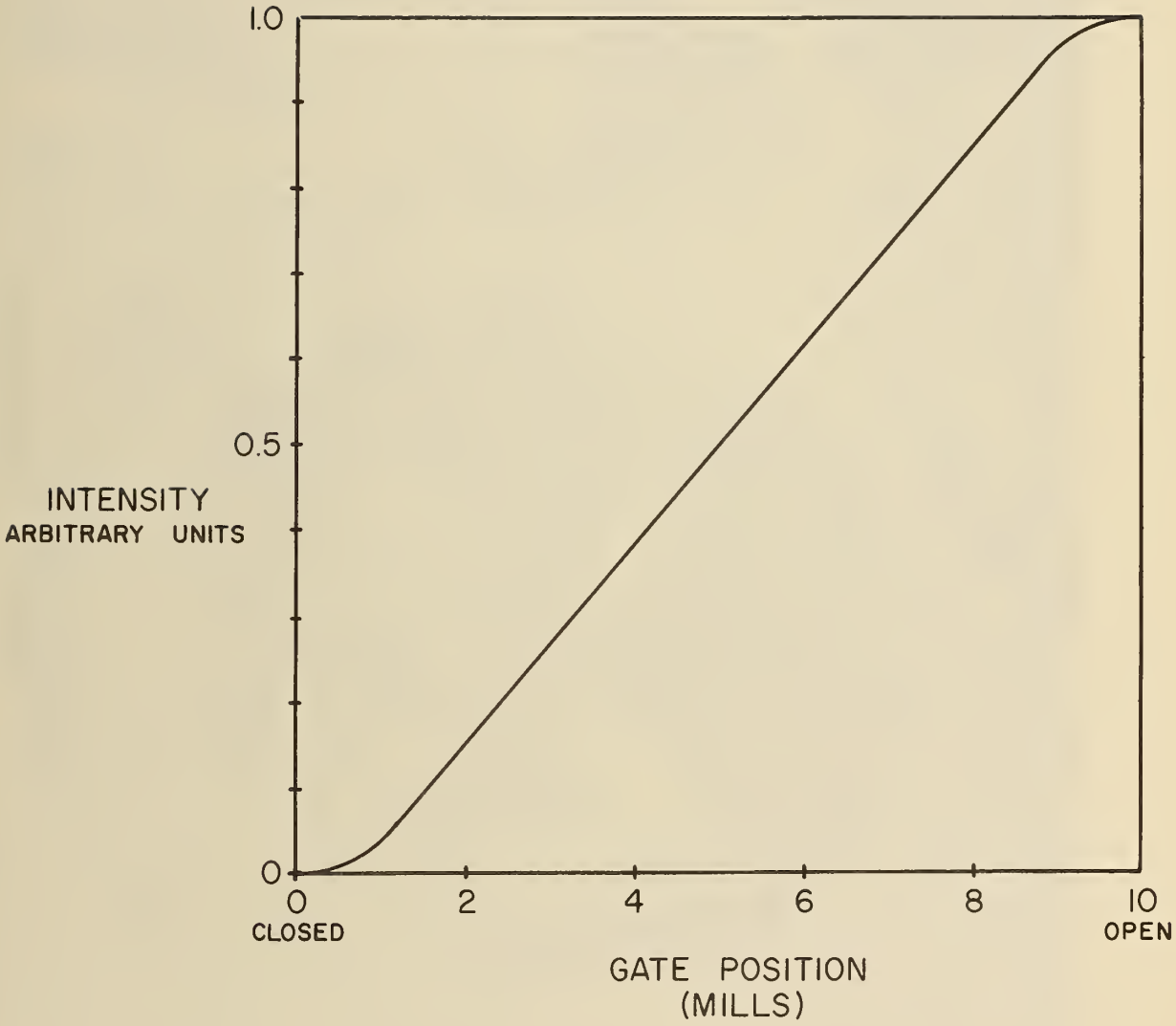
1.0
0.5
0
INTENSITY
ARBITRARY UNITS
0
CLOSED
2
4
6
8
10
OPEN
GATE POSITION
(MILLS)

Figure 2.

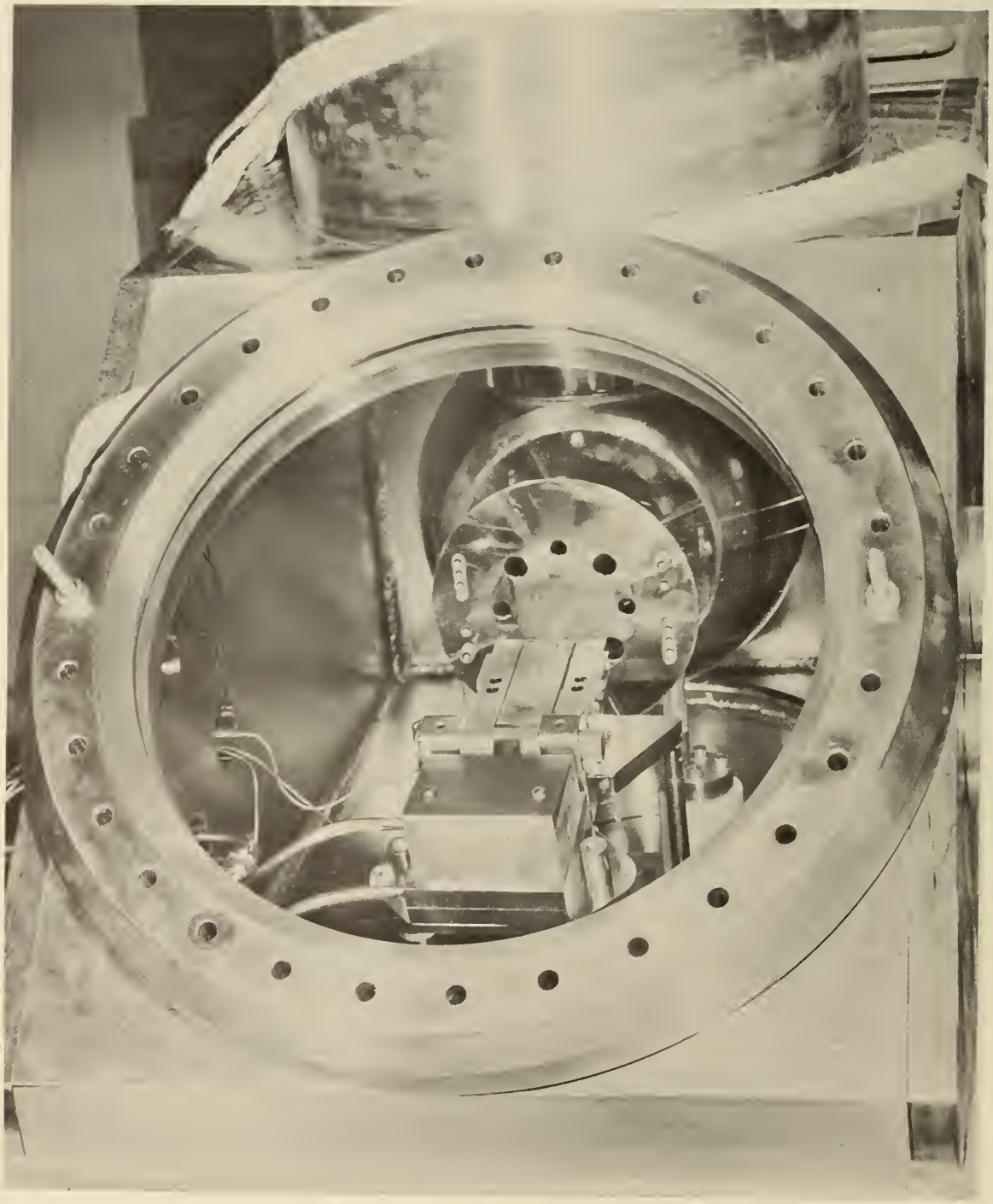

Figure 3

This photograph shows the electron beam focal electrodes in the background and next forward the diffraction grating in its adjustable mountings, then the small permanent magnets which deflect the electrons downward out of the line of sight, and in the immediate foreground the watercooled electron catcher which is made of silver and tungsten to absorb the avoidable X-rays due to collected high energy electrons. This is viewed through a 14" optical glass port.

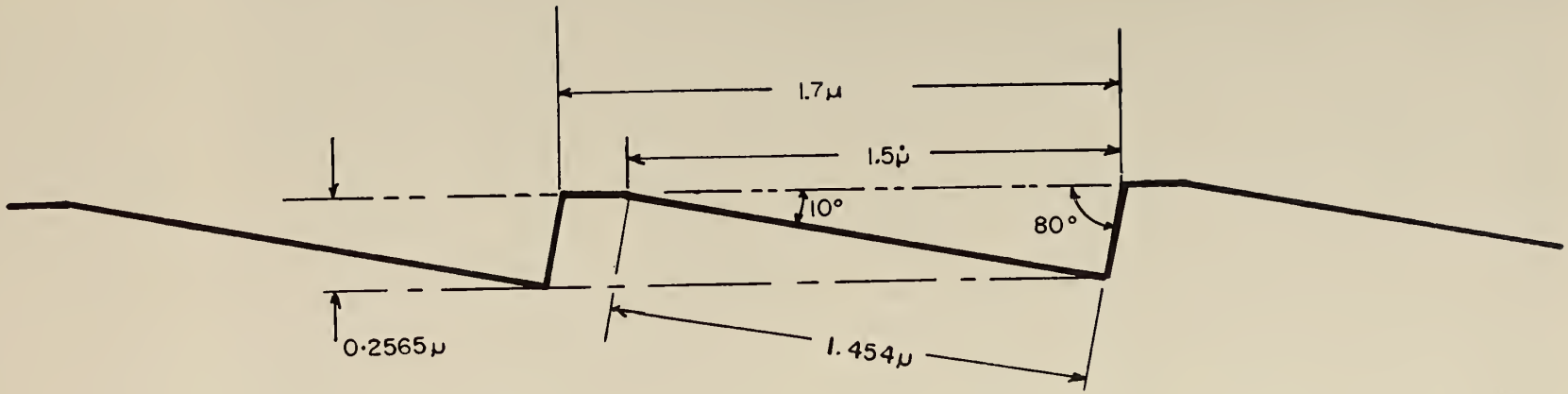

SCALE = 2 IN = 1μ

Figure 4

Profile of diffraction grating (15000 lines per inch).

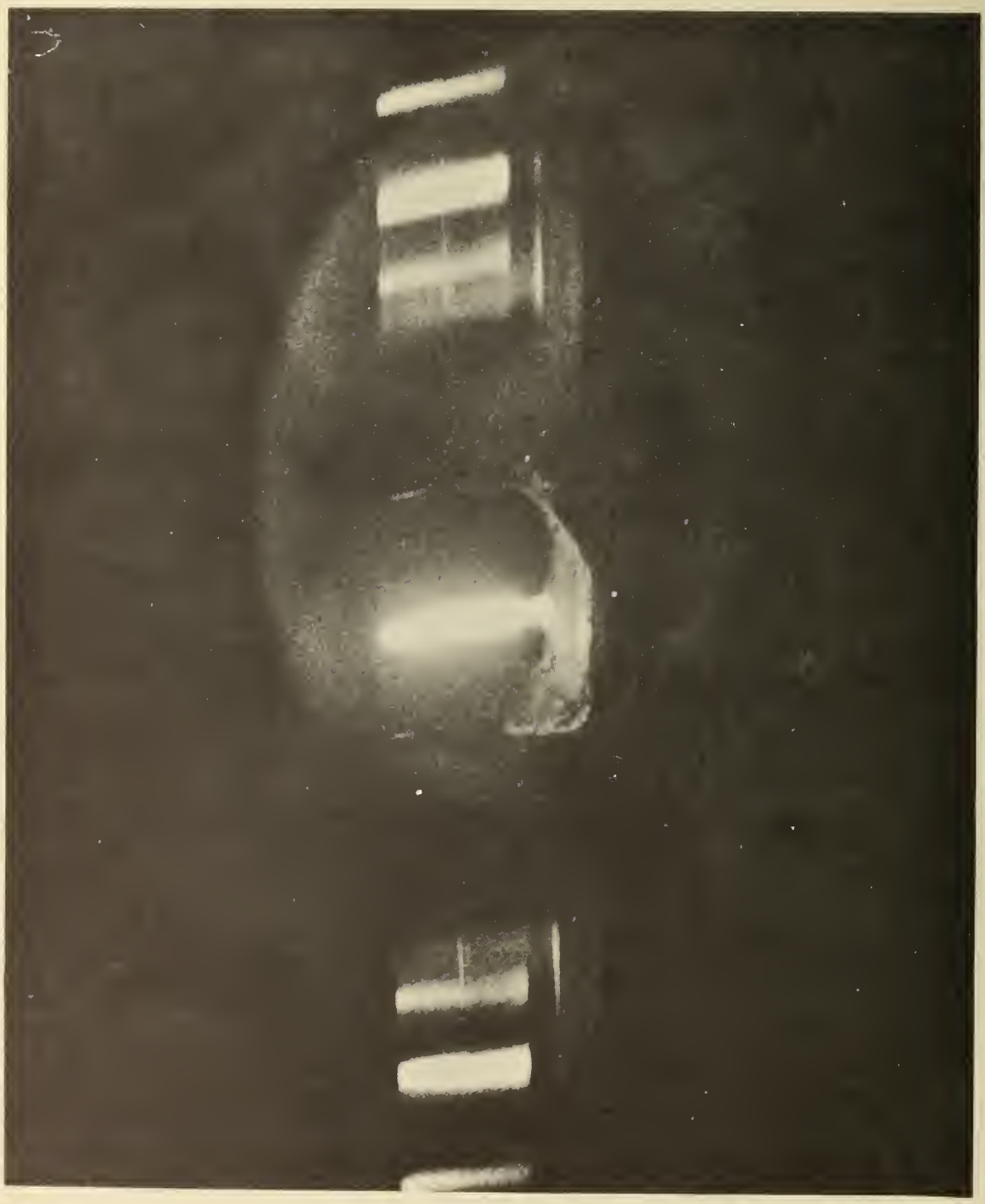

Figure 5

Four spectral images on each side of the central image. The colors in tne original photograph of the spectral images are, starting from the outside in sequence inward, red, green, blue, and violet. They represent the 4th, 5th, 6th, and 7th harmonic of the Fourier Series representing the grating profile.

GPO 841-146


DEPARTMENT OF COMMERCE
NATIONAL BUREAU OF STANDARDS